ACTA FORESTALIA FENNICA

200

ON THE COMBINATION OF MULTI-TEMPORAL SATELLITE AND FIELD DATA FOR FOREST INVENTORIES

MONIAIKAISEN SATELLIITTI- JA MAASTO-AINEISTON YHTEISKÄYTTÖ METSIEN INVENTOINNISSA

Peng Shikui

SUOMEN METSÄTIETEELLINEN SEURA 1987

Suomen Metsätieteellisen Seuran julkaisusarjat

ACTA FORESTALIA FENNICA. Sisältää etupäässä Suomen metsätaloutta ja sen perusteita käsitteleviä tieteellisiä tutkimuksia. Ilmestyy epäsäännöllisin väliajoin niteinä, joista kukin käsittää yhden tutkimuksen.

SILVA FENNICA. Sisältää etupäässä Suomen metsätaloutta ja sen perusteita käsitteleviä kirjoitelmia ja lyhyehköjä tutkimuksia. Ilmestyy neljästi vuodessa.

Tilaukset ja julkaisuja koskevat tiedustelut osoitetaan seuran toimistoon, Unioninkatu 40 B, 00170 Helsinki 17.

Publications of the Society of Forestry in Finland

ACTA FORESTALIA FENNICA. Contains scientific treatises mainly dealing with Finnish forestry and its foundations. The volumes, which appear at irregular intervals, contain one treatise each.

SILVA FENNICA. Contains essays and short investigations mainly on Finnish forestry and its foundations. Published four times annually.

Orders for back issues of the publications of the Society, and exchange inquiries can be addressed to the office: Unioninkatu 40 B, 00170 Helsinki 17, Finland. The subscriptions should be addressed to: Academic Bookstore, Keskuskatu 1, SF-00100 Helsinki 10, Finland.

ACTA FORESTALIA FENNICA 200

ON THE COMBINATION OF MULTITEMPORAL SATELLITE AND FIELD DATA FOR FOREST INVENTORIES

Peng Shikui

Tiivistelmä

MONIAIKAISEN SATELLIITTI- JA MAASTOAINEISTON YHTEISKÄYTTÖ METSIEN INVENTOINNISSA

To be presented, with the permission of the Faculty of Agriculture and Forestry of the University of Helsinki, for public criticism in Auditorium XII of the University Main Building, Fabianinkatu 33, February 26, 1988, at 12 o'clock noon

HELSINKI 1987

PENG SHIKUI. 1987. On the combination of multitemporal satellite and field data for forest inventories. Tiivistelmä: Moniaikaisen satelliitti- ja maastoaineiston yhteiskäyttö metsien inventoinnissa. Acta Forestalia Fennica 200. 95 p.

The study concerns with the methodology and efficiency of integrating multitemporal satellite image data with permanent sample plots in a continuous forest inventory and compartmentwise estimation. The genaralized least squares estimation for the population, and the unsupervised stratification for compartments, are the main estimation methods employed. The experimental material is composed of real and simulated multitemporal images (Landsat TM) and field data. Precision analyses for the estimation and comparisons for a number of estimation and updating methods, as well as statistical options are given.

Tutkimuksessa tarkastellaan eri ajankohtien satelliittikuvia ja pysyviä koealoja hyödyntäviä menetelmiä ja niiden tehokkuutta metsän otantatyyppisessä sekä kuvioittaisessa arvioinnissa. Perusmenetelmät ovat yleistetty, pienimpään neliösummaan perustuva ennustemenetelmä koko perusjoukolle ja kaksivaiheinen otanta osituksella kuvioittaisen arvioinnin yhteydessä. Tutkimusaineistot on saatu sekä todellisista että simuloiduista satelliittikuvista (Landsat 5) ja mitatuista ja simuloiduista relaskooppikoealoista. Tutkimuksessa on analysoitu estimoinnin tarkkuutta, vertailtu useita estimointi- ja ajantasallapitomenetelmiä sekä esitetty useita tilastotieteellisiä sovellusvaihtoehtoja.

Keywords: generalized least squares, multitemporal, stratification, two phase sampling, SPR
ODC 585+524.63

Author's address: Department of Forest Mensuration and Management, University of Helsinki, Unioninkatu 40 B, SF-00170 Helsinki, Finland.

ISBN 951-651-0787-7
Karisto Oy:n kirjapaino
Hämeenlinna 1987

CONTENTS

PREFACE

This study is a part of a project concerning the application of satellite imagery to forest inventories, which is being undertaken at the Department of Forest Mensuration and Management of the University of Helsinki.

The research topic was suggested by Professor Simo Poso, the supervisor of the project. He has also read several versions of the manuscript thoroughly and made valuable suggestions, comments and corrections. I would like to express my sincere gratitude for his encouragement and helpful advice.

Dr. Erkki Tomppo and Dr. Juha Lappi read and criticized the manuscript. I am greatly indebted to them for their valuable comments.

Mr. Markku Siitonen, one of the creaters of the MELA Programme, kindly helped me to use the programme. The compartment digitization and imagery registration in the study area were completed by Mr. Markku Similä. He also initially helped me to handle image material. Mr. Hannu Yli-Kojola collected and provided information about permanent sample plots in the Finnish National Forest Inventory. Dr. Ashley Selby checked the English. I wish to express my warm thanks to all of them. Also, I would like to take the opportunity to express my appreciation to those people who collected the field material in the study area.

I am especially grateful to all the staff members of the Department of Mensuration and Management for their providing such a fine atmosphere.

I am deeply indebted to the Finnish Natural Resource Foundation and the Foundation of Cooperative Research in Nordic Countries for financial support over two years and three months.

Acknowledgment is also due to the Finnish Forest Reseach Institute, the Faculty of Agriculture and Forestry of the University of Helsinki and the Technical Reseach Centre of Finland for the free use of the facilities and programmes, as well as to the Society of Forestry in Finland for publishing this paper.

Finally, I would like to thank the Chinese and Finnish governments for giving me the chance to study in Finland.

Helsinki, November, 1987

Peng Shikui

1. INTRODUCTION

11. Background of the continuous inventory

The development of forest inventory methods is often connected with i) the demand for the timber products, ii) the objectives of management planning and iii) considerations concerning the state policies and environmental protection. Forest inventory methods are also affected by the state of forest as well as the economical and technological levels in the country. To meet these demands single forest inventories have been used for more than a century.

In order to understand forest changes and to be able to control the effectiveness of management activities successive inventories are necessary (Loetsch and Haller 1973).

One type of successive inventory in the past was the repetition of the single inventory in the same area. Examples of this kind of inventory are the first seven national forest inventories in Finland and the first five in Sweden. The inherent drawback of this kind of successive inventory is the poor precision in estimating forest change.

An alternative to successive inventory is the continuous inventory, which is characterized by a periodical remeasurement of all the trees in a fidex area. The continuous inventory can be traced back to the "control method" which appeared in France hundred years ago and had been used in Switzerland for half a century (Spurr 1952). Since a compartment was used as the measuring unit, the method was laborious and expensive.

The continuous forest inventory (CFI) used in recent years was developed in Europe and North America during the years 1930–1950 (Loestch and Haller 1973). An important improvement of the CFI is that the permanent sample plots replaced the compartments. As defined by Stott and Semmens (1962) "Continuous forest inventory, or CFI, is a precise, frequently repeated, and directly comparable measurement of all commercial trees in systematically placed sample plots. These plots have fixed radii and are permanently located in the forest. Their treatment and the treatment of the surrounding forest must be analogous."

The CFI test in Finland was suggested by Nyyssönen (1967) and has been carried out by two large timber companies since 1958.

Along with increasing demand for monitoring the dynamic changes of both forest and environment, the CFI has been adopted by national forest inventories in several countries. China introduced the method to its national forest inventory in the 1970's. Permanent square plots were used in northern China and permanent relascope plots in southern China. Austria and Switzerland started using permanent sample plots in their national forest inventories at the beginning of the 1980's (Jaakkola 1986). Recently Sweden (Cruse et al. 1985) and Finland made this change in their national forest inventory by establishing permanent sample tracts. Nyyssönen (1967) pointed out that one of the reasons for not using the method in the Nordic countries earlier was that the technique based on temporary sample plots can offer the necessary information about growth and other factors in these countries.

The sampling technique used in the CFI is sampling with the partial replacement (SPR), developed by Jessen (1942) and discussed by Hansen et al. (1953) and Cochran (1977). The estimation theory, i.e. the minimum variance linear estimation (MVLE) or generalized least squares (GLS), the sampling design and the possible cases of the SPR have been comprehensively formulated and summarized by Ware and Cunia (1962), and Loetsch and Haller (1973) for the purposes of the continuous forest inventory. Subsequently, Cunia (1965), Cunia and Chevrou (1969), and Newton et al. (1974) further generalized the estimation and extended it to more than two occasions as well as the case for the multivariates. In addition, Frayer and Furnival (1967), Hazard (1977), Nyyssönen (1967), Hazard and Promnitz (1974), Dixon and Howitt (1979), Peng (1982, 1986), Peng and Zhu (1985), Scott (1984) have studied the CFI in theory and in practice. A distinct feature of the GLS method is that it can cope

with a variety of sample cases and estimate the current forest state and its change simultaneously with the minimum variance.

One problem often met in the CFI based only on permanent plots is the decrease of the correlation between the matched measurements over time. In order to alleviate the effect of the decrease on estimation precision, the whole area can be divided into the cut and the non-cut subareas. In a large forest region, however, determination of the cut and the non-cut areas tends to be difficult. Under such circumstances, it is worth examining the posibilities to improve the efficiency of SPR by using satellite imagery.

The sampling plan of the CFI is often designed for a large area. The fact that there exists a considerable number of sample plots in a large-scale forest inventory naturally leads to the desirability that these sample plots should also be applicable to smaller areas: subareas or compartments. This is because the inventory for a small area such as a compartment is labourious, even with the aid of ocular estimation and relascope plots.

A more popular approach towards both whole area and subarea inventories is two phase sampling. The sample plots in the first phase are usually those sample plots which are obtained under a low cost such as photo sample plots. The sample plots in the second phase are often the sample plots on the ground. The two phase sampling used in the national forest inventory in Finland was carried out by using relascope sample plots and aerial photo plots (Poso and Kujala 1971, 1978). The inventory method was adjusted when calculating results for districts. China has a similar approach. The national forest inventory in Jiling province in China was designed for the whole province, but the results were also used for each county by employing photo sample plots and regression models.

Because of the low price and the digital format of the satellite image data, the trend in using two phase sampling is for satellite imagery to replace the aerial photos. In Finland such a test began in 1984 (Poso et al. 1984). The research concerning the practical application of satellite imagery is still going on.

12. Satellite pictures and their application to forest inventory

The first satellite aimed at the global mapping of Earth resources was Landsat-1 lauched in 1972. The satellite imageries currently employed are Landsat MSS (Multispectral Scanning System), Landsat TM (Thematic Mapper) and SPOT (Systeme Probatoire l'Observation de la Terre).

MSS and TM refer to the sensors MSS and TM. The former have been installed in all Landsat satellites and the latter only in Landsat 4 and 5. TM has more spectral bands, more radiance levels and finer spatial resolution than MSS. SPOT was launched by France in 1986. It has a new type of scanner which has two modes: panchromatic and multispectral modes. The image data of these satellites covers both the visible and near infrared wavelengths.

The number of wavebands, spatial resolution and number of classes in spectral radiances are listed below,

	MSS	TM	SPOT	
			Mode 1	Mode 2
Wavebands	4	7	1	3
Spatial resolution	79 m	30 m (for six bands)	10 m	20 m
Grey levels	64	256		

where Mode 1 = panchromatic mode and Mode 2 = multispectral mode.

Jaakkola (1986) gave a broad summary of applications of MSS image data to forest inventories and forest management in the European countries, especially in the Nordic countries. The applications are directed to the sampling design, forest mapping and forest type classification, estimating the stand characteristics and monitoring forest changes.

The imagery is often used for forming the sample of the first stage in the multi-stage sampling. The three-stage sampling designed by the University of Freiburg (Jaakkola 1986) and the two-stage sampling used in Finland for estimating volume (Saukkola and Jaakkola 1983) are examples of the use of imagery.

Forest mapping and the classification of the land-use classes and forest types are perhaps the most common ways of using satellite imagery. Some applications have achieved an operational level. Jaakkola (1986) reviewed a number of successful applications in Europe such as mapping the poplar groves and beech forests in northern Italy, Forest cover-type mapping in Germany, and forest site-type mapping in Finland.

It seems that many methods for estimating the stand characteristics are still in the experimental stage. The correlation between image and ground characteristics is not particularly high. Some improvement can be obtained by employing ancillary material, e.g. from maps and aerial photographs.

Two basic methods utilized for estimating the stand characteristics are the regression technique and stratification. Jaakkola and Saukkola (1979), Tomppo (1987) and Peng (1987) have developed some regression models including the conventional models and the log-linear model for such studies.

Poso et al. (1984) presented a stratification model for compartmentwise estimation. The model can be used to estimate all the variables. Peng (1987) compared the two stratification methods (supervised and unsupervised) for some qualitative variables. The two methods gave similar results. However, the supervised method was regarded as problematic for the multiparameter inventory. Kilkki and Päivinen (1987) suggested an approach which resembles the supervised method, but it can be used for all the variables.

For estimating or monitoring change by using satellite image data, studies have concentrated on image transformations, approaches for detecting the mapping change and handling the multitemporal image data.

A typical transformation for detecting the changes of vegetation is the Kauth and Tomas transformation (Kauth and Tomas, 1976). Later Richardson and Wiegand (1977), Thompson and Wehmanen (1979), Badhwar et al. (1982) and Jackson (1983) developed and discussed the transformation. In addition, some other transformations such as multispectral ratios, logarithmic transformation etc. have been developed by Rouse et al. (1973), Goetz et al. (1975).

There are a number of approaches which can be used in detecting and mapping changes in the vegetation. A general approach for doing this is to make a comparison between the bitemporal image data acquired at two time points, as described and summarized by Goldberg et al. (1982) and Schowengerdt (1983). The approach is straightforward. Another method is "vector change" analysis (Malila 1980). In this approach the image data is first transformed into vegetation components. The image pixels are then classified according to the moving directions and the magnitudes of the first two vegetation components. The technique is designed for mapping vegetation changes. In Finland, Saukkola (1982) has developed a system for monitoring clear cuts. Häme (1987) has examined an approach which includes the segmentation and classification of clear cutting areas and the detection of forest damage.

Schowengerdt (1983) summarized a couple of techniques concerning how to handle multitemporal image data, including stacking the multitemporal image data and the maximum likelihood cascade in order to improve the accuracy of the interpretation.

In principle, most of the methods and techniques concerning the application of image data to forest inventories could be also suitable for CFI. However, a distinct feature of the application of the image data to the CFI is the multitemporal and two-phase data.

When the permanent sample plots are remeasured, every plot has two or more than two measurements for a variable of interest. If image data is available for each remeasuring period, every permanent plot also receives the associated two or more image values. Then, each of the permanent sample plots contains information concerning both the current state and change from both ground reality and imagery. As the number of remeasurements increases, the sample plots in the two phases: imagery and ground together with the different remeasuring periods might constitute a variety of sample cases.

13. Purposes of the study

This study is one of the research topics of the Department of Forest Mensuration and Management of the University of Helsinki in Finland on the application of the satellite data to the forest inventories.The key concern is how to handle the multitemporal and two-phase data or how to update data in the CFI with multitemporal imagery. This is the original motive of the study. The basic methodology is based on SPR and stratification. The emphasis of the study is put on the methods about the integration of permanent sample plots with image data for the continuous forest inventory and the compartmentwise estimation.

The purposes of the study are then

1. to present a general procedure for integrating the permanent plots with digital image data for the continuous forest inventory of the large areas and for compartment-oriented estimation.
2. to compare some basic estimation methods, updating techniques and statistical options used in the procedure.
3. to make efficiency analyses.

2. DESCRIPTION OF THE METHODS

21. Terminology and Notation

211. Terminology

Only most common and important terms used in the study are defined below.

Population, sample and phase

A population to be sampled is the aggregate from which the sample is chosen (Cochran 1977). In this study it is defined as the forest area. The population unit is the relascope plot. Therefore the population can be viewed as a set of all the relascope plots in the forest area.

The sample is a collection of the population units which are randomly or systematically drawn from the population. The unit in the sample is a sample plot or sample point.

The phase is an information concept (see Loetsch and Haller 1973). The first phase in the study is the image phase which contains only the information on the spectral values. The second phase in the study is the field phase which contains the stand characteristic information.

Image point, permanent sample plot and temporary sample plot

An image point or image plot is said to be a sample point in the first phase. Its centre corresponds to the centre of a relascope sample plot on the ground. The spectral value of the image point comes from the spectral value of the nearest pixel or the average spectral value of the nearest couple of pixels. The image sample consists of all the image points in the first phase.

A permanent sample plot in the study is a permanent relascope sample plot with BAF (Basal Area Factor) 2. It is laid out for the repeated observation. A permanent sample plot is drawn from the first phase and measured in the second phase. The permanent plot sample is composed of the permanent sample plots. A temporary sample plot is measured only once.

The image sub-sample is the remaining part of the image sample after removing those image points which have been drawn as the permanent sample plots.

Matched sample plots, matched image points, occasion and period

For each given target variable, a permanent sample plot has a pair of observations or matched observations on two occasions, i.e. two measuring time-points. Accordingly, the sample plots or image points with remeasurements are sometimes called matched sample plots or matched image points. A time interval between two occasions is said to be a period.

Current state, change, total growth and field variable

The current state refers to the forest state described by field variables on the present occasion such as the current volume, current species composition etc. The field variables relate to the stand characteristics.

The forest change, or change or net increase is the difference between two occasions with respect to the field variables. The total growth is said to be a sum of the net increase of volume and total drain during a period.

212. Notation

The notation of basic statistical symbols common to the whole study are as follows:

s_i^2 = sample variance of variable i
$s_{i,j}$ = sample covariance between variables i and j
$r_{i,j}$ = sample correlation coefficient between variables i and j
Σ_J = covariance matrix of vector J
$\Sigma_{J,K}$ = covariance matrix between vectors J and K

n_p = number of permanent sample plots
n' = number of image points of the image sample
n'_i = number of image points of the image sub-sample

The image points and permanent sample plots from different occasions might constitute a variety of sample cases. The following list is the notation of the sample cases, to be met in the study.

Notation of the sample	Image sample			Permanent plot sample		
	Occasion			Occasion		
	1	2	3	1	2	3
P12				*	*	
I1P1	*			*		
I2P2		*			*	
I2P12		*		*	*	
I12P1	*	*		*		
I12P12	*	*		*	*	
I1I2P12	*	*		*	*	
I123P12	*	*	*	*	*	
P23					*	*
I23P23		*	*		*	*
I2I3P23		*	*		*	*

Symbol "*" in the list indicates where the sample comes (phase and occasion). I in the notation represents the image sample, P denotes the permanent plot sample and the numbers refer to the occasions. If the image points in the image sub-sample come from two occasions but are not matched, the occasion numbers in the sample notation will be separated by I, I1I2 and I2I3, for instance. For the matched plots and points, the occasion numbers are connected one by one.

The abbreviations often used in the study are as follows:

D.B.H: diameter at the breast height
GLS: generalized least squares
MD: minimum distance
ML: maximum likelihood
P.C: principal component
PTM: probability transition matrix
RMSE: root mean square error
SPR: sampling with partial replacement
TPS: two phase sampling for stratification

22. Estimation methods for the population

The two phase sampling on the basis of the permanent sample plots and multitemporal image data can be regarded as a special case of SPR. The generalized least squares (GLS) estimation as a traditional estimation method for SPR is therefore adapted in the study. If the covariance matrix of the population is known, the estimates of the variables obtained with the GLS are the best unbiased ones.

The two phase sampling for stratification (TPS) or double sampling for stratification (Cochran 1977) is an alternative estimation method for the population. In fact the technique will be used mainly for the compartments in the study.

221. Generalized least squares estimation

Consider a two phase sampling with sample case I12P12. The image point in the first phase has a pair of observation vectors acquired on two occasions. Each vector is composed of q spectral values which represent q bands. In the second phase, there are n_p permanent sample plots. Each permanent sample plot also has two observation vectors; each observation vector covers q spectral values and p field variables.

Suppose that
(1) the samples are randomly selected;
(2) the population covariance matrix of observation vectors are known;
(3) the relationship between the observation vectors in the second phase and the state vector which is here defined as the mean vector of spectral values and field variables, can be linearly expressed in an observation equation as follows: (see Theil 1971 p. 236, Dixon and Howitt 1979)

$$Z = H X + v \qquad (22.1)$$

where Z = k-dimensional observation vector of sample means
X = h-dimensional state vector
H = observation coefficient matrix (kxh)
v = k-dimensional observation error vector.
$k = 2(p+q) + 2q$
$h = 2(p+q)$

Then, when Z, H and R_v where R_v = covariance matrix of v are given, vector X can be estimated by

$$\hat{X} = (H^T R_v^{-1} H)^{-1} H^T R_v^{-1} Z \qquad (22.2)$$

and the covariance matrix of $\hat{X}$ is produced by

$$P_X = (H^T R_v^{-1} H)^{-1} \qquad (22.3)$$

According to the order of the phase and the occasion, the detailed explanations in relation to Z, X, H, and R_v are as follows:

$$Z^T = [\, Z_2\ Z_1 \,]$$

where the subscripts refer to phases,

$$Z_2 = [\, Z_2^{(1)}\ Z_2^{(2)} \,] \text{ and}$$

$$Z_1 = [\, Z_1^{(1)}\ Z_1^{(2)} \,]$$

where the superscripts refer to occasions,

$$Z_2^{(1)} = [\, \tilde{z}_{2,1}^{(1)}, \tilde{z}_{2,2}^{(1)}, \ldots, \tilde{z}_{2,p}^{(1)}, z_{2,p+1}^{(1)}, \ldots, \tilde{z}_{2,p+q}^{(1)} \,]$$

= observation vector including means of p field variables in the second phase and q bands of spectral values on the first occasion

$$Z_1^{(1)} = [\, \tilde{z}_{1,1}^{(1)}, \tilde{z}_{1,2}^{(1)}, \ldots, \tilde{z}_{1,q}^{(1)} \,]$$

= spectral vector in the first phase on the first occasion

and $Z_2^{(2)}$ and $Z_1^{(2)}$ can be expressed in the same way.

$$X^T = [\, X^{(1)}\ X^{(2)} \,]$$

where

$$X^{(1)} = [\, \tilde{x}_1^{(1)}, \tilde{x}_2^{(1)}, \ldots, \tilde{x}_p^{(1)}, \tilde{x}_{p+1}^{(1)}, \ldots, \tilde{x}_{p+q}^{(1)} \,]$$

= state vector of means of p field variables and q bands of spectral values on the first occasion

and $X^{(2)}$ is on the analogy of $X^{(1)}$ but on the second occasion.

$$H = \begin{bmatrix} I & \\ 0^{(1)}\, I_1^{(1)} & 0 \\ 0 & 0^{(2)}\, I_1^{(2)} \end{bmatrix}$$

where

I = 2(p+q)dimension identity matrix
0 = qx(p+q) dimension 0 matrix
$0^{(1)}$ = qxp dimension 0 matrix
$0^{(2)}$ = qxp dimension 0 matrix
$I_1^{(1)}$ = q-dimensional identity matrix
$I_1^{(2)}$ = q-dimensional identity matrix

$$R_v = \begin{bmatrix} \Sigma Z_2 & 0_2 \\ 0_1 & \Sigma Z_1 \end{bmatrix}$$

where 0_1 = (2p+2q)×(2q) dimension 0 matrix
0_2 = (2q)×(2p+2q) dimension 0 matrix

For estimating a field variable's change and its variance during an interval, we multiply a vector A, which is of the form

$$A = [\, 0, \ldots, 0, -1, 0, \ldots, 0, 1, 0 \ldots, 0 \,]$$

to the left side of $\hat{X}$ and R_v, and A^T to the right side of R_v. The positions of −1 and 1 in A correspond to the positions of the target variable in vector $\hat{X}$ or matrix R_v at the previous and the present occasions respectively. The changes on a vector of p field variables can follow the way stated above by replacing p-1 pairs of -1 and 1 at the corresponding places in vector A.

In principle, equations (22.1), (22.2) and (22.3) are applicable to both the quantitative and qualitative variables. The estimation for a qualitative variable, however, is conducted in terms of classes of the qualitative variable. The values of a certain class of the qualitative variable are only two possibilities: 1, if the sample plot belongs to the class, or 0 otherwise. It should be noted that in order to avoid singularity, for each qualitative variable with m classes, only m-1 classes can be simultaneously involved in Eq. (22.1), (22.2) and (22.3). The estimate and its variance of the remaining one will be derived readily afterwards.

The GLS for other cases can be made in a similar way. So long as vectors Z and X are determined, H and R_v can be be arranged by following the order and intercorrelations among the components on Z and X.

In reality the population covariance matrix would be unkown. Then the permanent plot sample covariance is used instead.

222. Two phase sampling for stratification

When the population is large enough, the estimate and variance of the mean value of a target variable in a population are of the following approximate forms when using TPS (see Cochran 1977, p. 333)

$$\bar{x}_{st} = \Sigma w_i \bar{x}_i \qquad (22.4)$$

$$s^2_{\bar{x}_{st}} = \Sigma w_i^2 \, s^2_{\bar{x}_i} + \Sigma w_i (\bar{x}_i - \bar{x}_{st})^2 / n' \qquad (22.5)$$

where w_i = weight of stratum i
$\bar{x}_i$ = mean value of the variable of interest in stratum i
$s_{\bar{x}_i}$ = standard deviation of $\bar{x}_i$

It should be mentioned that for sample case I12P12, the stratification is made on the basis of the image data from two occasions.

223. Class area transitions of the qualitative variables

In order to appraise the past activities of silviculture and to estimate the drain and growth of the forests, an analysis would be required of the trend and the amount of class areas of a qualitative variable during a period. In such a situation, a convenient way is to create a class (area) transition table or matrix.

A class (area) transition table which shows how sample plots move from a class to other classes can be easily constructed on the basis of two measurements of the permanent sample plots. For a single variable, the class transition table can be expressed as follows: where $n_{i,j}$ refers to the number of sample plots of class i on the first occasion and class j on the second occasion.

It is easy to see how the plots of a qualitative variable in classes change during a period, i.e. the direction and the amount of the change. For example, $n_{1,2}$ indicates that $n_{1,2}$ sample plots of a certain variable originally belonged to class 1, and that in one period it has moved to class 2. Since each sample plot can represent a certain amount of the forest area, the transition of the sample plots can be extrapolated to the whole forest area. Furthermore, $n_{i,j}$ can be replaced by the corresponding proportion of $n_{i,j}$ to the total

Table 2.1 Class transition table.

		Occasion 2			
		Class 1	Class 2 . . .	Class j . . .	Class m
Occasion 1	Class 1	$n_{1,1}$	$n_{1,2} \cdots$	$n_{1,j} \cdots$	$n_{1,m}$
	Class 2	$n_{2,2}$	$n_{2,2} \cdots$	$n_{2,j} \cdots$	$n_{2,m}$
	. . . . .				
	Class i	$n_{i,1}$	$n_{i,2} \cdots$	$n_{i,j} \cdots$	$n_{i,m}$
	. . . . .				
	Class m	$n_{m,1}$	$n_{m,2} \cdots$	$n_{m,j} \cdots$	$n_{m,m}$

number of permanent sample plots in class i on occasion 1, then the table becomes a probability transition matrix as in a Markov chain.

From Table 2.1 the probability transition matrix can be transformed accordingly,

$$P = \begin{bmatrix} p_{1,1} \; p_{2,2} \cdots p_{1,j} \cdots p_{1,m}, \\ p_{2,1} \; p_{2,2} \cdots p_{2,j} \cdots p_{2,m}, \\ \cdots\cdots \\ p_{i,1} \; p_{i,2} \cdots p_{i,j} \cdots p_{i,m}, \\ \cdots\cdots \\ p_{m,1} \; p_{m,2} \cdots p_{m,j} \cdots p_{m,m}, \end{bmatrix} \qquad (22.6)$$

where $p_{i,j} = n_{i,j}/n_i$, and
n_i = number of the sample plots of the i class on occasion 1

With the image data in the first phase, the probability transition matrix can be obtained by GLS or TPS. The application of GLS for estimating the transition probabilities is the same as for estimating the proportions of the qualitative variables mentioned in section 221 but it is now carried out in terms of classes on both occasions.

By using the TPS estimation, the weighted probability transition matrix of the population can be given by

$$P = \sum_{i=1}^{L} w_i P_i \qquad (22.7)$$

where P_i = probability transition matrix in stratum i
w_i = weight of stratum i
$= n_i'/n'$
n_i' = number of image sample points in stratum i
L = number of strata

The estimates of transition in quantities or probabilities, and their confidence limits or precisions can be obtained according to (22.3) and (22.5) in section 22.

The transition matrix can also be used for handling multitemporal image and field data.

23. Estimation methods for compartments

Two estimation methods: TPS estimation and regression estimation will be used for the compartments in the investigation.

For the compartmentwise estimation, TPS can be divided into two sub-methods, supervised and unsupervised methods. The unsupervised method is the basic method in the study.

If multitemporal image and field data are available, the working steps and associated statistical options when using the unsupervised method for the compartments in the study are as follows:

Working step	Statistical options
Data preprocessing including compartment delineation and digitization	
Data registration	
Filtering	Filtering for spatial and time series
Transformation	Principal component analysis (P.C) Canonical variable transformation (C.V) Vegetation index transformation (V.I)
Stratification including Pre-strafification	
Classification	Classifying: K-means clustering or equal interval classifying Classifier: minimum distance classifier (MD) or maximum likelihood classifier (ML)
Compartment-oriented estimation including calculation of estimates in strata	
Calculation of estimates in compartments	

Most working steps and the statistical options for the unsupervised method are also suitable for the supervised method.

For the regression estimation, the working steps and statistical techniques in the study are:

Data preprocessing including compartment delineation and digitization	
Data registration	
Transformation	Principal component analysis
Fitting regression models	
Application of the models to the compartments	

231. Filtering

Filtering is a conventional technique used in image data processing. The main objective of filtering is to remove the random error in the image data and to improve the estimation.

2311. Time filtering

Time filtering is filtering for time series. It is a technique for handling multitemporal image data.

Theoretically, for a stationary time series c_t, a linear time invariant filter is of the form (Harvey 1981, p. 70),

$$y_t = \sum_{j=t-v}^{t+u} w_j c_{t-j} \qquad (23.1)$$

where w_j = weight of c_{t-j} at time t-j.
u and v = positive integers or 0

In a continuous forest inventory, it is difficult to obtain a sufficiently large sample for a time series of a certain target variable because of the long remeasurement period. Thus, instead of using a time series acquired at a great number of time points, a sample consisting of a large amount of spatial sample plots obtained from two successive observations in time is often available in a continuous forest inventory. The weighted expression concerning a time filter such as (23.1) can be thought of as a weighted linear transforma-

tion or a kind of adaptive filtering (Niblack 1985) which is not time-invariant. For the case of two time points, the weighted transformation of image variables is of the form

$$y_2 = w_0 c_2 + w_1 c_1 \qquad (23.2)$$

and $w_0 + w_1 = 1$,

where c_1 and c_2 are the image variables on occasions 1 and 2 respectively, w_1 and w_0 are their weights. In order to estimate a certain field variable, a practical way to determine w_0 and w_1 is to maximize the correlation coefficient between y_2 and the field variable with respect to w_0 or w_1. Maximizing the correlation between y_2 and the field variable, i.e.

$$dr_{y_2,x}/dw_1 = 0$$

where $r_{y_2,x}$ = correlation coefficient between y_2 and x
x = a certain field variable

then, the w_0 and w_1 can be obtained as follows:

$$w_1 = a_2 / (a_1 + a_2) \qquad (23.3)$$
$$w_0 = a_1 / (a_1 + a_2) \qquad (23.4)$$
$$a_2 = r_{c_1,x} s_{c_2} - r_{c_2,x} r_{c_1,c_2} s_{c_2} \qquad (23.5)$$
$$a_1 = r_{c_2,x} s_{c_1} - r_{c_1,x} r_{c_1,c_2} s_{c_1} \qquad (23.6)$$

and the optimum correlation can be expressed in the following way:

$$r^2_{y_2,x} = (r^2_{c_1,x} + r^2_{c_2,x} - 2 r_{c_1,x} r_{c_2,x} r_{c_2,c_2}) / (1 - r^2_{c_1,c_2}) \qquad (23.7)$$

(23.7) can be rewritten as follows:

$$|r_{y_2,x}| = |r_{c_2,x}| [1 + (q_r - r_{c_1,c2})^2 / (1 - r^2_{c_1,c_2})]^{1/2} = |r_{c_2,x}| G_r \qquad (23.8)$$

where $q_r = r_{c_1,x}/r_{c_2,x}$

G_r is defined as the gain in the correlation because $|r_{y_2,x}| > |r_{c_2,x}|$ (or $|r_{c_1,x}|$) always holds. $|r_{c_2,x}|$ is here supposed to be greater than $|r_{c_1,x}|$, i.e. we can select the greater value of $r_{c_1,x}$ and $r_{c_2,x}$ as the denominator of q_r.

If x is the current state of a field variable, the weights w_1 and w_0 usually have positive signs. Then y_2 is a weighted average of the image variables on two occasions. The filter takes on "low path" characteristics. If x is the net increase, the signs of the weights are often opposite. Then, y_2 is a weighted difference between image variables on two occasions. The filter takes on "high path" characteristics (Niblack 1985, Showengerdt 1983).

2312. Spatial filtering

Spatial filtering is a filtering for spatial series. A linear and shift-invariant spatial filtering can be expressed in the following way (Showengerdt 1983, p. 16–22)

$$g(x,y) = \int\int f(x',y') h(x-x',y-y') dx' dy' \qquad (23.9)$$

where x and x′ = horizontal coordinates of spatial points
y and y′ = vertical coordinates of spatial points
g(x,y) = output of the linear system
f(x′,y′) = input of the linear system
h(x-x′,y-y′) = point spread function or weights of f(x′,y′)

It is obvious that the spatial filtering is also a weighted process.

In the discrete case, (23.9) for a finite range can be written as follows:

$$g(i,j) = \sum_{k=i-v}^{i+v} \sum_{l=j-u}^{j+u} f(j,l) h(i-k,j-l) \qquad (23.10)$$

For the one-dimension case,

$$g(i) = \sum_{k=i-v}^{i+v} f(k) h(i-k) \qquad (23.11)$$

(23.11) resembles (23.1).

Spatial filtering can be used to blur the image (smoothing filtering) or to enhance the edges (edge enhancement filtering) in order to produce different visual effects. On the other hand, there is another kind of filtering which is designed to maximize a certain goodness criterion rather than the visual effect. For instance, in a forest inventory image processing attempts to improve the correlation of the image variable with the field variable. It follows that spatial filtering in a forest inventory, as with time filtering mentioned above, should also attempt to maximize the correlation in question.

In spatial filtering, the adjacent pixels are naturally the most effective for correlation maximizing. A central pixel, in which an image point falls, and all its adjacent pixels can form a 3 × 3 pixel window. Then, the filtering of the pixel window could be taken into account.

Consider a spatial filter of two adjacent pixels. The filter can be expressed as (23.2) except that the subscripts refer to two adjacent pixels . Assumes $s_{c_1} = s_{c_2}$.

Then weights of the filter for maximizing the correlation can be simplified from (23.5) and (23.6) as follows:

$$a_2 = r_{c_1,x} - r_{c_2,x} r_{c_1,c_2} \qquad (23.12)$$

$$a_1 = r_{c_2,x} - r_{c_2,x} r_{c_1,c_2} \qquad (23.13)$$

The weights of the filtering window, which is a pixel window to be involved in filtering, can be simply obtained by summing all the two-pixel filters, each of which consists of the central pixel and one of its neighbours.

The spatial filter may also consist of a couple of the nearest image pixels around the image point. In this case, the filter becomes unidimensional, as in (23.11), although the nearest pixels might come from different directions.

232. Transformation

A transformation of satellite digital data, in principle, proceeds from two considerations: i) reducing or removing the influence of factors such as atmospheric scattering, topographic relief or sun elevation on the satellite imagery; ii) compressing the redundant data, which will result in inefficient analysis due to the high correlations between spectral bands. In accordance with whether information about the field variables is involvled or not, the transformation can be divided into the transformation with and without the ground observations. Typical transformations, suitable for both, are principal component analysis and canonical variable analysis. The latter deals with two sets of variables. In addition, the vegetation index transformations related to forest change will be also presented.

The transformation is made for the sample, following which the transformation coefficients, e.g. eigenvectors in the principal component analysis, will be used for the image plots in the compartments.

2321. Principal component transformation

The transformation of spectral values can be expressed in the following form (see Anderson 1984, p. 451)

$$Y = A^T C \qquad (23.14)$$

where Y is a vector of principal components, A is a matrix which is composed of eigenvectors, C is an original spectral vector. Let β be a eigenvector in A. β can be solved from the equation

$$|\Sigma_C - \lambda I| \beta = 0 \qquad (23.15)$$

Where λ is a Langrange multiplier and I is an identity matrix. Matrix A can be calculated from either a covariance matrix (non-standardized transformation) or a correlation matrix (standardized transformation). In most of cases, the choice between the two matrices depends on the ultimate application. As Singh and Harrison (1984) mentioned, "whether standardization is desirable is, in the ultimate analyses, to be decided on non-statistical grounds". For the forest inventory, the choice is often decided on the purposes of the inventory, the variance proportion distribution into principal components and correlations between the stand characteristics and principal components. Since the standardized transformation is able to remove temporally or spatially-varying gain (which is a multiplier to the spectral bands) and bias to a certain extent, the choice from the view point of normalizing the image data is in favour of the correlation matrix. In this study, the standardized transformation will be used in the main procedure, but the non-standardized transformation also will be dealt with for comparison.

2322. Canonical analysis

Canonical variable analysis (see Anderson 1984, p. 480) is also a linear transformation but deals with the correlation between two

sets of variables: the image variables and the field variables in the study. The motive for using canonical analyses is to maximize the correlation between the transformed image variable and the transformed field variable. For a single quantitative variable, for instance the volume, the correlation between the canonical variable and the quantitative variable is equivalent to the multiple correlation between the quantitative variable and all the spectral bands.

Subject to maximizing the correlation between two sets of transformed variables, the linear transformation can be written as follows:

$$Y_c = A^T C \tag{23.16}$$

$$Y_x = B^T X \tag{23.17}$$

where Y_c = vector of canonical variables for spectral bands.
Y_x = vector of canonical variables for stand characteristics
C = original vector of spectral bands
X = original vector of stand characteristics
A and B = coefficient matrices

Let α and β be vectors in A and B respectively, α and β can be solved from the following equation:

$$\begin{bmatrix} -\lambda\Sigma_C & \Sigma_{C,X} \\ \Sigma_{X,C} & -\lambda\Sigma_X \end{bmatrix} \begin{bmatrix} \alpha \\ \beta \end{bmatrix} = 0 \tag{23.18}$$

The canonical variables for both sets of variables are independent of each other and the corresponding correlation coefficients are ordered in a descending way.

2323. Vegetation index transformation

Using MSS Landsat data, Kauth and Thomas (1976) developed a linear transformation to produce four orthogonal indices. These indices are termed brightness (BR), greenness (GN), yellowness (YE) and nonsuch (NS). Later Wiegand and Richardson (1982) created a 2-dimensional orthogonal vegetation index (PVI) based on the same principle. The original purpose for developing this procedure was to extract an efficient component, which is concerned with the phytomass, on the basis of Landsat data. The most effective index is the green one which remains after the soil background and random errors have been removed. The index is therefore helpful in estimating the biomass and detecting change. In fact, the principle can be also used in TM data. By way of comparison, we will construct the first two indices, the soil index and the green index, based on the TM data available for the study area.

In order to separate BR and GN, the soil line should be selected. Image data for two points on the ground are needed, i.e. a wet point and a dry point (see Jackson 1983). Then a data point which represents the green index is required for forming the second vector orthogonal to the first. The Gram-Schmit algorithm employed can be found in Freiberger (1960) and Jackson (1983).

233. Stratification estimation

Stratification is often encountered in the statistical literature concerning sampling techniques. In fact, its use in the study is rather like classification. Considering that it is a part of the two-phase sampling, we call it the "stratification". Thus, the term in this study has a dual meaning.

Although some differences exist between stratification and classification, the terms are not separated in the subsequent sections unless stated otherwise.

In order to improve the stratification efficiency by using the image data, it is essential that the pre-stratification has to be made using additional information such as aerial photos, topography maps, ready-made forest type maps and any other material. As a result, only the forest area is included in the stratification. Also, in order to estimate growth the investigated area should be divided into cut and non-cut areas. This partition should be made for either the sample or the image points in compartments.

The classification is a decision-making process in which every image point will be assigned to a stratum to which the point is closest in light of predetermined statistical rules. Four steps are involved:

1. determining the stratification factors and the number of strata;
2. classifying or clustering;
3. creating the classifier for the image points in compartments and calculating the estimates for strata;
4. assigning a stratum code to each image point in the compartment.

The second and third steps are conducted for the sample only in the second phase.

The stratification can be categorized into the supervised and the unsupervised methods according to the stratification factor. The image variable is the stratification factor for the unsupervised method, and the estimated field variable for the supervised method.

2331. The unsupervised method

A. Classification

To make classification more efficient, the spectral values of imagery bands, as stratifying factors, would be transformed, for instance into principal components.

The number of the tranformed variables are determined by the variance proportion and the correlation concerned. For TM image data, the first three principal components are frequently selected as the stratifying factors because the remaining three are less important.

For the unsupervised method, it is difficult to precisely determine the number of strata. " There are no satisfactory methods for determining the number of clusters for any type of cluster analyses " (Everitt 1979, 1980). The main reason for the difficulty in determining the number of strata arises, perhaps, from the fact that the threshold of an efficient number of strata itself can not be exactly decided. Cochran (1977) discussed the number of strata in a stratification; under the assumptions that the regression of a estimated variable y of interest on a stratification factor is linear and every stratum has the equal number of sample units, the variance of the estimate of the mean value of y can be approximately expressed in the form

$$s_{\bar{y}}^2 \geq s_y^2 [r^2 / L^2 + (1 - r^2)] / n \tag{23.19}$$

where s_y^2 = sample variance of y without strafifying
n = number of sample plots
r = correlation coefficient between y and the strafifying factor
L = number of strata

The part of (23.19) in the brackets can be regarded as a ratio of the variances between stratification and non-stratification. Since r^2 / L^2 is much less than $(1 - r^2)$(when L is fairly large), the effect of the stratification is not sensitive to the number of strata. If the number of strata is over ten, there is no a sharp threshold for the number of strata. According to (23.19), Cochran concluded that the effect of the number of strata on the variance is little beyond L = 6, unless $r > .95$. Although (23.19) might be oversimplified in some cases, it reveals at least some property concerning the relationship between the number of strata and the correlation coefficient.

In practice, a useful approach for determining the number of strata, and which is concerned with all the stratifying factors and variables of interest, is to plot the number of strata against R^2, where R^2 is ratio of the sum of squares between strata divided by the total (corrected) sum of squares (SAS 1982). Usually, with an increase of strata, R^2 also increases. The number of strata at which R^2 tends to stabilize can then be selected.

In order to classify the sample into homogeneous strata in terms of the image variable, clustering is a common technique. k-means clustering (see section 2333) is rather popular in this aspect. An alternative is the equal interval classifying method. This classifies the image variables into a number of classes with an equal interval. Both of methods will be optionally used in this investigation.

Creating the classifier means creating a decision rule for assigning an image point to an appropriate stratum. A number of options could be selected for this purpose. These include the minimum distance method, the paralleleipiped method, the neighborhood method, the maximum likelihood estimation, the generalized linear models etc. (Hand 1981).

One of the simplest ways to determine the stratum code of an image point, called the minimum distance (MD) method, is to assign

the image point to the stratum to which the point is the nearest, according to the distance.

Statistically, the maximum likelihood (ML) classifier (see section 2333) is more efficient, compared to the MD classifier, if the statistical prerequisites are satisfied. Once the ML classifier is accepted and applied to the sample, a process called the ML iteration might be required because of the redistribution of the sample plots in the strata. The iteration will continue until no further change of the sample plots between strata.

These two classifiers will be optionally used in the study due to their simplicity and efficiency.

By using the selected classifier, the image points in the compartments are classified, i.e. the last step is completed.

It should be pointed out that the above discussion is only confined to a pure classification which partitions all image points into a number of strata and decides to which stratum an image point belongs. The estimation of stand characteristics has not so far been dealt with. This will be formulated in the next section since stand characteristics constitute a basis for the compartment estimation, and can therefore be viewed as a part of the estimation.

B. Compartment-oriented estimation

Compartment-oriented estimation means that the estimates of the stand characteristcs in strata are extended to compartments through the stratum codes of the image points within them. The method includes:

- calculating estimates for each stratum
- extending the estimates of each stratum to the compartments.

The main ideas of the compartmentwise estimation have been outlined by Poso et al. (1984). The method is now demonstrated with respect to two types of compartment characteristics.

The quantitative characteristics usually include age, diameter, height, volume, total growth, removal, mortality and so on. The qualitative characteristics in Finland involve the site class, stoniness, taxation class, development class, main species and so forth. For application, these two types of stand characteristics will be treated in different ways.

Statistically, a common way to describe a population or a sample is by mean values for the quantitative variables and by frequencies or proportions for the qualitative variables. The same method can be applied with respect to acquiring the estimates of stand characteristics for the strata.

Suppose that $\bar{x}_{i,j}$ refers to a mean value of the jth quantitative characteristic in stratum i, then the mean vector of p quantitative characteristics in stratum i can be given by

$$X_i = [\, \bar{x}_{i,1}, \bar{x}_{i,2}, \ldots, \bar{x}_{i,j}, \ldots, x_{i,p} \,] \qquad (23.20)$$

For the qualitative characteristics, a stratum may include more than one class. In this case, a frequency-distribution (F-D) matrix, instead of a vector, can be utilised to represent the stand characteristics for the stratum.

Assume that there are q qualitative standcharacteristics in the strata; the maximum number of classes in all the qualitative variables is m; the the F-D matrix for stratum i can be expressed in the following way:

$$F_i = \begin{bmatrix} f_{1,1} & f_{1,2} & \ldots & f_{1,k} & \ldots & f_{1,m} \\ f_{2,1} & f_{2,2} & \ldots & f_{2,k} & \ldots & f_{2,m} \\ \ldots & \ldots & & \ldots & & \ldots \\ f_{j,1} & f_{j,2} & \ldots & f_{j,k} & \ldots & f_{j,m} \\ \ldots & \ldots & & \ldots & & \ldots \\ f_{q,1} & f_{q,2} & \ldots & f_{q,k} & \ldots & f_{q,m} \end{bmatrix} \qquad (23.21)$$

where $f_{j,k} = n_{j,k} / n_i$ and $\sum_k f_{j,k} = 1$, $k = 1,2, \ldots, m$

n_1 = number of permanent plots in class for qualitative variable j

n_i = number of permanent plots in stratum i

q = number of the qualitative variables.

The mean vectors and F-D matrices are then available for the compartment-oriented estimation in the next step.

The estimates of charateristics in a compartment can be denoted in the same way as the estimates of the stand characteristics in the strata.

For the quantitative characteristics, a mean vector in the compartment can be achieved simply by averaging the mean vectors over all the image points in the compartment. The expression of a compartment mean vector is given by

$$X_c = \sum_i n'_i X_i / n'_c \quad i = 1,2, \ldots, n'_c \qquad (23.22)$$

where X_i = vector of mean values of quantitative variables in stratum i

n'_i = number of image points of stratum i in the compartment

n'_c = number of total image points in the compartment

For qualitative characteristics, the estimated result for a compartment is also a F-D matrix as (23.21). The operation can be written as follows:

$$F_c = \sum_i n'_i F_i / n'_c \quad i = 1, 2, \ldots n'_c \qquad (23.23)$$

where F_i refers to the F-D matrix of stratum i.

Based on the F-D matrix, we can readily make a decision for all the qualitative characteristics in a compartment. Of course, we may select the dominant class as a representative of the nominal characteristic in the compartment and calculate the mean class code for the ordinal variables or just let the F-D matrix stand for all the qualitative characteristics in the compartment.

2332. The supervised method

If the sample units in the second phase are viewed as the training areas and the field variables are used as the stratification factors, the stratification is implemented in the so-called supervised way.

Although the supervised method can also cover the four steps mentioned in the unsupervised method, the first two steps are quite simple because the strata can be decided directly, especially for the qualitative variable. For the quantitative target variable, the strata can be obtained by equal interval classifying.

The most important step in the supervised method is to determine the classifier. In many cases, the ML classifier would be acceptable. It is effective for both the qualitative and the quantitative target variables if the required conditions are satisfied. The MD classifier can be also used for the quantitative variables.

The mean vector for the strata is still needed for the supervised method because the quantitative variables have to be classified by equal intervals. The F-D matrix for the qualitative variable is generally not necessary for the strata , but it is required for the compartments. This is because by using the ML classifier for every image point in the compartments what we actually obtain is the probability distribution of an image point rather than an exactly determined class.

2333. Statistical techniques in the stratification

A. K-means clustering

The algorithm (see MacQueen 1967, Hartigen 1975) begins by selecting k starting points which can be used as the centers of the k clusters. Then every image point is assigned to the nearest cluster in terms of the distance from the point to the center of the cluster. After all image points have been so treated, means of the k new clusters are recalculated and used as the coordinates of the new centers of the k clusters. Based on the new centers every image point is reassigned. The process is repeated until the image points involved in each cluster have no longer relocated. The distance used is Euclidean.

B. Maximum likelihood classification and the Bayes rule

The matter has been dealed e.g. by Tou and Gonzalez (1974), Schowengerdt (1983), or Swan and Davis(1978). Let X be a n-dimensional spectral vector, p(i) be the a priori probability that X comes from stratum or category i, and let $p(X \mid i)$ be a conditional probability density function of stratum or category i , then the likelihood ratio is of the form

$$l(X) = p(X|i)/p(X|j) \qquad (23.24)$$

where $p(X \mid j)$ is a conditional probability density function of stratum or category j.

For an image point with spectral vector X, the decision rule for assigning the point to one of two strata or categories (i and j) is defined as follows:

if $l(X) > T(X)$ then the image point belongs to stratum or category i, otherwise stratum or category j, where T(X) is a threshold value expressed as

$$T(X) = p(j)/p(i) \qquad (23.25)$$

The above decision rule also can be expressed by discriminant functions. From (23.24) and (23.25) the discriminant functions can be derived as follows:

$$d_i(X) = p(X \mid i)p(i)$$

$$d_j(X) = p(X \mid j)p(j)$$

and the Bayes decision rule can be rewitten in the following way:

if $d_i(X) > d_j(X)$, then the image point ε i

if $d_i(X) < d_j(X)$, then the image point ε j

More often, $d_i(X)$ and $d_j(X)$ take the natural logarithm form, i.e.

$$d_i(X) = \ln[p(X \mid i)p(i)]$$

and

$$d_j(X) = \ln[p(X \mid j)p(j)]$$

Assume that the image variables in stratum or category i obey a multivariate normal distribution with mean vector μ_i and covariance matrix Σ_i, then the probability density function is of the form

$$p(X \mid i) = 1/(2\pi \mid \Sigma_i \mid)\exp[-(1/2)(X-\mu_i)^T\Sigma_i(X-\mu_i)]$$

in turn,

$$d_i(X) = \ln[p(i)] - \ln(2\pi)/2 - (X-\mu_i)^T\Sigma_i(X-\mu_i)/2 - \ln(\mid\Sigma_i\mid)/2 \qquad (23.26)$$

If there are m categories for a target variable, then the probability (posterior probability) belonging to category k for an image point can be expressed as follows:

$$p(k \mid X) = \exp[d_k(X)]/\sum_i \exp[d_i(X)] \quad i = 1, 2, \ldots, m \qquad (23.27)$$

When the a priori probabilities are unknown, a common way to determine the a priori probability is initially to assume that they are equal to each other or they are proportional to class (or category) sizes. For the multitemporal cases, the posterior probability of an image point on the previous occasion and the transition probability can be used for estimating the a prior probability on the present occasion (see section 24).

234. Regression estimation

2341. Conventional regression models for the quantitative variables

Regression models will be used in the study for the purpose of comparison. Two models will be adopted for estimating the volume and the net increase. For the volume, the model is of the form

$$V = \exp[(a_0 + a_1 \ln(b_1 + p_{c1}) + a_2 \ln(b_2 + p_{c3})] \qquad (23.28)$$

where p_{c1} = first principal component
p_{c3} = third principal component and

a_0, a_1, a_2, b_1 and b_2 are the parameters to be estimated. For the net increase, the model is of the form

$$D_v = a_0 + \exp(b_0 + b_1 p_{c1} + b_2 p_{c2}) \qquad (23.29)$$

where p_{c2} = second principal component and

a_0, b_0, b_1 and b_2 are the parameters to be estimated. It should be pointed out that the principal components used in the models are obtained on the basis of the tranformation of the bitemporal image data.

2342. Log-linear and logistic regression models for the qualitative variables

The log-linear or the logistic regression model is applicable to the qualitative variables, and especially to the nominal variables.

For the multinomial variables, the response of a sample plot to a multinomial variable is one of the possible categories of this variable. If the sample is partitioned into a number of cells (see SAS 1985) through classifying in terms of image variables, the estimate of the category probabilities of a multinomial variable for a cell can be denoted by the proportion of the counts of the category to the total counts in the cell.

Suppose that for a certain qualitative variable, the sample is classified into L cells; for each cell, there are m possible categories. Then the log-linear model can be expressed in the following way

$$Y_i = X_i\beta + \varepsilon_i \quad i = 1,2, \ldots, L \qquad (23.30)$$

where $Y_i = [f_{i,1}, f_{i,2}, \ldots, f_{i,j}, \ldots, f_{i,m-1}]^T$
$f_{i,j} = \ln(p_{i,j}/p_{i,m})$
$p_{i,j} = n_{i,j}/n_i$
$p_{i,m} = n_{i,m}/n_i$
n_i = number of sample plots in cell i
$n_{i,j}$ = number of sample plots of category j in cell i
$n_{i,m}$ = number of sample plots of category m in cell i
β = parameter vector
X_i = independent variable (image variables) matrix
ε_i = error vector of the model

β can be solved by the weighted least squares method (McCullagh and Nelder 1983, SAS 1985).

The drawback of the log-linear model is that the sample has to be classified into cells. Where some cells probably remain containing only a few observations, which would cause the zero proportion for many categories, then they have to be given a small value in order to derive a solution. This may produce a biased estimation. An alternative choice for avoiding such a situation is to select the logistic regression model instead of the log-linear model.

A logistic model can be expressed in the following way:

$$P_i = Q_i + \varepsilon_i \qquad (23.31)$$

where $P_i = [p_{i,j}, p_{i,j}, \ldots p_{i,m-1}]^T$
$Q_i = [q_{i,1}, q_{i,2}, \ldots, q_{i,m-1}]^T$
$q_{i,j} = \exp(x_j\beta)/[(1 + \sum_j \exp(x_j\beta)]$
$i = 1, 2, \ldots, L \quad j = 1, 2, \ldots, m\text{-}1$
x_j = the jth row vector in X_i in (23.30)
β = parameter vector
ε_i = error vector of the model

β in (23.33) can be solved by means of the maximum-liklihood method (Cox 1970, McCullagh and Nelder 1983, SAS 1985, Press and Wilson 1978).

24. Updating by using multitempotal image and field data

241. Multitemporal data handling

Updating here is concerned with handling the multitemporal image and field data in order to obtain accurate results for the new inventory.

The multitemporal data can be handled in several ways:

- separately by occasions
- by stacking
- recursively.

The first way is inefficient for both the current state and the forest change. This is because the multitemporal image data become the separate unitemporal data and the permanent plots are used in the same way as the temporary plots.

Stacking multitemporal data is a common way for data updating because it covers all the available information. In addition, the estimation of both the current state and change can be conducted simultaneously. The estimation methods presented in the previous sections are based on stacked image data. A transformation for stacked multitemporal image data could be implemented as follows:

(1) the transformation is run once by using all or a part of bands on all occasions
(2) the transformation is made separately by occasions
(3) the transformation is based on time filtered image data.

Data recursion is a further treatment of results obtained by using the multitemporal data separately. In this case, the estimates obtained on one occasion can be used for modifying the estimates on another occasion.

242. Updating methods

Updating methods are methods for handling multitemporal image and field data by means of the estimation methods.

Four updating methods will be discussed in this study, of which stacking multitemporal data and time filtering have been presented already. The remaining two are:

- ML cascade
- estimate-modifying.

Both of these methods are recursive.

A maximum likelihood cascade, called as ML-PTM-ML model in this study, was developed by Swain (1978). PTM is an abbreviation of Probability Transition Matrix. The model re-determines the probability distribution of the image points in the compartments with the help of a priori distribution derived from a probability transition matrix and the probability distribution on the previous occasion.

Similarly, another maximum likelihood cascade, called the ML-ML model in the study, is the special case of the ML-PTM-ML. In this model the probability distribution of the image points obtained by using the ML classifier on the previous occasion can be used as the a priori probabilities for the ML classifier on the present occasion without the PTM. This model can be used in the case where there is no big change during the interval.

The framework of the two methods is illustrated in Figures 2.1 and 2.2 where the frames with the dash lines refer to the operation.

For the ML-PTM-ML model, the a priori probability of an image point can be derived as follows

$$p_j = \sum_i p_i\, p_{i,j} \quad i = 1, 2, \ldots, m_2 \qquad (24.1)$$

where p_j = a priori probability of an image point which falls in category or stratum j on the present occasion

p_i = probability of the image point in category i or stratum on the previous occasion

$p_{i,j}$ = transition probability from category i on the previous occasion to category j on the present occasion

m_2 = number of categories or strata on the present occasion

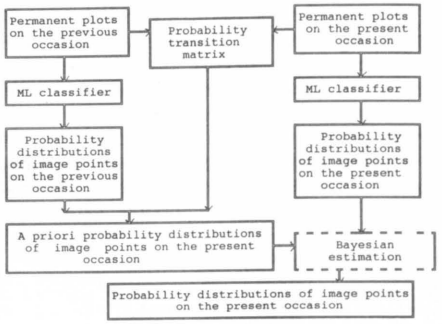

Figure 2.1. Maximum likelihood cascade (ML-PTM-ML model).

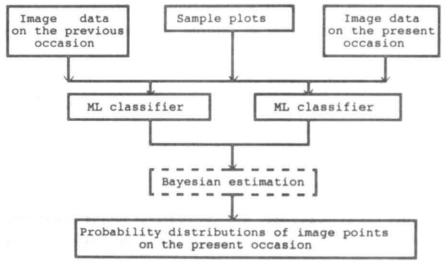

Figure 2.2. Maximum likelihood cascade (ML-ML model).

The probability transition matrix can be easily constructed following the same method mentioned in section 223. The maximum likelihood classification and the Bayesian rule were already presented in section 23. Although the ML cascade was originally designed for the supervised method, both ML-PTM-ML and ML-ML models can be adapted for updating data on the basis of the permanent sample plots. However, it should be noted that for the supervised and unsupervised methods, the construction of the transition probability matrix is different. The former is based on the field variables while the latter is based on the image variables. In addition, the ML-ML model can be also used for updating data based on temporary sample plots measured on two occasions or on a single occasion but with multitemporal image data.

Estimate-modifying in the study means updating data by weighting two estimates: one is based on the stratification by using the newly obtained image data; another is based on the statification by using the old image data. The weights are equal to the reciprocals of the variances of the estimates.The method is time-consuming. In addition, it should be implemented separately for both the cut and non-cut areas.

243. Updating data for different sample cases

Basic sample cases for two occasions are as follows (cf, sestion 212):

- I12P12
- I1P12
- I12P1

The updating methods described above are mostly for sample case I12P12, but they can be applied to the other two cases. Some updating features for the last two cases are now presented.

Case I1P12

When the image data , together with the permanent sample plots are involved from the previous forest inventory, and only the permanent sample plots have been remeasured in the present forest inventory without new image data, the data updating is relatively simple. The area is divided into non-cut and cut areas and the strata previously obtained are adjusted, new compartmentwise estimation is made by using the newly remeasured results from permanent plots. If the supervised method is used in the stratification, updating data by using only the new measurements of the permanent sample plots can be carried out through the probability transition matrix.

Case I12P1

Without random bias and gain (see section 2321), updating by only using the new image data is also straightforward. The updating can be completed simply by using the new image data and the old models which were created on the basis of the image data and the measurements from the previous occasion.

However, beyond the forest change, the image data acquired at different time points often possesses random biases and gains generated by seasons, atmosphere, sun elevation etc. over time. In this case, the image data should be normalized by means of special techniques such as the multispectral ratio, the vegetation index transformation and the standardized principal component transformation. Among these techniques, the standardized principal component transformation can remove both the biases and the gains.

In practice, none of these normalized techniques could effectively remove the random biases and gain but still maintain the forest change for the normalized image data. More often, beside the random errors these techniques may also remove a certain amount of image change information generated from the forest change. In order to remove the random bias and gain but maintain the image changes caused by the forest changes, the normalization of the image data may still require ground plots.

25. A framework of the main procedure in the study

The generalized least squares (GLS) estimation for the population and the unsupervised stratification for the compartments by using the stacked bitemporal image and field data (sample case I12P12) constitute the main procedure in the study. A framework for the main procedure is illustrated in Figures 2.3 and 2.4.

The frames formed with dash lines in Figures 2.3 and 2.4 denotes data acquiring or processing, whereas the frames formed with solid lines refer to results following the previous processing.

The left part of Figure 2.3 illustrates the connection of the procedure for the population when using GLS, while the middle and right parts illustrate the connections of the

procedure for the compartments when using the unsupervised stratification.

Figure 2.4 demonstrates the connection of the statistical options in the stratification step shown in Figure 2.3.

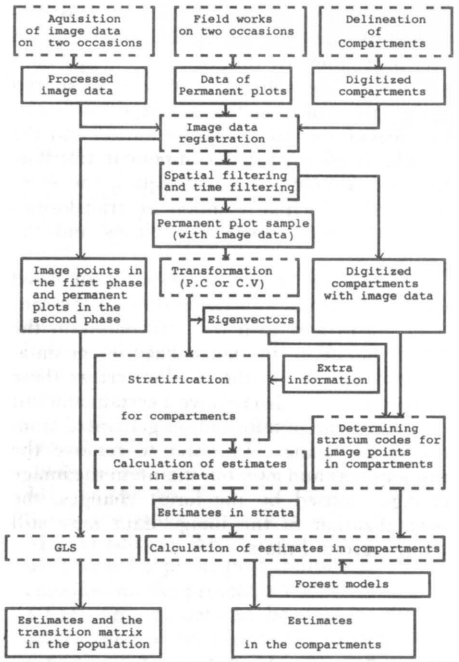

Figure 2.3. The estimating framework for the population and compartments.

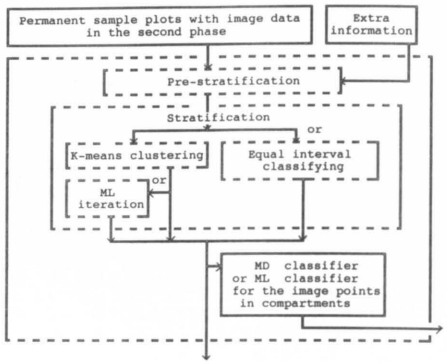

Figure 2.4. Stratification for the compartments.

3. DESCRIPTION OF THE MATERIAL

31. The study area

The study area is located in Hyytiälä, the forest experiment station of Helsinki University, situated about 210 kilometers north of Helsinki in Finland (Figure 3.1). This area and the data described later in the paper have been already outlined in the previous studies (Poso et al. 1987; Peng 1987). Its geographic position is 61°50′ N and 24°18′ E. With low hills, the terrain slopes gently. The highest altitude is 190 m but most of the area is situated between 140 and 160 m above the sea level. The total area amounts to 198.2 hectares, which consists of 194.3 hectares forest land, 3.3 hectares water area and .6 hectares other non-forest land.

The forest land is dominated by Norway spruce and Scots pine mixed with a small amount of birch and other species. The average height, the D.B.H and the volume in the forest area are 16.2 m, 19.8 cm and 176 m^3 respectively. The frequencies for some stand characteristics are based on 1472 field plots and are presented in Table 3.1.

The explanations on the codes of Table 3.1 are given in section 33.

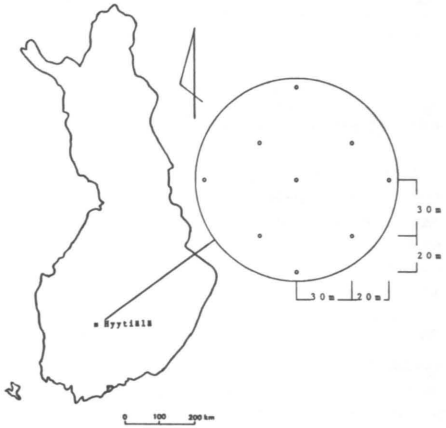

Figure 3.1. The location of the study area and a scheme of the layout of the sample plots.

32. Sample plots on the ground

Relascope plots with a basal area factor of 2 were applied in 1983−84. The total number of plots measured was 1472 from which 1401 sample points fell on forest land. The distances between two points are 50 m latitudinally and some 25 m longitudinally (See Figure 3.1). These sample plots, with the associated image information, will be employed in as follows:

1. 1472 sample points will later serve as an set of input data for simulating the ground observation and spectral values for the coming periods.
2. The 1401 sample plots on forest land will be used as a test sample for checking the estimated results.
3. The permanent plot sample consists of 387 field plots which are drawn from the test sample. The initial measurements of the sample plots are used as the measurements of the permanent sample plots on the first occasion. The remeasurements of all the sample plots for the coming occasions will be simulated (see section 35).

33. Stand characteristics of the sample plots in the study area

The stand characteristics for the sample plots were defined acccording to Kuusela and Salminen (1969). These studied more thoroughly here are as follows: (the number refers to the code of a class)

Land classes

1. Forest land.
2. Poorly productive land.

Table 3.1 Distributions of the stand characteristics.

Main species

	Pine	Spruce	Birch	Other species
%	44.2	49.3	5.4	1.1

Age classes (year)

	0–19	20–39	40–59	60–79	80–99	100–119	120–139	> 139
%	14.9	12.7	6.4	15.3	28.2	12.3	8.9	1.3

Volume classes (m^3 /ha)

	0–39	40–79	80–119	120–159	160–199	200–239	240–319	> 319
%	18.6	8.9	7.3	10.2	13.0	12.0	16.7	13.3

Development classes (code)

	1	2	3	4	5	6	7	8
%	16.1	13.9	33.0	33.8	0.4	0.2	1.9	0.7

Soil classes (code)

	1	2	3
%	82.1	6.1	11.8

Site classes (code)

	1	2	3	4	5
%	0.1	14.9	57.8	16.4	10.8

Stoniness (code)

	1	2	3	4	5	6	7	8
%	56.8	18.3	1.6	4.5	0.7	0.2	8.4	9.5

Taxation classes (code)

	1	2	3	4	5
%	10.0	43.2	28.8	14.2	3.8

3. Waste land.
4. Agricultural land.
5. Building site.
6. Roads.
7. store area.
8. Others.
9. Water.

Soil classes
1. Mineral site.
2. Spruce swamp.
3. Pine swamp.
4. Open swamp.

Site classes
1. Very rich site with the main type OMaT (*Oxalis Maianthemum*).
2. Rich site with the main type OMT (*Oxalis Myrtillus*).
3. Damp site with the main type MT (*Myrtillus*).
4. Sub-dry site with the main type VT (*Vaccinium*).
5. Dry site with the main type CT (*Calluna*).

Stoneness
1. Less stony.
2. Stony.
3. More stony.
4. Swampy.
5. Natural peatland.
6. Drained peatland.
7. Others.
8. Heathy peatland.

Taxation classes
1. IA including OMaT, OMT and etc.
2. IB including MT and etc.
3. II including VT and etc.
4. III including CT and etc.
5. IV including the productive pine swamp.

Development classes
1. Seedling.
2. Young stands at thinning stage.
3. Middle aged stands.
4. Regeneration maturity stands.
5. Shelter wood stands
6. Under-productive stands: poorly forested.
7. Under-productive stands: unsuitable species, too old or defective.
8. Open area.

Main species
0. no trees
1. Pine.
2. Spruce.
3. Birch (*Betula verrucosa*).
4. Birch (*Betula pubescens*).
5. Aspen.
6. Alder.
7. Other broad leaved species.
8. Other conifers.

Age (year).
Basal area in m^2 /ha.
Average height in m.
Average D.B.H in cm.
Volume in m^3 /ha.
Composition (10 %): pine, spruce, and broad leaved species.

Beside the stand characteristics listed above, there are others, such as type of thinning, forest improvement measures etc., which were used as stand characteristics in the field work but were not used in the study.

34. Satellite image data for the study area

The Landsat-5 TM image data used in the study were acquired in September of 1984 and in June of 1985. That means that for the study there are two sets of digital image data in the same area but acquired at different occasions with an interval of nine months. The two sets of image data acquired in 1984 and 1985 are called ID-84 and ID-85 respectively.

The prominent features of the TM image data are the reduced pixel size (30 m × 30 m for bands 1–5 and band 7), more spectral bands and the wider range of the grey levels (256 for the maximum value), in comparison with the Multispectral Scanner (MSS). Except the thematic band 6, the other 6 spectral bands which consist of three visible bands and three infrared bands are arranged from the blue band to the near infrared band. The wavelengths of the TM spectral bands are given in Table 3.2.

The histograms of the two sets of image data are shown in Figures 3.2(a)–(b).

The spectal values of the ID-84 and ID-85 indicate large differences. The numeric values of ID-85 are much higher than those of ID-84.

The histograms also show that with respect to magnitude and range of variation, bands 4 and 5 are superior to other bands.

The correlation coefficients of ID-84 and ID-85 are shown in Table 3.3. For the qual-

Table 3.2. Wavelengths of TM bands.

Band	1	2	3	4	5	7
Wavelength (μ m)	.45–.52	.52–.60	.63–.69	.76–.90	1.55–1.75	2.08–2.35

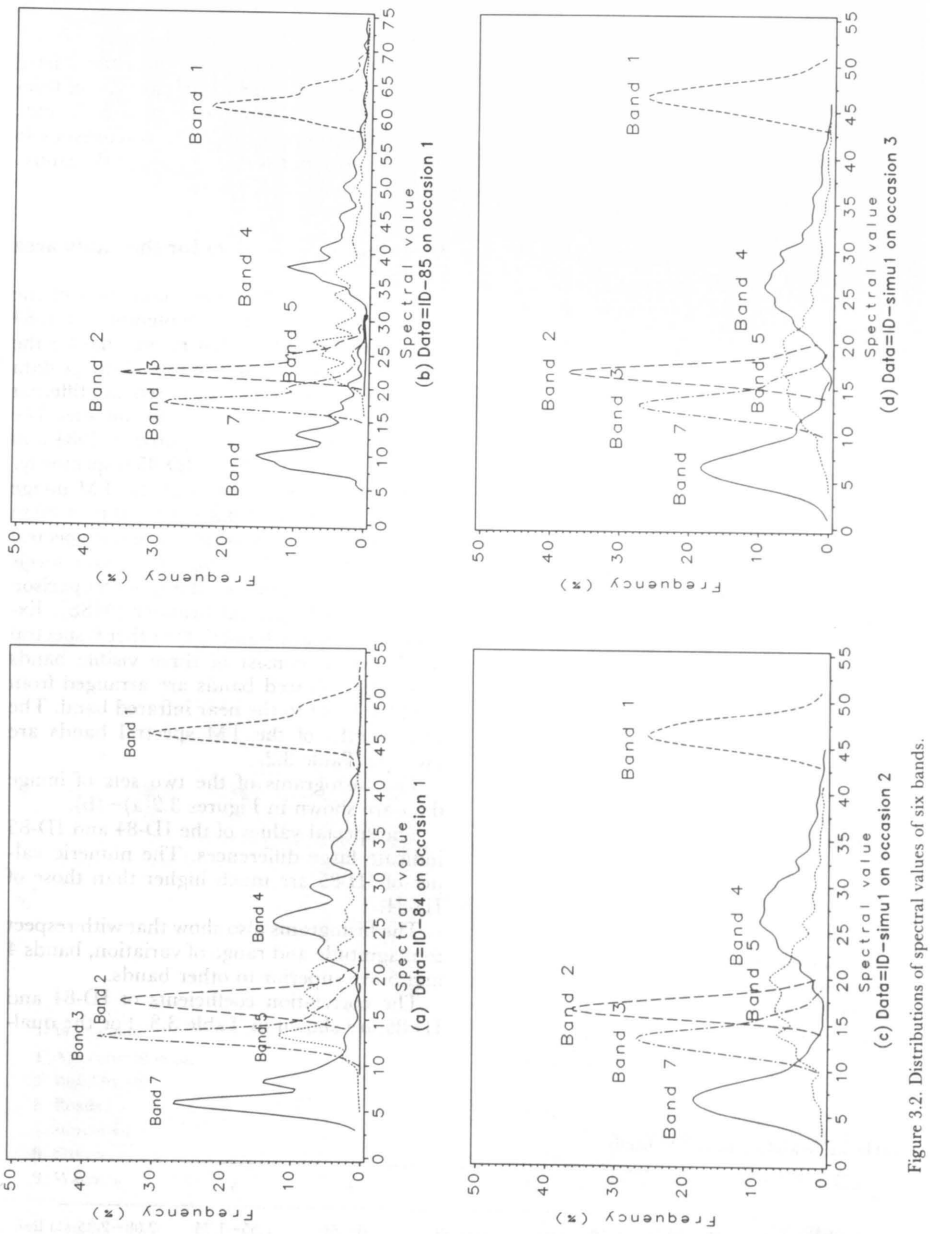

Figure 3.2. Distributions of spectral values of six bands.

Table 3.3. Correlation coefficients between stand characteristics and spectral values of six bands.

	Band 1	Band 2	Band 3	Band 4	Band 5	Band 7
			Data = ID-84			
Soil class	0.074	0.130	0.131	0.021	0.142	0.136
Site class	0.235	0.293	0.289	0.126	0.277	0.285
Stoniness	0.109	0.112	0.102	0.090	0.107	0.086
Tax. class	0.159	0.224	0.201	0.082	0.194	0.206
Main species	0.333	0.442	0.470	0.344	0.482	0.470
Dev. class	0.422	0.530	0.556	0.605	0.582	0.531
Age	−0.427	−0.557	−0.554	−0.665	−0.590	−0.522
D.B.H	−0.443	−0.566	−0.578	−0.638	−0.606	−0.556
Height	−0.487	−0.611	−0.621	−0.673	−0.661	−0.608
B.A	−0.453	−0.532	−0.557	−0.578	−0.592	−0.556
Volume	−0.436	−0.558	−0.551	−0.609	−0.587	−0.537
Composition:						
Pine	0.245	0.321	0.333	0.158	0.332	0.345
Spruce	−0.315	−0.436	−0.445	−0.325	−0.485	−0.468
B.L	0.086	0.154	0.152	0.267	0.205	0.149
			Data = ID-85			
Soil class	0.135	0.106	0.166	0.095	0.201	0.216
Site class	0.334	0.261	0.414	0.121	0.374	0.445
Stoniness	0.132	0.125	0.130	0.125	0.139	0.151
Tax. class	0.222	0.169	0.288	0.129	0.264	0.324
Main species	0.410	0.399	0.460	0.496	0.567	0.553
Dev. class	0.547	0.663	0.602	0.570	0.576	0.546
Age	−0.514	−0.626	−0.531	−0.619	−0.558	−0.498
D.B.H	−0.537	−0.644	−0.578	−0.559	−0.579	−0.537
Height	−0.591	−0.700	−0.640	−0.591	−0.642	−0.604
B.A	−0.540	−0.644	−0.595	−0.532	−0.598	−0.572
Volume	−0.525	−0.627	−0.569	−0.545	−0.597	−0.557
Composition:						
Pine	0.342	0.277	0.411	0.023	0.418	0.469
Spruce	−0.401	−0.377	−0.446	−0.308	−0.563	−0.556
B.L	0.037	0.094	−0.019	0.467	0.178	0.070
			Data = ID-simu1			
Soil class	0.092	0.091	0.083	0.054	0.083	0.102
Site class	0.201	0.256	0.250	0.052	0.223	0.254
Stoniness	0.095	0.076	0.097	0.097	0.098	0.102
Tax. class	0.134	0.205	0.170	0.043	0.149	0.174
Main species	0.306	0.387	0.388	0.307	0.403	0.409
Dev. class	0.478	0.570	0.610	0.629	0.615	0.616
Age	−0.461	−0.565	−0.590	−0.628	−0.616	−0.581
Height	−0.532	−0.640	−0.680	−0.672	−0.705	−0.673
D.B.H	−0.509	−0.616	−0.658	−0.649	−0.675	−0.644
B.A	−0.485	−0.526	−0.565	−0.579	−0.594	−0.565
Volume	−0.510	−0.579	−0.605	−0.605	−0.630	−0.602
Composition:						
Pine	0.114	0.148	0.134	−0.039	0.109	0.134
Spruce	−0.312	−0.395	−0.388	−0.273	−0.397	−0.402
B.L	0.024	0.049	0.027	0.104	0.052	0.038

Note that Dev. class = Development class, B.L = Broad Leaved species, B.A = Basal Area and Tax. class = Taxation class.

itative variables such as soil class, site class, main species, taxation class, development class and so on, the correlation coefficient between a spectral band and a qualtitative variable was calculated as follows:

$$r = \sum_{i=1}^{m} \sum_{j=1}^{n'_i} (c_{i,j} - \bar{c})(\bar{c}_i - \bar{c}\,)/$$
$$\{ [\sum_{i=1}^{m} \sum_{j=1}^{n'_i} (c_{i,j} - \bar{c})^2][\sum_{i=1}^{m} \sum_{j=1}^{n'_i} (\bar{c}_i - \bar{c})^2]\}^{1/2} \qquad (3.1)$$

where r = correlation coefficient between a spectral band and a qualitative variable

$c_{i,j}$ = spectral value of the jth image point in class i of the qualitative variable

$\bar{c}_i$ = mean value of the spectral band of image points in class i

$\bar{c}$ = mean value of the spectral band of all image points

m = number of classes of the qualitative variable

n'_i = number of image points in class i for the qualitative variable

This resembles the correlations between the scores and the dependent variable in a regression model containing the dummy variables. Similarly, the correlations of these qualitative variables appear as positive values.

From Table 3.3, it can be seen that the correlations between variables concerned with the biomass like the volume, basal area, height, D.B.H, age and development class, are similar. For the data in the fall these variables are more related to the near infrared bands (band 4 and band 5) than the visible bands (e.g. band 3 and band 2). For the image data in the summer, however, they are more correlated with band 2, then bands 3, 5 and 4.

On the other hand, the variables concerned with water and the colour such as main species, tree species composition, soil class, site class and taxation class, are always more correlated with the near infrared bands (band 5 and 7), especially for the data in the fall. This is because the reflectance and the absorbed range of both the vegetation and the soil are placed in the infrared bands (see Curran 1985).

The correlations between a spectral band and the different classes in regard to each qualitative variable are not the same. Figure 3.3 displays the correlations between the different categories (classes) of the major qualitative variables and data ID-84. These correlations are computed by means of the binary variables 1 and 0. It follows that if the spectral values of a certain class is lower than the rest, the class indicates a negative correlation and vice versa. For instance, with the lower spectral values, spruce as the main species and development class 4 display negative correlations.

One may find that the correlations of band 4 with most classes of the main species, soil class, taxation class and site class are lowest, but it is high with many of the development classes.

The correlations between the differences of the spectral values on the first two occasions and the net increase of the field variables are shown in Table 3.4. The image data on the first occasion comes from ID-84 and the spectral values on the second occasion come from the simulated image data : ID-simul (see section 35). Although the correlations are quite low, the relationship of the correlation with the spectral bands remains similar to those of image data ID-84 in Table 3.3.

35. Simulation

The true field data available for the study is based on a single measurement. The available image data are bitemporal although, the interval is only nine months and corresponds to only a unitemporal field data. Consequently, for the purposes of the study the multitemporal image and field data for the coming occasions had to be simulated for the purposes of the study.

351. Simulation of the ground variables

The simulation of the forest characteristics for sample plots was manipulated by means of a special programme called MELA created by the Finnish Forest Research Institute. The programme was originally aimed at long term forestry planning (Siitonen 1983, Kilkki 1985), and it consists of two stages: the simulation of the possible management schedules (production model) and the decision stage.

In the first stage, in which a compartment is used as a calculation unit, the simulation principally includes a natural growth process (ingrowth, growth and mortality) and man-made measures such as thinning, clear cutting and other silvicultural treatments.

In the second stage, linear programming was applied to determining an optimal production. According to the requirement of the present study, the second stage was im-

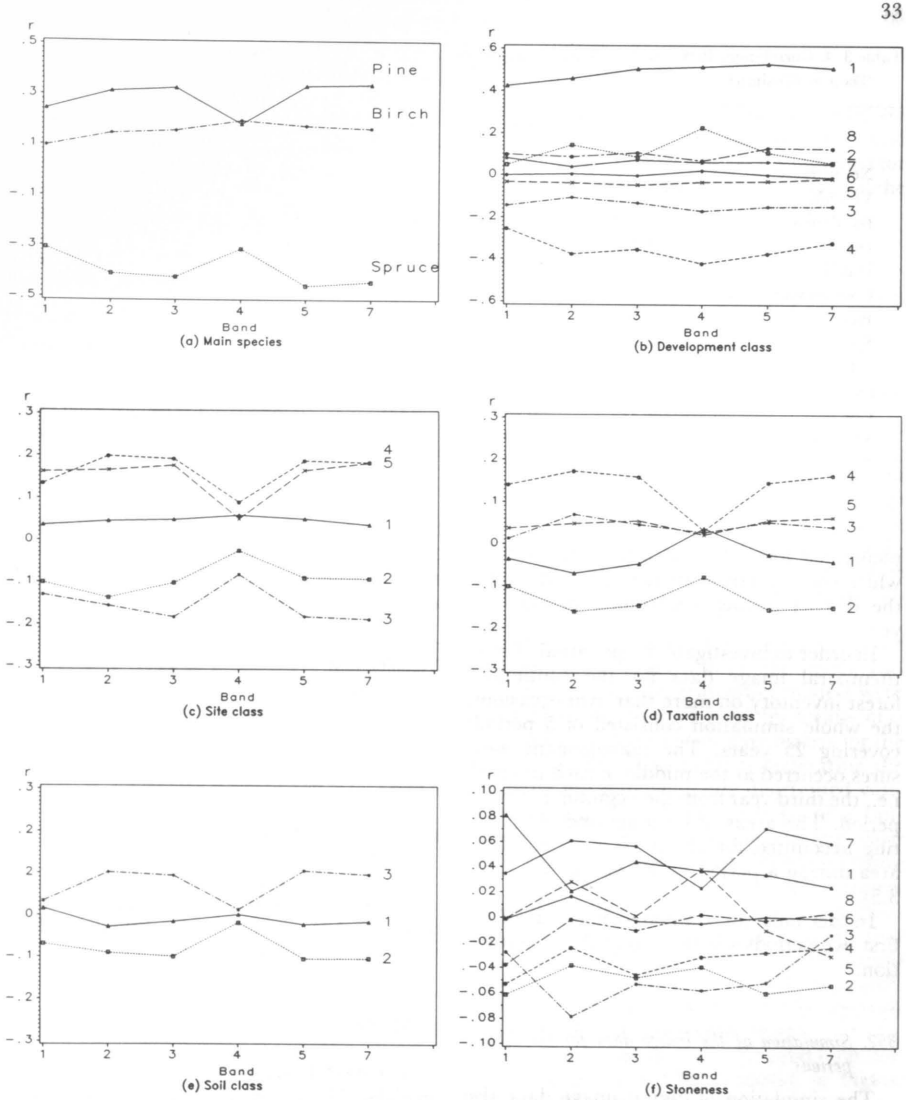

Figure 3.3. Correlation coefficients between variable classes and spectral bands.

Table 3. 4. Correlations between the differences of the spectral values on the first two occasions and the net increase (Data = ID-simu1)

	Band 1	Band 2	Band 3	Band 4	Band 5	Band 7
Net increase						
Volume	−0.110	−0.157	−0.168	−0.187	−0.148	−0.134
Basal area	−0.148	−0.190	−0.212	−0.230	−0.200	−0.184
Height	−0.129	−0.145	−0.183	−0.241	−0.231	−0.196
D.B.H	−0.121	−0.123	−0.168	−0.184	−0.203	−0.196
Composition:						
Pine	−0.083	−0.121	−0.154	−0.145	−0.163	−0.149
Spruce	0.001	0.017	0.004	−0.039	−0.035	−0.024
B.L	−0.052	−0.124	−0.105	−0.128	−0.095	−0.099
Drain:						
Cut	0.115	0.155	0.171	0.167	0.156	0.150
Mortality	0.012	−0.009	0.020	−0.035	0.003	0.032

plemented for achieving a fixed net income which corresponds to an average yield level in the district during a planning period of 5 years.

In order to investigate the potential of multitemporal image data for the continuous forest inventory on more than two occasions, the whole simulation consisted of 5 periods covering 25 years. The management measures occurred at the middle of each interval, i.e., the third year from the beginning of every period. The areas of thinning and clear cutting accounted for about 10 % of the total area during a period of five years (see Table 3.5).

In fact only the simulated material of the first two periods will be used in this investigation.

Table 3. 5. Cutting areas in the first two periods.

	Periods 1	2
Thinning (ha)	22.97	4.05
Clear cutting (ha)	–	9.54

352. Simulation of the image data for the coming periods

The simulation of digital image data also consisted of two steps: (1) model fitting, and (2) randomization.

A prediction model for digital data at each period was based on the test sample which contains both the field variables and the spectral values (image data ID-84). The independent variables involved in the multivariate regression model deal with most stand characteristics including the soil class, site class, stoneness, taxation class, main species, age, basal area, height, D.B.H, volume and species composition.

In order to investigate the potential efficiency of the different image data, two regression models, which were fitted by least squares, were chosen for the simulation.

Model 1

The model consisted of two regression submodels. First, the predicted image values were generated from these two sub-models. Then they were weighted. The reason for using two additive models was to yield image data such that the correlations of all the stand characteristics with spectral values are close to the original ones.

The independent variables in the first submodel include the site class, the taxation class, basal area and D.B.H.The model is of the form:

$$c_i = a_0 + \sum_{j=1}^{m1} \delta_{1,j}\, a_{1,j} + \sum_{j=1}^{m2} \delta_{2,j}\, a_{2,j} + b_1 G + b_2 \ln(D+3) + \varepsilon \qquad (3.2)$$

where c_i = spectral values of band i
a_0 = constant
$a_{1,j}$ = score of class j of the site class
$a_{2,j}$ = score of class j of the taxation class
$\delta_{i,j}$ = 1 if the sample plot belongs to class j of site class, or 0 otherwise
$\delta_{2,j}$ = 1 if the sample plot belongs to class j of the taxation class, or 0 otherwise
D = D.B.H
G = basal area
m_1 = number of site classes
m_2 = number of taxation classes
b_1–b_2 = regression coefficients to be estimated
ε = model error

The independent variables in the second sub-model cover main species, stoniness, age, height, basal area, D.B.H and compositions for three species and the group of species which can be expressed as follows:

$$c_i = a_0 + \sum_{j=1}^{m1} \delta_{1,j}\, a_{1,j} + \sum_{j=1}^{m2} \delta_{2,j}\, a_{2,j} + b_1 A + b_2 H + b_3 D + b_4 \ln(G+3) + b_5 P + b_6 S + b_7 B + \varepsilon \qquad (3.3)$$

where $\delta_{1,j}$ = 1 if the sample plot belongs to the j class of stoniness, or 0 otherwise
$\delta_{2,j}$ = 1 if the sample plot belongs to class j of main species, or 0 otherwise
$a_{1,j}$ = score of class j of stoniness
$a_{2,j}$ = score of class j of main species
A = age
H = mean height
P = proportion of pine
S = proportion of spruce
B = proportion of deciduous species
m_1 = number of classes of stoniness
m_2 = number of main species
b_1–b_7 = regression coefficients to be estimated

The scores, regression coefficients, R^2 and residual mean squares for six bands can be found in Appendix 1. The image data (including five periods) produced by this model, together with the associated ground measurements, is called ID-simu1. In the rest of the paper, the stratification and the estimation by using the multitemporal image data are mainly based on this data.

Model 2

The image values in the second model are highly correlated to the quantitative stand charateristics. This image data is intended for both the analysis and comparison-stage of the investigation. The model is of the form

$$c_i = a_0 + b_1 H + b_2 \ln(H+3) + b_3 V + b_4 \ln(V+10) + b_5 [(\ln(V+10)]^2 + \varepsilon \qquad (3.4)$$

where V = volume
H = height
b_1–b_5 = regression coefficients to be estimated

The aim of using only these independent variables in (3.4) was to obtain those image data which are hightly correlated with the these field variables. The regression coefficients of (3.4) are listed in Appendix 1. The data derived from this model is known as ID-simu2.

In the second step of the simulation of the multitemporal image values, the image values predicted by the regression models were adjusted to the desired level by means of a randomizer and the correlation matrix for the spectral bands. It includes i) generating the normally but independently distributed variables for each band on the basis of a randomizer; ii) regenerating the random variables with joint normal distribution by using the transformation of a triangle matrix (Rubinstein 1981) based on the given correlation matrix and on the results from the first step. The second step was repeated several times, modifying the given correlation matrix until the correlation matrix of the spectral bands reached a satisfactory level.

The histogram of data ID-simu1 on the second occasion in 1989 is shown in Figure 3.2 and the relevant correlations are presented in Table 3.3. It can be seen that the distributions and the correlations of the simulated spectral values with the simulated stand characteristics are similar to those of the original values.

The data we now have are the multitemporal image and field data on six occasions (five periods). The data on the first occasion consist of the unitemporal field data and bitemporal image data (ID-84 and ID-85).

The data on the subsequent occasions are simulated.

36. Computer programmes in the study

Beyond programmes MELA and NALLE, the computer programmes used in the study consist of FORTRAN programmes and SAS programmes (SAS 1985).

The FORTRAN programmmes, except those for the image data registration, were made by the author of this paper and used for the following aspects:

- multitemporal image data simulation
- image data registration (made by Markku Similä)
- spatial and time filtering
- vegetation index transformation
- GLS and double sampling for the population
- Stratification and compatmentwise estimation
- updating data: ML-PTM-ML and ML-ML models, estimate-modifying.

The following SAS procedures are used in the study:

- PRINCOMP for the principal component analysis
- CANCORR for the canonical variable transformation
- CATMOD for the logistic and log-linear models
- NLIN for the non-linear regression models
- FASTCLUS for k-means clustering.

4. RESULTS

41. Data preprocessing

411. Compartment delineation

With the aid of field work the whole area was delineated into 68 management compartments (of which 65 compartments belong to forest land) on the photograghs. Then the compartment boundaries were digitized by the NALLE programme developed by Timo Pekkonen in the Finnish Forest Research Institute. The average compartment area was 3.0 hectares. The size distribution is as follows:

Compartment size (hectare)	<1.0	1.0–2.9	3.0–4.9	5–9.9	≥10
Frequency (%)	33.8	33.9	16.9	2.3	3.1

412. Image registration

The registration used in the study consists of two steps which have been described by Poso et al. (1987). The first step is a coordinate transformation which is accomplished by a two-variate linear function. The transformation has been checked using 16 control points for the ID-84 data and 13 control points for the ID-85 data with the corresponding standard deviation (distance) 13 m and 15 m respectively.

The second step was to seek an optimum overlapped position of satellite imagery with respect to the study area on the map. This was accomplished by shifting the imagery and calculating the respective correlation coefficients between the spectral values and the ground truth. This method is motivated by an inference that an optimum overlapping should produce a maximum correlation. The experimental results indicate that the correlation is sensitive to the movement.

After the shifting, the correlation coefficients between the main measurements such as volume, age, diameter and height, and the spectral values were increased 0.1 for the ID-84 and 0.05 for the ID-85. The causes of the location error have been discussed by Poso et al. (1987).

The optimum positions are not precisely the same for all the spectral bands and all the field variables. For instance, the optimum position for volume may not be the optimum one for main species, or an optimum position for band 2 may not be the optimum one for band 5. In this case, spatial filtering may provide help.

413. Filtering

4131. Spatial filtering

The weights needed for the simplest two-pixel filter can be calculated from (23.12) and (23.13). The parameters required for the calculation are obtained from the sample.

Figure 4.1 illustrates the autocorrelations between pixels with respect to the spectral values and Figure 4.2 illustrates the correlations between the field variable (volume and composition) and the spectral values of the pixels as a function of the spatial distance.

It can be seen from Figures 4.1 and 4.2 that both the autocorrelations between the pixels with respect to the spectral values and the correlations between the field and image variables show slight differences caused by different directions of shift. The correlation curves of Figures 4.1 and 4.2(a) are close to those concerning the spatial autocorrelations with respect to volume (see Nyyssönen et al. 1967). The behaviour of the correlation curves for pine proportionis different from the others which may have importance in spatial filtering.

As an extention to the filtering of two adjacent pixels in all directions, a filtering window with 3×3 pixels can be formed.

According to (23.13), (23.14), (26.9) and image data ID-85, the weights of the filters covering two adjacent pixels and the gains in the correlations in four directions are presented in Table 4.1.

It can be seen that the weights of different filters, which represent different bands and

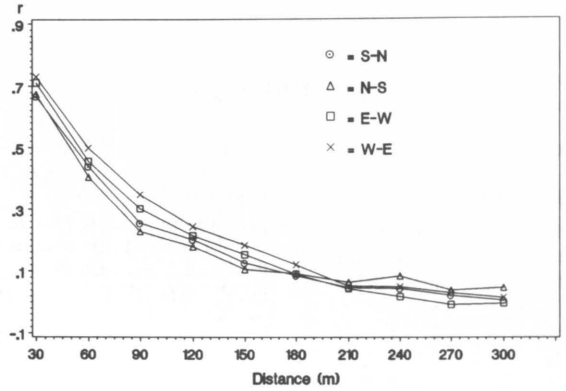

Figure 4.1. Autocorrelations between spatial pixels (Band 2 from ID-85).

different directions, are different although, in most cases the weights are larger for the central pixel, i.e. w > .5. However, we may find that the weights of some bands are less than .5 with a higher gain in the correlation (band 5 and 7 for volume from North to South, and the weights of the filters of bands 1−4 for the proportion of pine from South to North).

The reason for this is that the registered position of the image data is not optimum for all the bands and for all the variables. For example, the position of the image on bands 5 and 7 for volume should be moved further to the North.

The conflict between the optimum positions of the bands or the field variables is most likely caused by random variation. This is probably smoothed by using spatial filtering.

However, if the optimum position for a certain band or variable is found, the gain in the correlation for the band or the variable through spatial filtering tends to be low, except for those bands or variables in which the original correlations are low. For example, bands 1−4 have reached the best position for volume. The gains in the correlations for bands 2-4 are so small that they can practically be ignored. Only band 1 achieved a meaningful gain in the correlation. The original correlation of band 1 with volume was quite low.

Further, those variables which smoothly vary over space probably show a good gain in correlation. For instance, the gains for species composition are higher than those for the volume (see Table 4.1).

Another type of spatial filter is composed of the nearest 2−3 pixels to an arbitrary image

Table 4.1. Weights and gains of the spatial filters.

	Directions								
	N-S			S-N		W-E		E-W	
				For volume					
	r*	w	Gain	w	Gain	w	Gain	w	Gain
Band 1	−.53	.69	1.044	.72	1.032	.63	1.062	.76	1.023
Band 2	−.63	.81	1.012	.82	1.011	.88	1.004	.80	1.011
Band 3	−.57	.78	1.015	.84	1.007	.77	1.013	.81	1.009
Band 4	−.55	.93	1.001	.89	1.002	1.06	1.001	.76	1.010
Band 5	−.60	.49	1.051	1.17	1.009	.54	1.038	1.21	1.007
Band 7	−.56	.49	1.063	1.21	1.008	.64	1.028	.95	1.000
				For proportion of pine					
Band 1	.34	.60	1.079	.45	1.159	.58	1.086	.54	1.098
Band 2	.28	.72	1.027	.32	1.193	.73	1.020	.56	1.061
Band 3	.41	.78	1.015	.45	1.103	.74	1.018	.59	1.047
Band 4	.02	−.40	1.564	−1.32	2.869	−.89	1.853	−.70	1.725
Band 5	.42	.80	1.007	.54	1.042	.51	1.044	.82	1.006
Band 7	.47	.75	1.013	.64	1.029	.67	1.023	.71	1.017

Note that N-S = from North to South, W-E = from West to East and so on; w represents the weight of the central pixel of a pixel window; the weight of the adjacent pixel is therefore 1-w; and r* denotes the correlation before filtering.

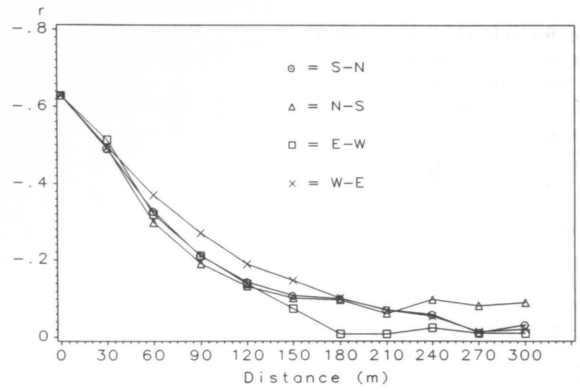

(a) Between band 2 and volume (data = ID-85)

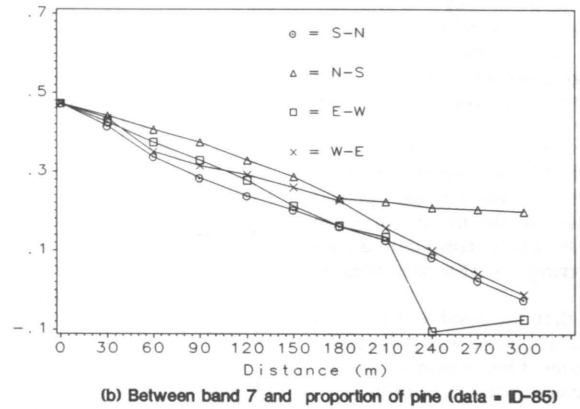

(b) Between band 7 and proportion of pine (data = ID-85)

Figure 4.2. Correlations of spectral values and variables as a function of the distances.

point. The reason for selecting the nearest 2−3 pixels is that in many cases the fourth nearest pixel is no longer the adjacent pixel to the image point side by side. The average distances from an arbitrary image point to the 3 nearest pixels are 11.4 m, 21.0 m and 27.3 m which are calculated as follows:

$$d = \int_l^k \int_u^v (x^2 + y^2)^{1/2}\, dy\, dx/(15^2/2) \qquad (4.1)$$

where x = horizontal coordinate
y = vertical coordinate
k, l, v and u = parameters for the integration

When an image point is located in the shade part in Figure 4.3, the first three nearest pixels to the image point are illustrated in Figure 4.3. The integration ranges of (4.1) are illustrated in Figure 4.4. Numbers 1, 2 and 3 refer to the first, second and third nearest pixels to the image point in Figure 4.3, and the associated integration ranges in Figure 4.4.

Table 4.2 lists the weights of the nearest pixel of the two-pixel filters: one is composed of the nearest and the second nearest pixels; another is composed of the nearest and the third nearest pixels. The corresponding correlations after filtering are also presented in the table.

It can be seen that the results of the two filters in Table 4.2 are fairly near, especially for the case of volume. One reason is that the difference of the average distances of the second and the third nearest pixels to the image point is only six meters.

In comparison with the results in Table 4.1, the results in Table 4.2 look better for species composition but worse for volume. The gain in the correlation regarding volume is insignificant except in band 1. With random selection of the image points the results of the two filters should be analogous. The ground sample plots, however, are allocated systematically and hence might have a periodical coincidence, more or less, with pixels. If the centres of most of the ground sample plots are located within the range formed by directions E-W and S-N, the gain in the correlation for volume might be low. This is because along these two directions the gain in the correlation for volume is weak when using the filtering window (see Table 4.1).

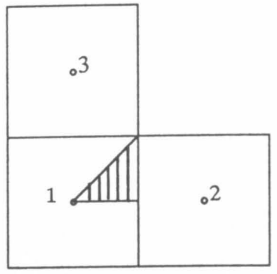

Figure 4.3. The area of image points for 3 nearest pixels.

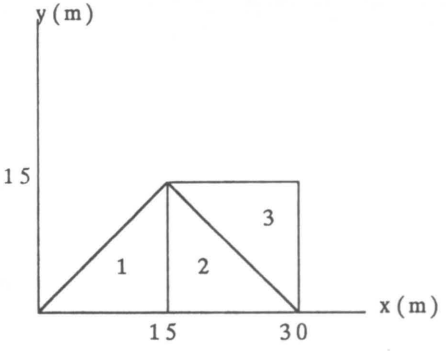

Figure 4.4. The integration ranges for 3 nearest pixels.

The gains in correlations between volume and some bands in Table 4.1 look higher. But in this case, also, there are big variations within the spectral bands. As a result, the multiple correlation based on all of the spectral bands for the field variable might not increase as much as does the correlation between a single spectral band and the field variable.

The next set up describes two filter windows. Their weights are given in Table 4.1.

.2/8	.2/8	.2/8
.2/8	.8	.2/8
.2/8	.2/8	.2/8

−.2/8	−.2/8	.2/8
−.2/8	.84	.5/8
.2/8	.5/8	.5/8

Table 4. 2. Weights of the nearest pixel of two-pixel filters and the corresponding gains.

	Filter of the first and the second nearest pixels		Filter of the first and the third nearest pixels	
	w	Cain	w	Gain
		For volume		
Band 1	.71	1.031	.78	1.016
Band 2	.90	1.002	.86	1.005
Band 3	.87	1.004	.89	1.003
Band 4	.92	1.001	.91	1.001
Band 5	.99	1.000	1.12	1.002
Band 7	.90	1.002	.96	1.000
		For proportion of pine (species composition)		
Band 1	.52	1.092	.56	1.071
Band 2	.57	1.055	.64	1.033
Band 3	.55	1.055	.70	1.019
Band 4	−.30	1.405	−1.18	2.230
Band 5	.60	1.027	.77	1.008
Band 7	.65	1.024	.74	1.011

Table 4. 3. Correlations obtained by using the filtering window (3 × 3 pixels).

	Band					
	1	2	3	4	5	7
			For volume			
Correlation	−.551	−.634	−.579	−.549	−.622	−.579
Gain	1.048	1.008	1.016	1.005	1.038	1.036
			For proportion of pine			
Correlation	0.378	0.305	0.436	0.035	0.430	0.476
Gain	1.099	1.089	1.056	1.207	1.021	1.008
Multiple correlation before filtering			−.666			
Multiple correlation after filtering			−.670			

The left window above is for bands 1−4 and the right window is for bands 5 and 7. Although the weights of these two filters do not exactly follow the optimum weights in Table 4.1, for most bands they approach the best ones. After filtering, the correlations and the associated gains by using the two filter windows stated above are presented in Table 4.3.

It can be seen from Table 4.3 that the gain in the multiple correlation is rather weak. In addition, the window which was designed for volume proves to be useful for the estimation of tree species proportions. The gain for the proportion of pine in Table 4.3 is higher than the gain for volume.

4132. Time filtering

The weights of the time filters concerned with volume, age, and species proportions (pine and spruce) for image data ID-84 and ID-85, according to (23.3) and (23.4), are listed in Table 4.4.

Table 4.4 shows that the weights of the filters regarding volume and age are favorable to data ID-84, except for bands 5 and 2, while the weights of the filters regarding species composition are mostly in favour of ID-85. One reason for this is that most bands of ID-85 which were acquired in the summer indicate higher correlations with the species composition than those of ID-84 acquired in the fall. This feature is not specific to volume or age. This suggests the use of separate time filters for the images of different seasons.

For comparison, two time filters, of which one is for volume and another for species composition, are used for the compartment estimation. The correlations before and after filtering are presented in the lower part of Table 4.4. It can be seen that although the filter is for volume, the correlation concerned with age is also improved for most bands. The weights of the filter for species composition are the average values of two filters in which one is for pine and the other for spruce. Also, the correlations for most bands are enhanced by using the filter for species composition.

414. Transformation

4141. Principal component analysis

The eigenvectors and the correlations between stand characteristics and the principal components, which are obtained in a standar-

Table 4.4. Weights and correlations related to the time filters.

	Volume		Age		Species proportion			
					Pine		Spruce	
	Weights							
	ID-84	ID-85	ID-84	ID-85	ID-84	ID-85	ID-84	ID-85
Band 1	.55	.45	.56	.44	.30	.70	.44	.56
Band 2	.56	.44	.44	.56	.73	.27	.75	.25
Band 3	.59	.41	.71	.29	.17	.83	.44	.56
Band 4	.83	.17	.76	.24	1.82	−.82	.92	.08
Band 5	.48	.52	.73	.27	−.06	1.06	.19	.81
Band 7	.60	.40	.75	.25	.01	.99	.31	.69
	Correlations before filtering							
Band 1	−.457	−.479	−.442	−.453	.224	.349	−.307	−.384
Band 2	−.563	−.584	−.517	−.590	.321	.285	−.416	−.360
Band 3	−.560	−.547	−.537	−.473	.323	.429	−.425	−.467
Band 4	−.602	−.522	−.637	−.586	.131	−.010	−.261	−.210
Band 5	−.551	−.583	−.527	−.495	.354	.454	−.469	−.556
Band 7	−.514	−.527	−.465	−.426	.390	.531	−.482	−.578

	Correlations after filtering			
	Filtering for volume		Filtering for species composition	
Band 1	−.556	.532	.358	−.414
Band 2	−.632	−.612	.336	−.432
Band 3	−.606	−.554	.430	−.488
Band 4	−.612	−.657	−.047	−.178
Band 5	−.601	−.534	.454	−.558
Band 7	−.560	−.478	.530	−.582

dized transformation for 12 stacked bands from two occasions are shown in Tables 4.5, 4.6 and 4.7. The results in Tables 4.5 and 4.6 are calculated on the basis of all the image points (1401). The transformed image variables, as described in the previous paper (Peng 1987), have some distinctive features.

First, all the twelve elements of the first eigenvector have positive signs. This implies that the first principal component is the weighted summation of all the image bands on two occasions.

Secondly, the first six elements of the second eigenvector are positive, while the remaining six elements are negative. Meanwhile, the first six elements correspond to the six bands on the first occasion and the rest elements are the transformation coefficients for the six bands on the second occasion. Thus the second principal component is the weighted difference of the image data on two occasions. The first two principal components seem to be the results obtained by using a smooth (summation) or "low path" filter, and an edge enhacement (difference) or "high path" filter.

As a natural result of the preceding features, the first principal component is often correlated with the current states of field variables, whereas the second principal component relates to forest change.

In comparison with results using the image data on a single occasion (see Table 4.6), using the image data from two occasions

Table 4. 5. Eigenvectors of bitemporal image data (12 stacked bands and 1401 image points).

	Data = ID-84 plus ID-simu1			Data = ID-84 plus ID-85		
	P.C 1	P.C 2	P.C 3	P.C 1	P.C 2	P.C 3
Occasion 1:						
Band 1	0.2275	0.2852	0.9041	0.2364	0.2176	0.5855
Band 2	0.2817	0.3032	−.1689	0.2888	0.2738	0.1292
Band 3	0.2899	0.3163	−.0402	0.3006	0.2273	0.2081
Band 4	0.2772	0.2770	−.3284	0.2752	0.4506	−.2419
Band 5	0.3025	0.3016	−.1527	0.3188	0.1586	0.0380
Band 7	0.2884	0.3029	−.1159	0.3054	0.1182	0.1499
Occasion 2:						
Band 1	0.2605	−.2875	−.0023	0.2722	−.3806	0.0059
Band 2	0.2988	−.2817	0.0275	0.3004	−.2180	−.2293
Band 3	0.3070	−.2846	0.0364	0.2948	−.3707	0.0821
Band 4	0.2944	−.2688	−.0555	0.2515	0.2294	−.6654
Band 5	0.3167	−.2705	0.0361	0.3081	−.2523	−.1034
Band 7	0.3077	−.2800	0.0337	0.2998	−.3708	0.0419

increases the correlations of the first principal component with most variables by 5−10 %. The results are similar to those obtained by using time filtering for the current state.

Table 4.6 presents the correlations obtained when using all and a part of important spectral bands on two occasions. It can be seen that the results are very similar. One of the reasons is that the different band combinations differ in the variance proportions of the first three principal components. The variance proportion of the first three principal components for the transformation using all the bands is less than those for the transformation using only some of bands (see Table 4.6).

Table 4.7 presents the results based on the transformations using the standardized and non-standardized matrices regarding image data ID-84 and ID-85.

From Table 4.7 one may find that as a whole, there are no big differences between the two transformations. If considering only the first principal component, the standardized transformation on the summer image data is better than the non-standardized transformation, especially regarding volume and height. For the image data aquired in the fall, the conclusion is quite the opposite. The reason for this is that for volume and height the best spectral bands of the image data in the fall are bands 4 and 5 which have the large variation (see Figure 3.2), they therefore have more weights than other bands in the non-standardized transformation. The best bands for volume and height in the summer imagery are bands 2 and 3, i.e. those bands whose distributions are narrow.

4142. Canonical variable transformation

Table 4.8 presents the canonical coefficients for 12 bands transformed on the basis of the volumes on two occasions.

Except a few bands, the second canonical coefficient vector in Table 4.8, like the second eigenvector of the principal component transformation is associated with the changes of the stand characteristics.

Table 4.9 demonstrates a comparison on the correlations. One set of correlations is between the principal components and field variables and the other set is between the canonical variables and field variables. It can be seen that for most quantitative variables the correlations concerned with the first canonical variables are better than those concerned with the first principal component. Furthermore, the canonical transformation is not only good for volumes on two occasions, it is also beneficial for all the stand charateristics in relation to the tree size, such as height, D.B.H, age and basal area, but not for the species composition.

By using the bitemporal image data, the second canonical variable like the second principal component is usable for estimating the net increase (see Table 4.9).

4143. Vegetation indices

For forming the Kauth and Thomas's vegetation indices, a key step is to select dry and wet points on the ground. Since there was no such materials to hand, the selection has to be made from the image points falling on the open sites in the study area. Two points (the dry and the wet) selected in this way have the highest and the lowest spectral values respectively. Unfortunately, after transformation, the correlations between the greenness and

Table 4. 6. Correlation coefficients between principal components and field variables (from 1401 image points).

	P.C 1	P.C 2	P.C 3	P.C 1	P.C 2	P.C 3	P.C 1	P.C 2	P.C 3
	(ID-84 plus ID-simul)			(ID-84 plus ID-85)			(ID-84)		
Band 1−6	Band 1−6 on two occasions			Band 1−6 on two occasions			on single occasion		
On occasion 1:									
Dev. class	−0.479	−0.061	0.069	−0.418	0.048	−0.171	−0.441	0.082	−0.122
Age	−0.702	−0.056	0.082	−0.664	0.168	−0.086	−0.631	0.098	−0.160
Volume (V)	−0.710	−0.030	0.040	−0.659	0.029	−0.076	−0.623	0.063	−0.095
Basal area (G)	−0.706	−0.033	0.004	−0.655	0.002	−0.074	−0.622	0.026	−0.027
Height (H)	−0.786	−0.047	0.044	−0.719	0.036	−0.125	−0.697	0.069	−0.079
D.B.H (D)	−0.742	−0.018	0.052	−0.661	0.067	−0.123	−0.644	0.077	−0.097
Composition:									
Pine	0.311	0.125	0.053	0.318	0.435	0.098	0.331	0.034	−0.169
Spruce	−0.454	−0.161	0.014	−0.520	−0.245	−0.009	−0.472	0.032	0.146
Broad leaves	0.167	0.097	−0.122	0.287	−0.382	−0.147	0.194	−0.113	0.087
During occasions 1−2:									
Net increase for									
H	0.074	0.220	0.000	—	—	—	—	—	—
D	−0.134	0.209	0.026	—	—	—	—	—	—
G	0.077	0.230	−0.011	—	—	—	—	—	—
V	−0.015	0.184	−0.020	—	—	—	—	—	—
Total growth	−0.311	0.068	−0.101	—	—	—	—	—	—
Variance proportion of the first three principal components			0.84			0.84			0.92
	Band 3,4,5,7 on two occasions			Band 3,4,5,7 on occasion 1 Band 2,3,5,7 on occasion 2					
On occasion 1:									
Age	−0.707	−0.043	−0.232	−0.647	−0.126	−0.255	—	—	—
Volume	−0.706	−0.021	−0.124	−0.661	−0.036	−0.183	—	—	—
Composition:									
Pine	0.297	0.128	−0.289	0.396	−0.192	−0.202	—	—	—
Spruce	−0.447	−0.170	0.209	−0.527	0.097	0.221	—	—	—
Between occasion 1−2:									
Net increace for V	−0.028	0.185	0.049	—	—	—	—	—	—
Variance proportion of the first three principal components			0.91			0.91			—
	Band 4,5,7 on two occasions			Band 4,5,7 on occasion 1 Band 2,5,7 on occasion 2					
On occasion 1:									
Age	−0.709	−0.043	−0.225	−0.650	−0.161	−0.262	—	—	—
Volume	−0.705	−0.022	−0.119	−0.662	−0.061	−0.204	—	—	—
Composition:									
Pine	0.277	0.128	−0.279	0.382	−0.227	−0.171	—	—	—
Spruce	−0.435	−0.170	0.207	−0.528	0.152	0.164	—	—	—
During occasions 1−2:									
Net increase (V)	−0.024	0.179	0.052	—	—	—	—	—	—
Variance proportion of the first three principal components			0.94			0.94			—

Note that Dev. class = Development class.

Table 4.7. Correlations between principal components and field variables based on the correlation matrix and the covariance matrix.

	Correlation matrix			Covariance matrix		
	P.C 1	P.C 2	P.C 3	P.C 1	P.C 2	P.C 3
	Data = ID-84 (in the fall)					
Main species	.474	.109	.185	.470	.228	.114
Site class	.284	.087	.147	.246	.228	.141
Volume	−.624	.064	−.096	−.627	−.113	−.057
Height	−.697	.069	−.080	−.702	−.107	−.062
variance proportion (%)	77.2	8.6	5.8	86.9	9.0	1.8
	Data = ID-85 (in the summer)					
Main species	.518	.453	.291	.556	.457	.222
Site class	.346	.466	.176	.244	.539	.131
Volume	−.649	−.131	−.041	.639	.015	−.151
Height	−.715	−.129	−.091	−.690	.020	−.211
Variance proportion (%)	77.1	10.7	5.5	80.6	16.6	1.6

most of the field variables are quite low. A natural way to improve the correlations concerned with the greenness is to change the direction of the soil line (the line between the dry and wet points). This is done by simply fixing the dry point, then repeatedly changing the direction from the dry point to the wet point for each of six bands to find out the effective direction on the basis of the correlations obtained.

Based on the iterative process, the effective direction for the greenness is mostly decided on band 4 and band 5 for data ID-84 (in the fall), and bands 1, 2 and 3 for data ID-85 (in the summer). The vegetation index coefficients, for data ID-84 and ID-85 are presented in Table 4.10.

It can be seen that for ID-85 the greenness index is just the weighted difference between the visible bands and near infared bands, but for data ID-84, it is the difference of bands 5 and 1 with other bands. It should be pointed out that although the transformation is for the greenness, the brightness also has the good correlations with most field variables (see Table 4.11). Consequently, if the brightness and the greenness are involved in the stratification, the results would be beneficial for the estimation of most field variables.

Table 4. 8. Canonical coefficients of 12 bands for the volumes on two occasions (C.C refers to the canonical coeffecient).

	Band					
	1	2	3	4	5	7
	Occasion 1					
C.C 1	.096	.108	.066	.341	.085	−.075
C.C 2	−.309	−.298	−.498	−.274	.042	.658
	Occasion 2					
C.C 1	.149	.086	−.011	.200	.068	.178
C.C 2	.087	−.814	.599	.893	−.686	.591

42. Estimation for the population

421. Current states and changes

The GLS (Generalized Least Squares) estimates and variances of current states and changes for volume and main species (pine) within a period of five years are indicated in Table 4.12. For comparison, the results of five sample cases, the TPS (Two Phase Sampling for stratification) and the test sample (TS) are listed in the table. The table covers two periods: occasions 1−2 and occasions 2−3.

Table 4. 9. Correlations of the canonical variables (C.V) and the principal components with image data on two occasions (from 387 image points).

	C.V 1	C.V 2	P.C 1	P.C 2	P.C 3
			Occasion 1		
Volume (V)	−.729	.041	−.713	−.023	−.014
Basal area (G)	−.727	−.014	−.721	−.004	−.033
Height (H)	−.792	.004	−.776	−.047	.002
D.B.H (D)	−.767	−.012	−.749	−.026	.001
Pine	.242	−.095	.319	.119	−.030
Spruce	−.383	.087	−.447	−.136	.035
B.L	.153	−.083	.116	.112	−.047
Age	−.704	.029	−.665	−.059	−.013
			Occasion 2		
Volume	−.714	−.059	−.702	.036	.011
Basal area	−.639	−.164	−.642	.105	.006
Height	−.810	−.031	−.796	.005	−.003
D.B.H	−.773	−.021	−.755	.011	−.005
Pine	.167	−.139	.242	.147	−.022
Spruce	−.435	.090	−.495	−.110	.019
B.L	.099	−.132	.063	.167	−.051
			During occasions 1−2		
Net increase for					
V	.031	−.215	.023	.128	.055
G	.130	−.225	.118	.164	.060
D	−.101	−.049	−.102	.213	−.036
H	.204	−.146	.190	.235	−.021
CUT1	−.102	.178	−.109	−.103	−.063
Composition change:					
Pine	−.211	−.137	−.211	−.090	.023
Spruce	−.268	.024	−.264	.082	−.055
B.L	−.193	−.148	−.184	.164	−.006

Table 4. 10. Transformation coefficients for the vegetation indices.

	Band 1	2	3	4	5	7
Data = ID-84						
Brightness	.1413	.0565	.0537	.2204	.9608	.0480
Greenness	.0471	−.1510	−.3587	−.4372	.1620	−.7920
Data = ID-85						
Brightness	.6315	.2706	.5413	.2977	.3022	.2346
Greenness	.4194	.0618	.2068	−.3887	−.7667	−.1963

Table 4. 11. Correlations of some variables with the vegetation indices.

	Brightness	Greenness
Age	.620	.647
Volume	.610	.619
Height	.685	.691
D.B.H	.631	.647
Compositions:		
Pine	.319	.256
Spruce	.477	.407
B.L	.218	.223

In the first period, there was no clear cutting, only thinnings producing small changes in the species composition, were imposed on six compartments. In the second period, three compartments were regenerated by clear cutting and no compartment was treated by thinning. Although the total drain in the first period is greater than that in the second period, the intensity of cutting is lower in the former. The results reveal a strong dependency of the variances of the estimates on the correlations. The variance of case I12P12 in the first period was reduced by 35 % for the volume and by 25 % for the proportion of pine in comparison with case P12, i.e. the case in which only the permanent sample plots were used for the estimation.

In comparison with case P12, the reduction in the variance of the total growth of volume for case I12P12 was 17 %. Furthermore, we might find that the gains in precision for the current states of volume and main species in both periods 1 and 2 are rather similar, simply because their correlations with the image variables for the two periods are close to each other.

The analysis described above is also applicable for the net increase of volume. During the first period, the reduction of the variance of the net increase for case I12P12 is only 5 % in comparison with case P12. The reduction is much less than that attained by the current volume. This is because the correlation coefficients between the net increase of volume and the image varaibles are very low (around −.2).

The variance of the net increase of volume during the second period is large owing to the clear cutting. The reduction of the variance of the net increase of volume for case I23P23 is 32 % as compared to case P23. It is almost the same as that attained by the current state of volume since the absolute value of the relavent correlation coefficient is over .60.

Large changes tend to increase the variance of the net increase but at the same time the correlation of the net increase of volume with image variables increase as well. It follows that the increase of the variance of the net increase can be partly offset by image data. In other words, with the help of image data the whole area can be roughly splitted into the cut and non-cut areas.

Table 4.12 shows that the variances of estimates which result from the double sampling for stratification, i.e. TPS, is higher than that in the GLS. However, the results of the two estimations sometimes approximate to each other if the stratification is good. Unlike the GLS, the double sampling for stratification does not only rely on the permanent plot

Table 4.12. Estimates and variances for five cases.

Case	Current state Estimate	Current state Variance	Net increase Estimate	Net increase Variance	Total growth Estimate	Total growth Variance
			Volume (m^3/ha)			
Period 1:						
P12	186.33	40.97	16.91	8.78	30.24	.54
I2P12	188.24	27.02	17.24	8.66	30.35	.48
I12P12	188.21	25.74	16.88	8.48	30.34	.45
I1I2P12	188.18	24.25	16.84	8.50	30.34	.45
I123P12	187.78	25.49	16.38	8.36	30.28	.44
TPS	187.05	29.70	17.08	9.18	30.29	.55
TS	190.70	11.35	14.87	2.74	30.22	.16
Period 2:						
P23	195.29	43.57	8.96	23.54	31.26	.77
I23P23	196.41	27.03	8.39	16.06	31.19	.70
I2I3P23	196.49	25.70	8.16	17.05	31.19	.70
TPS	194.18	29.60	7.95	17.20	31.26	.77
TS	201.05	12.54	10.35	5.89	31.03	.22
			Main species (Pine %)			
Period 1:						
P12	48.04	6.48	2.09	1.227	—	—
I2P12	47.05	5.62	1.80	1.189	—	—
I12P12	47.00	5.17	1.66	1.176	—	—
I1I2P12	47.00	5.09	1.69	1.180	—	—
I123P12	47.12	5.03	1.61	1.156	—	—
TPS	46.84	6.11	1.87	1.879	—	—
TS	46.29	1.78	2.04	.398	—	—
Period 2:						
P23	51.86	6.47	2.66	1.155	—	—
I23P23	51.34	5.31	2.94	1.021	—	—
I2I3P23	51.29	5.22	2.96	1.033	—	—
TPS	50.42	6.20	3.15	1.816	—	—
TS	50.30	1.79	2.60	.272	—	—

sample and the number of image points, but also on the stratifying factors, specified number of strata, method of clustering etc.

422. Class probability transition for the qualitative variables

Here, only two qualitative variables (development classes and main species) when the simulated material is used, change over time. It can be seen from Table 4.13 and Table 4.14 that most of the change of main species appeared in pine and broad leaved species because of both cutting and growth during the period. The change is slow for the species but more rapid for the development classes. Most development classes had a movement of about 20–40 % upwards during the five-year period. The estimates and the variances of the transition matrices using the GLS, and the estimates on the basis of the test sample are shown in Tables 4.13 and 4.14.

Table 4.13. Probability transition matrices for main tree species.

(a) GLS (Case I12P12)

Estimates

Occasion		2							
		0	1	2	3	4	6	7	8
	0	.308	.692	.000	.000	.000	.000	.000	.000
	1	.018	.949	.033	.000	.000	.000	.000	.000
	2	.000	.053	.942	.000	.005	.000	.000	.000
1	3	.000	.079	.112	.809	.000	.000	.000	.000
	4	.000	.136	.162	.000	.702	.000	.000	.000
	6	.000	.000	.000	.000	.500	.000	.500	.000
	8	.000	.190	.622	.000	.188	.000	.000	.000

Variances

Occasion		2							
		0	1	2	3	4	6	7	8
	0	.0703	.2108	.0000	.0000	.0000	.0000	.0000	.0000
	1	.0001	.0026	.0002	.0000	.0000	.0000	.0000	.0000
	2	.0000	0003	.0023	.0000	.0000	.0000	.0000	.0000
1	3	.0000	.0075	.0074	.0009	.0000	.0000	.0000	.0000
	4	.0000	.0201	.0200	.0000	.1000	.0000	.0000	.0000
	6	.0000	.0000	.0000	.0000	.2170	.0000	.2170	.0000
	8	.0000	.0305	.0966	.0000	.0356	.0000	.0000	.0000

(c) Test sample

Estimates

Occasion		2							
		0	1	2	3	4	6	7	8
	0	.333	.667	.000	.000	.000	.000	.000	.000
	1	.011	.948	.036	.000	.005	.005	.000	.000
	2	.002	.055	.935	.000	.008	.000	.000	.000
1	3	.036	.214	.036	.714	.000	.000	.000	.000
	4	.000	.154	.154	.000	.692	.000	.000	.000
	6	.000	.000	.000	.000	.800	.000	.200	.000
	8	.000	.063	.323	.000	.625	.000	.000	.000

Table 4.14. Probability transition matrix for the development classes.

(a) GLS

Estimates

Occasion		2							
		1	2	3	4	5	6	7	8
	1	.706	.294	.000	.000	.000	.000	.000	.000
	2	.059	.637	.203	.101	.000	.000	.000	.000
	3	.038	.000	.523	.421	.018	.000	.000	.000
	4	.035	.000	.015	.837	.113	.000	.000	.000
1	5	.000	.000	.000	.716	.284	.000	.000	.000
	6	.000	1.00	.000	.000	.000	.000	.000	.000
	7	.250	.528	.000	.000	.222	.000	.000	.000
	8	1.00	.000	.000	.000	.000	.000	.000	.000

Variances

Occasion		2							
		1	2	3	4	5	6	7	8
	1	.0071	.0046	.0000	.0000	.0000	.0000	.0000	.0000
	2	.0010	.0087	.0030	.0014	.0000	.0000	.0000	.0000
	3	.0003	.0039	.0032	.0002	.0000	.0000	.0000	.0000
	4	.0003	.0000	.0001	.0036	.0007	.0000	.0000	.0000
1	5	.0000	.0000	.0000	.1621	.0597	.0000	.0000	.0000
	6	.8038	.0000	.0000	.0000	.0000	.0000	.0000	.0000
	7	.0519	.1125	.0000	.0000	.0606	.0000	.0000	.0000
	8	.2809	.0000	.0000	.0000	.0000	.0000	.0000	.0000

(b) Test sample

Estimates

Occasion		2							
		1	2	3	4	5	6	7	8
	1	.738	.262	.000	.000	.000	.000	.000	.000
	2	.063	.626	.258	.053	.000	.000	.000	.000
	3	.048	.463	.461	.028	.000	.000	.000	.000
	4	.036	.000	.015	.827	.122	.000	.000	.000
1	5	.000	.000	.000	.600	.400	.000	.000	.000
	6	1.000	.000	.000	.000	.000	.000	.000	.000
	7	.591	.364	.000	.000	.045	.000	.000	.000
	8	1.000	.000	.000	.000	.000	.000	.000	.000

43. Estimation for compartments

The results in this section are based on sample case I12P12 and the unsupervised method by using the principal component transformation, K-means clustering and MD classifier.

431. Stratification

4311 Number of strata

For the unsupervised method, the number of strata is determined by the R^2 (defined in section 2331) in the study. Figure 4.5 shows

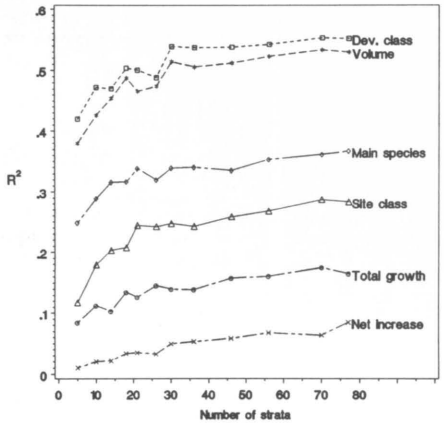

Figure 4.5. Relationship between R^2 and the number of strata.

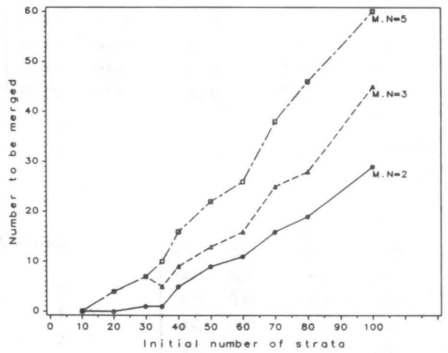

Figure 4.6. Numbers to be merged with respect to numbers of strata (M.N=minimum number of sample plots in a stratum).

the dependency of the number of strata on R^2 for six variables which have different correlations with the image data based on data ID-84 and ID-simu1. It can be noted in Figure 4.5 that i) for most of the field variables the maximum level was almost achieved with 30 strata; ii) as a whole, the efficient stratum number is not sensitive to the correlation coefficients between the field variables and the stratification factors; iii) for the field variables which are almost uncorrelated with the stratifying factors such as net increase, there is no identifiable threshold for determining the stratum number.

In practice, an increase in the number of strata can readily make tedious the job of merging the small strata into the larger strata. Figure 4.6 illustrates the numbers to be merged as a function of initial number of strata. The number to be merged rises rapidly when the given number of strata exceeds 35.

In consideration of the cases stated above, the initially given number of strata in the study was 35, of which only two strata had no more than a single sample plot.

The minimum number of permanent sample plots specified for a stratum is two simply because of the minimum requirement for estimating the sample variance.

4312. Classification

K-means clustering was used for the classification. The initial seeds are 35 observations. After merging, the final number of the strata, in which every stratum has at least two sample plots, was 34. The distributions of the sample plots as well as the distributions of cluster centres for each pairs of stratification factors are shown in Figures 4.7(1a)-4.7(3a) and Figures 4.7(1b)-4.7(3b) where the number in parentheses is the number of the sample plots in the cluster (stratum). Note that the distribution of the clusters closely matches the distribution of the sample plots, though some strata are quite large.

Figure 4.8(a) demonstrates the means of the first and the second principal components by strata as a function of the volume of the growing stock. In the figure r refers to the correlation coefficient between the means of the volume and the principal component in the strata. It is evident that the volume is highly related to the first principal component but only weakly related to the second one.

Note that the first principal component with positive values changes fairly rapidly from the open area to the young stand. The change of the values around zero becomes gentler. This part of the principal components corresponds to the middle-aged and

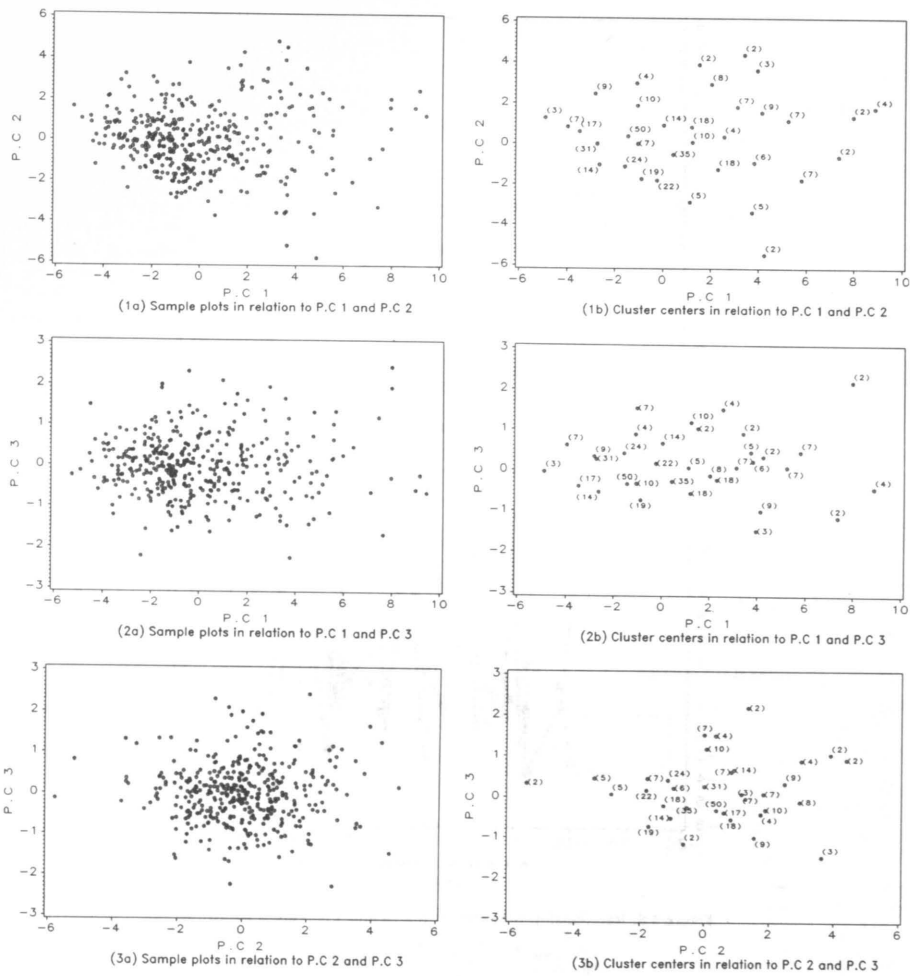

Figure 4.7. Distributions of sample plots and cluster centers in relation to P.C-values.

mature forests. It suggests that it might be easier to detect the natural changes in the open areas and the young stands than in the middle-aged and mature forests. It follows that clear cutting can be found easily, while the forest thinning is difficult to detect.

Figure 4.8(b) illustrates the mean values of the first and the second principal components by strata as a function of the net increase (volume). The fluctuations of both principal components among the strata are large. The correlation (r) for the second P.C shows a higher value than that for the first one.

432. Estimates of the stand characteristics by strata

Estimates of volume, height and species proportion are shown in Figure 4.9, where the strata are arranged in an ascending

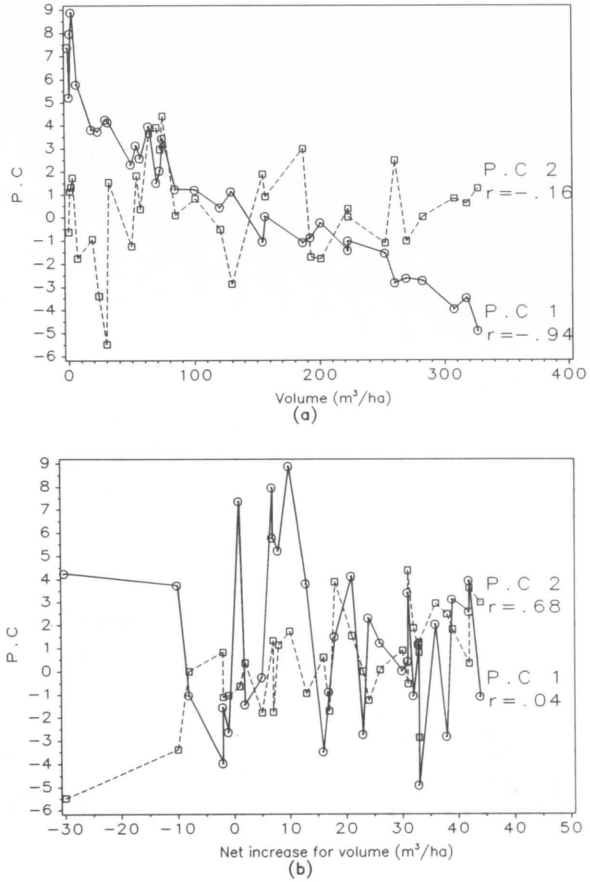

Figure 4.8. Relationship between estimates and P.C-values by strata.

order by volume and the proportion of pine on the basis of occasion 1. It can be seen that estimates of the volume in the strata are evenly distributed within a range of 0–420 m^3 /ha and most of the strata indicate a positive growth.

If the strata characterized by the negative growth consisted only of the cut and thinned permanent plots, they would produce good net increase estimates for the compartments. Unfortunately, those strata contain only a small proportion of the cut permanent plots. Other cut permanent plots are scattered in those strata which have a positive growth. This fact causes a slight underestimation in the net increase for the non-cut compartments and a serious overestimation of the net increase for the cut compartments.

In Figure 4.10, the variances are shown of the estimates of volume and net increase in the strata where the number of permanent sample plots is more than ten. The variances of the low-volume strata are small, but the variation coefficients remain higher than those of the high-volume strata (see Figure 4.10).

It should be pointed out that the weighted

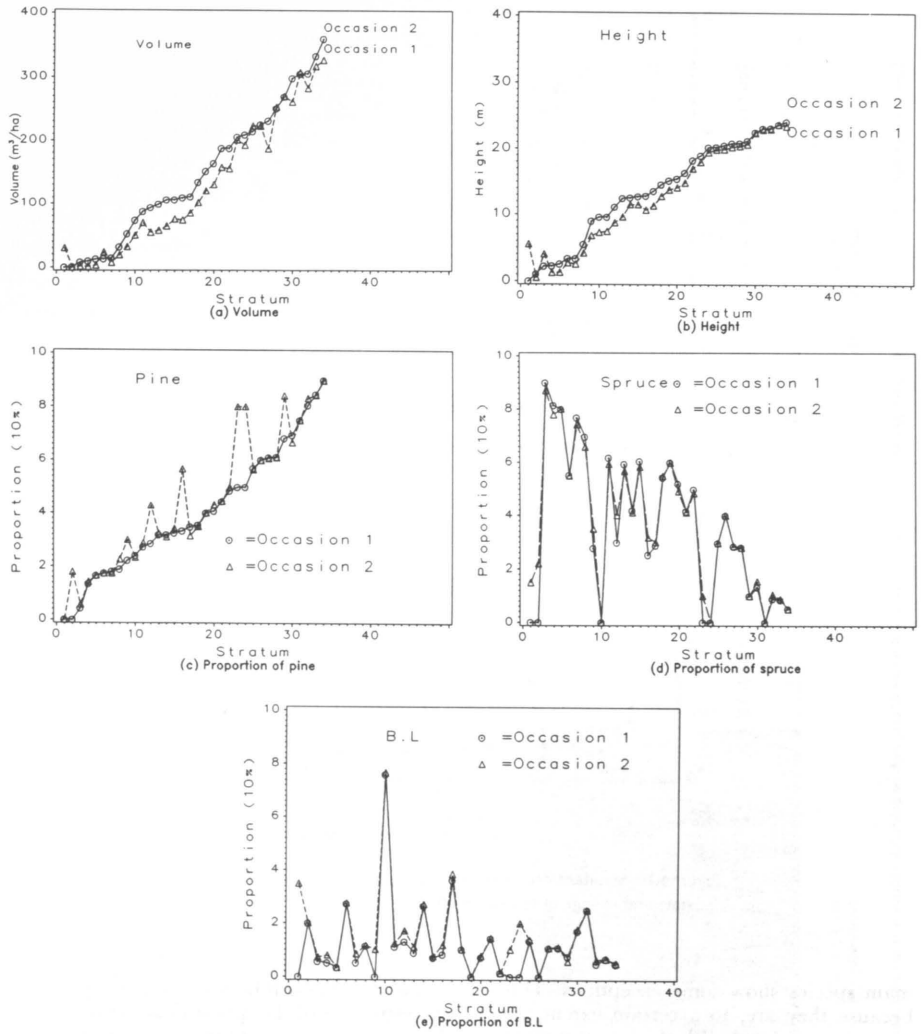

Figure 4.9. Illustration of stratum-wise means of some field variables for two occasions.

average variances over all strata, whose roots are denoted by the dash lines in Figure 4.10, are very close to the residual mean squares of a linear model formed by these variables and the image variables in the study. It follows that the weighted average variances might be estimated approximately from the sample variance and the correlation coefficient between the stratifying factors and a certain field variable.

For the qualitative variables, as can be seen in Figure 4.11, in most strata no classes have a proportion of more than 50 %. As a result, the coefficients of variation for the qualitative variables are large (see Figure 4.11). However, the development class and

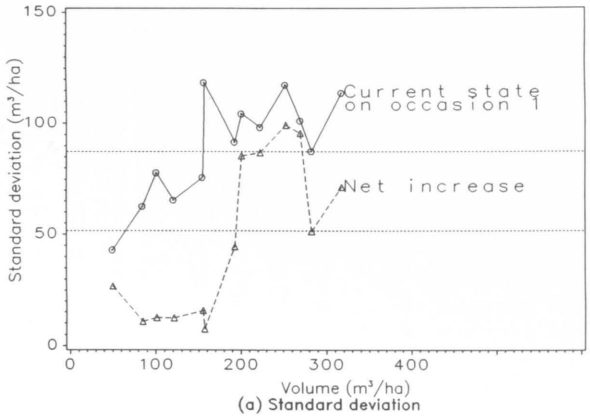

Figure 4.10. Standard deviations and variation coefficients of the current state and change of volume in strata.

main species show some exceptions. This is because they are, to a certain extent, more strongly correlated with the image variables.

433. Estimates of the compartment characteristics

A list of the estimates of the basic characteristics in a compartment is given in Appendix 2. For each quantitative variable, the mean values, standard deviations, and coefficients of variation are listed. For the qualitative variables, the frequency distributions are presented.

Two criteria will be adopted for appraising the estimates of the quantitative variables in the compartments. One is the correlation coefficient between the estimates and measurements, and another is the root mean square error (RMSE).

For the qualitative variables, the criterion for estimation accuracy used here is the proportion of the number of the correctly estimated compartments to the total number of compartments.

Figure 4.13(a–c), Tables 4.15 and 4.16 demonstrate the accuracy of the estimation of several important characteristics. Figure 4.13

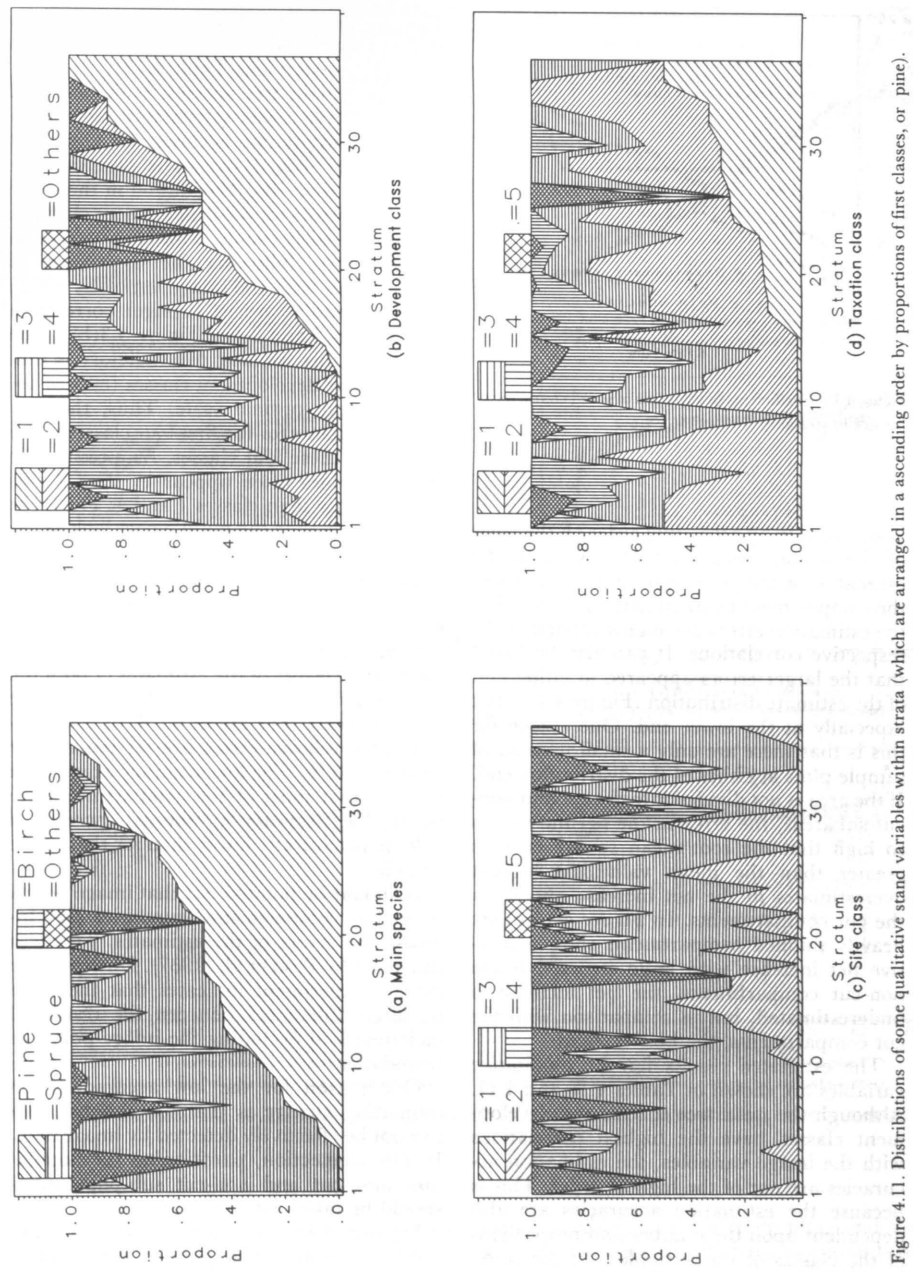

Figure 4.11. Distributions of some qualitative stand variables within strata (which are arranged in a ascending order by proportions of first classes, or pine).

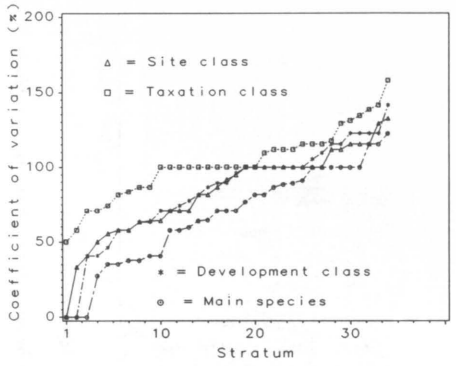

Figure 4.12. Coefficients of variation of stand characteristics in strata.

is arranged in an ascending order on the basis of the volume measurements. As with the estimates for the population, the estimates of the compartment characteristics indicate that the estimation errors are highly related to the respective correlations. It can also be found that the larger errors appeared at either end of the estimate distribution (Figure 4.13), but especially at the lower end. One reason for this is that there are only a small number of sample plots at either of the distribution end. If the area is not divided into the cut and non-cut subareas, the error in the net increase is so high that the root mean square error is greater than the mean value.The highest overestimates in the net increase appear in the cut compartments. In Figure 4.13(c) six heavily thinned compartments show a positive net increase with large errors. For the non-cut compartments, the net increase is underestimated, but in comparison with the cut compartments, the bias is slight.

The estimated results for the qualitative variables are shown in Tables 4.16 and 4.17. Although the main tree species and development classes have the highest correlations with the image variables, the estimation accuracies are not of the highest order. This is because the estimation accuracies are also dependent upon the number and proportions of the classes of the variables. In the study area, the dominant soil class is the mineral soil (over 80 % of the whole area, see Table 3.1), the accuracy therefore looks good. In fact, the accuracies for the other soil classes are equal to zero (see Table 4.17).

For the main tree species, both pine and spruce achieve rather satisfactory accuracies. The lower estimation accuracy for birch and other broad leaved species is probably explained by their low distribution in the study area. The errors for the development class are distributed fairly evenly. This situation seems contradictory, following the correlation of these classes with the image variables where classes 1 and 4 are in stronger correlation than classes 2 and 3 (see Figure 3.3(b)). The reason for this seeming contradictory is that the first four development classes (classes 1–4) are on an ordinal scale. Thus, the representative class for the first four classes is the average of these four classes. As a result, the average values often appear in class 2 and class 3 rather than classes 1 and 4. Therefore the accuracies for the middle part look better than the edge part. If the development class is treated in the nominal scale, the most accurate results are still obtained by classes 1 and 4 (see Table 4.17).

Figure 4.14(a)-(b) plots the distributions of the relative errors of the estimates of both the volume and the net increase of volume in the compartments. For about 60 % of compartments the relative errors are for the volume less than 30 %. The low accuracy arises from the fact that most of the compartments are small. The accuracy for the net increase of volume is naturally lower than for that of the volume.

It should be pointed out that image points located at compartment boundaries may increase the errors of the estimates. This was discussed by Poso et al. (1987). However, the present experiment indicates that there are no large differences between the results of including and excluding the image points at boundaries.

One reason for the low accuracy when estimating change is that the thinned area can not be effectively detected by image data. In this connection, partitioning the population into cut and non-cut sub-populations should be taken into account.

Figures 4.13 (d-f) and 4.14 (c-d) and Tables 4.15 and 4.16 present the effect of dividing the area into cut and non-cut subareas. It can be seen that the partition is more

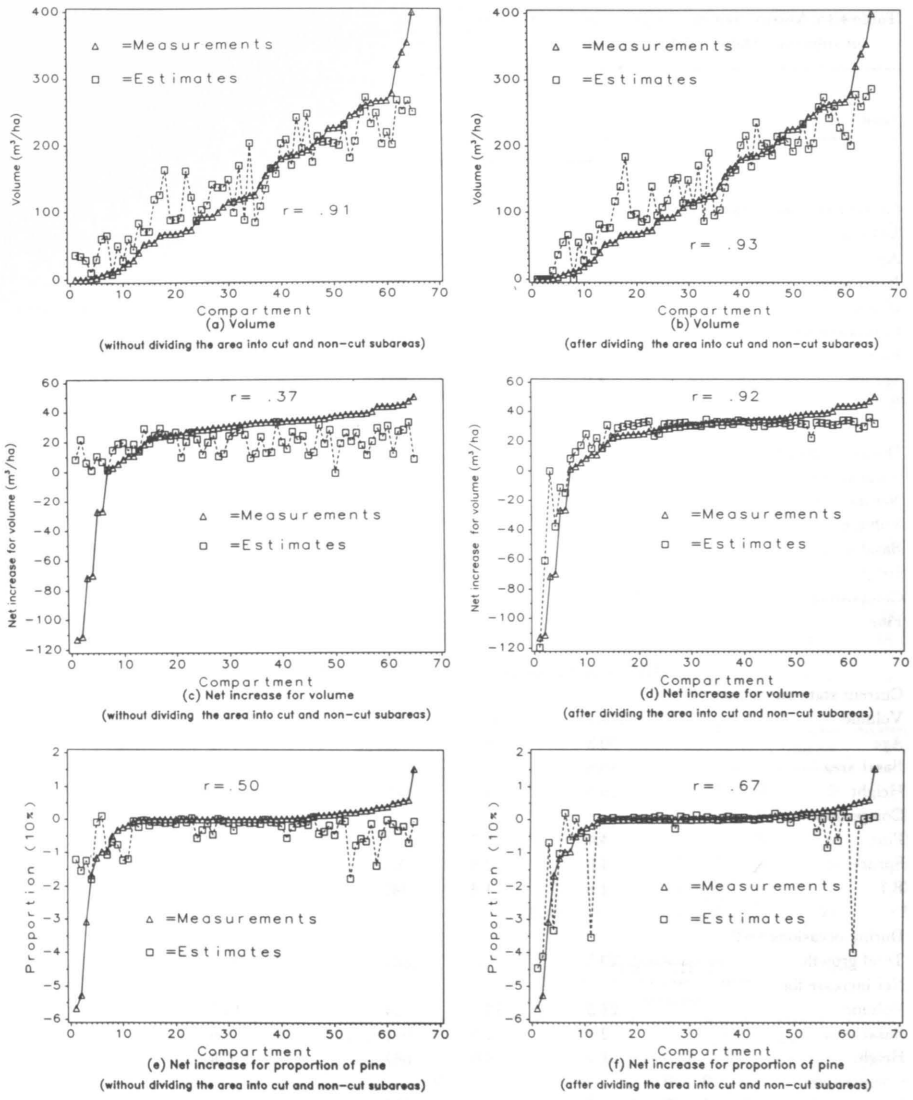

Figure 4.13. Estimates and measurements in compartments (which are arranged in a ascending order by measurements).

beneficial for the estimates of the net increase but less beneficial for the estimates of the current states of the field variables.

Of course, to partition the area into cut and non-cut subareas, the sample plots and the estimated compartments have to contain the relevant information which may require extra work.

Table 4.15. Means, root mean square errors and the correlations without and after dividing the area into cut and non-cut subareas (Data = ID-84 plus ID-simu1).

Variable	Compartments			Image points		
	Mean	RMSE	Correlation	Mean	RMSE	Correlation
Without dividing the area into cut and no-cut subareas						
Current state on occasion 2:						
Volume	140.4	45.6	.911	190.7	90.6	.697
Age	50.3	18.9	.848	74.2	27.6	.723
Basal area	18.6	3.7	.904	20.2	8.3	.612
Height	16.2	3.5	.909	17.0	4.4	.813
Composition:						
Pine	4.4	2.8	.528	4.0	3.7	.414
Spruce	4.0	2.6	.653	4.5	3.2	.581
B.L	1.6	1.7	.229	1.5	2.0	.193
During occasions 1–2:						
Total growth	29.5	8.8	.720	30.2	14.2	.355
Net increase for						
Volume	21.5	30.8	.371	14.9	61.0	.186
Basal area	2.9	3.8	.425	1.6	6.6	.264
Height	1.2	1.5	.736	0.8	2.1	.428
Composition:						
Pine	−.2	.9	.505	−.3	1.4	.295
After dividing the area into cut and non-cut subareas						
Current state on occasion 2:						
Volume	140.4	41.2	.925	190.7	89.9	.704
Age	50.3	18.7	.852	74.2	27.1	.733
Basal area	18.6	3.7	.941	20.2	7.7	.683
Height	16.2	3.6	.888	17.0	4.2	.829
Composition:						
Pine	4.4	2.7	.581	4.0	3.5	.502
Spruce	4.0	2.5	.705	4.5	3.1	.627
B.L	1.6	1.6	.383	1.5	1.9	.264
During occasions 1–2:						
Total growth	29.5	7.6	.801	30.2	13.6	.426
Net increase for						
Volume	21.5	13.8	.924	14.9	44.5	.698
Basal area	2.9	1.8	.911	1.6	4.7	.728
Height	1.2	1.0	.867	0.8	1.8	.653
Composition:						
Pine	−.2	.9	.672	−.3	1.3	.496

Note that the units of the mean and RMSE are m^3/ha for volume, year for age, m^2/ha for basal area, m for height and 10 % for composition. The same to the subsequent tables.

Table 4.16. Estimation accuracies (%) of the qualitative variables in the compartments (Data = ID-84 plus ID-simu1).

Compartments						Sample points					
Soil Class	Tax. class	Site class	Stoneness	Main species	Dev. class	Soil class	Tax. class	Site class	Stoneness	Main species	Dev. class
Without the cut partition											
90	63	66	80	78	61	81	43	57	57	67	47
After the cut partition											
90	60	67	81	73	63	82	45	55	57	68	55

Table 4.17. Classification accuracies for the qualitative variables in compartments (without the cut partition).

	Soil class Estimates						Site class Estimates						
Class	1	2	3	Correct number	Accuracy (%)	Class	2	3	4	5	Correct number	Accuracy (%)
1	59	0	0	59	100	2	0	6	0	0	0	0
2	1	0	0	0	0	3	0	40	0	2	40	95
3	5	0	0	0	0	4	0	11	0	0	0	9
Sum	65	0	0	59	91	5	0	3	0	3	3	50
						Sum	0	60	0	5	43	66

	Main Species Estimates						Taxation class Estimates							
Species	Open area	Pine	Spruce	Birch	Correct number	Accuracy (%)	Class	1	2	3	4	5	Correct number	Accuracy (%)
Open area	0	2	0	0	0	0	1	0	2	1	2	0	0	0
Pine	0	32	3	0	32	91	2	1	36	1	1	0	36	92
Spruce	0	8	19	0	19	70	3	0	10	0	1	0	0	0
Birch	0	0	1	0	0	0	4	0	2	1	5	1	5	56
Sum	0	42	23	0	51	78	5	0	1	0	0	0	0	0
							Sum	1	51	3	9	1	41	63

	Development class (based on the ordinal variable) Estimates							Development class (based on the nominal variable) Estimates							
Class	1	2	3	4	5	Correct number	Accuracy (%)	Class	1	2	3	4	5	Correct number	Accuracy (%)
1	8	6	0	0	0	8	57	1	14	2	0	0	0	14	89
2	0	10	7	0	0	10	59	2	4	9	2	5	0	9	45
3	0	1	18	0	0	18	95	3	0	1	0	8	0	0	0
4	0	0	9	4	0	4	31	4	0	1	0	17	0	17	94
5	0	0	2	0	0	0	0	5	0	0	0	2	0	0	0
Sum	8	17	36	4	0	40	61	Sum	18	13	2	32	0	40	61

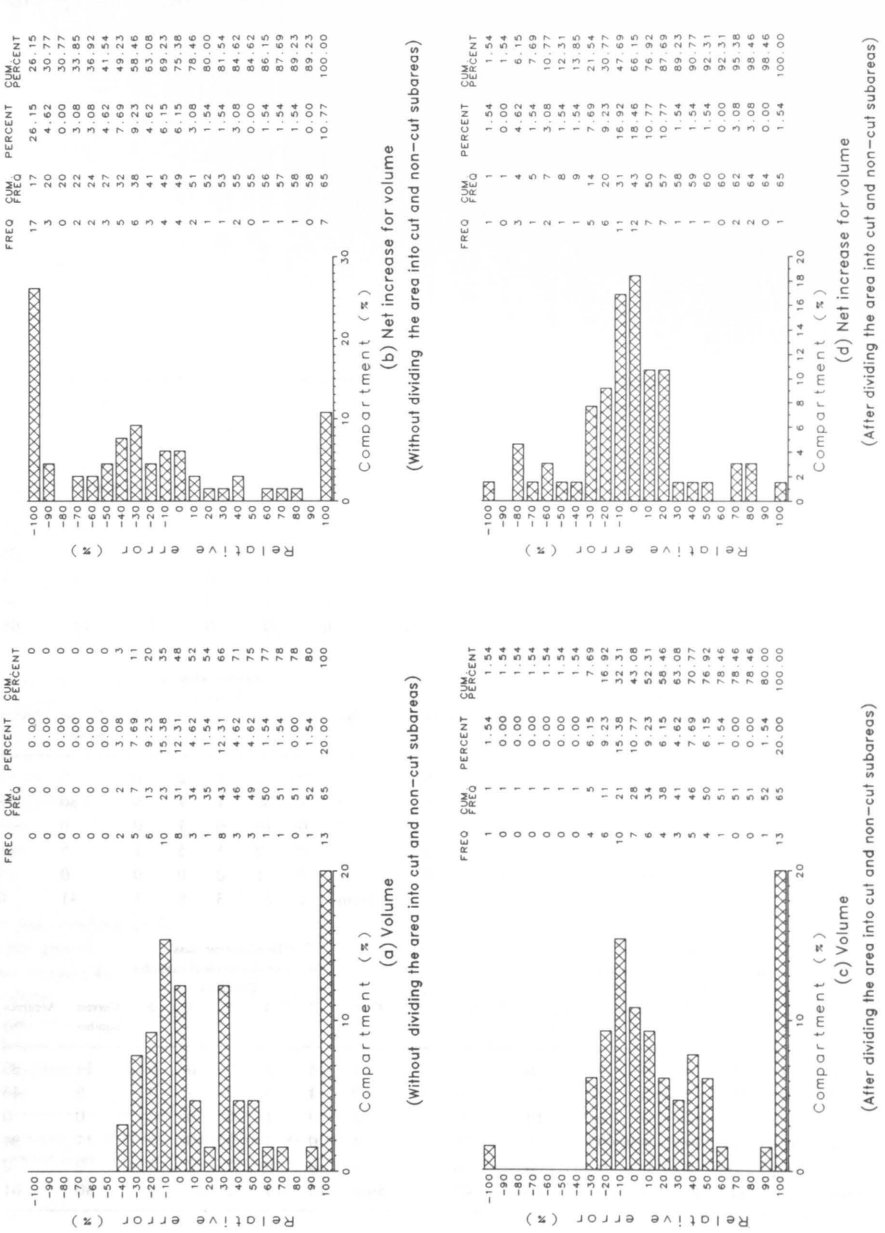

Figure 4.14. Distribution of compartments into classes of relative errors in estimation.

44. Effects of the statistical options and methods

The three criteria for the quantitative and qualitative variables used in section 43 will be used to evaluate the statistical options and methods in the compartmentwise estimation.

441. Transformation options

The results listed in Table 4.18 are based on the unsupervised stratification using different transformation techniques and various combinations of spectral bands. The initial numbers of clusters (strata) are the same for all the transformations.

Table 4.18(a) demonstrates that if the first three principal components are used as the stratification factors, the best combination is not the case in which all the image bands are utilized in the transformation. Instead, the combinations which cover only 3–4 effective bands on two occasions give better results. Beside the randomness of the sample, the reason for this is that the first three principal components contain more variance for these spectral bands (see Table 4.6). The results for the standardized and non-standardized principal component transformations coincide with the results in section 4141. For the image data acquired in the fall (data ID-84 and ID-simu1), the non-standardized principal component transformation shows better results than does the standardized transformation. For the image data acquired in the summer (data ID-85), the reverse seems to be true.

The canonical variable transformation in the study was calculated for volume, species composition and main species. The real image data such as the bitemporal image data (ID-84 plus ID-85) and unitemporal image data (ID-84) produces nearly the best estimates (see Tables 4.18(b) and 4.19).

On the other hand, for a single quantitative variable, the canonical variable transformation seems better when compared with a qualitative variable with several classes.

The transformation using the first four principal components did not improve the accuracy. The improvement might require an increase in the number of strata.

442. Classification options

In order to remove the effect of the sample in the second phase of the comparison, the results in Tables 4.20–4.25 were calculated on the basis of 1014 image points in the first phase, and the image points (387) associated with the sample plots in the second phase, are not included.

A. Clustering and equal interval classifying

Table 4.20 shows that interval classification is also rather effective, especially for the case with a single stratification factor as in the case of a single canonical variable (see Table 4.19). The interval used in the single canonical variable is .3 producing 18 strata (classes).

When the investigated area is homogeneous, the clustering method is likely to lead to a few over-large strata, which may reduce the efficiency of the stratification. In the study area, for instance, most of sample plots are centered on the mature or nearly mature forest stands, the estimated results for these compartments using the equal interval classifying method appear better than those using the clustering method.

B. Classifiers MD (Minimum distance) and ML (Maximum likelihood)

As mentioned in section 23, the ML classification in the unsupervised method may require an iteration process. To accomplish the iteration, the minimum number of image points in a stratum is specified 5 in this study; 2 for the MD method. The 35 strata were therefore merged into 25. In the first iteration, 20 image points from 387 moved from their original strata to others. Six iterations were required for completion, i.e. no further image point changed stratum. Figure 4.15 illustrates the changes of the numbers of strata when using the iteration based on bitemporal image data (ID-84 plus ID-simu1). It can be seen that after the iteration, the number of the image points decreased in the large strata, and increased slightly in some small strata.

In Tables 4.20 and 4.21 both the MD and ML classifiers show very similar results. It

Table 4.18 (a). Means, root mean square errors and correlations by using different transformations.

Band combination	Number of P.C or C.V	Estimated variable	Compartments Mean	Compartments RMSE	Compartments Correlation	Image points Mean	Image points RMSE	Image points Correlation
		Data = ID-84 plus ID-simu1 for occasion 2 (Case I12P12)						
		Principal component transformation (standardized)						
3,4,5,7	3	Volume	140.4	43.0	.921	190.7	89.3	.707
		Age	53.1	16.7	.893	74.2	26.1	.757
		Net increase (V)	21.5	29.4	.495	14.9	61.0	.198
		Composition:						
		Pine	4.4	2.3	.721	4.0	3.5	.464
		spruce	4.0	2.0	.866	4.5	3.2	.562
		B.L	1.6	1.7	.312	1.5	2.1	.193
4,5,7	3	Volume	140.4	41.6	.931	190.7	91.2	.695
		Age	53.1	14.4	.931	74.2	26.0	.761
		Net increase (V)	21.5	29.2	.570	14.9	61.0	.184
		Composition:						
		Pine	4.4	2.4	.712	4.0	3.5	.454
		Spruce	4.0	2.3	.779	4.5	3.2	.541
		B.L	1.6	1.6	.387	1.5	2.0	.270
1,2,3,4,5,7	4	Volume	140.4	46.7	.906	190.7	92.0	.685
		Age	53.1	17.3	.885	74.2	26.9	.731
		Net increase (V)	21.5	30.2	.446	14.9	61.0	.186
		Composition:						
		Pine	4.4	2.7	.581	4.0	3.6	.419
		Spruce	4.0	2.5	.697	4.5	3.2	.539
		B.L	1.6	1.7	.252	1.5	2.0	.184
		Principal component transformation (non-standardized)						
1,2,3,4,5,7	3	Volume	140.4	43.8	.903	190.7	89.7	.705
		Age	53.1	15.6	.910	74.2	25.9	.760
		Net increase (V)	21.5	29.9	.459	14.9	61.0	.184
		Composition:						
		Pine	4.4	2.5	.660	4.0	3.5	.455
		Spruce	4.0	2.2	.788	4.5	3.2	.563
		B.L	1.6	1.6	.436	1.5	2.0	.218
3,4,5,7	3	Volume	140.4	41.6	.912	190.7	90.1	.701
		Age	53.1	15.7	.914	74.2	26.0	.756
		Net increase (V)	21.5	29.4	.572	14.9	61.0	.184
		Composition:						
		Pine	4.4	2.7	.575	4.0	3.5	.450
		Spruce	4.0	2.4	.737	4.5	3.2	.553
		B.L	1.6	1.7	.303	1.5	2.0	.226
		Canonical variable transformation (for volumes on two occasions)						
1,2,3,4,5,7	2	Volume	140.4	44.9	.912	190.7	91.9	.689
		Age	53.1	16.3	.898	74.2	26.9	.736
		Net increase (V)	21.5	27.1	.700	14.9	62.9	.149

Table 4.18(a) cont.

Band combination	Number of P.C or C.V	Estimated variable	Compartments Mean	Compartments RMSE	Compartments Correlation	Image points Mean	Image points RMSE	Image points Correlation
		Canonical variable transformation (for composition)						
3,4,5,7	2	Composition:						
		Pine	4.4	2.2	.770	4.0	3.6	.505
		Spruce	4.0	2.2	.814	4.5	3.3	.518
		B.L	1.6	1.6	.377	1.5	2.0	.265
		Vegetation indix transformation						
1,2,3,4,5,7	2	Volume	140.4	43.5	.922	190.7	89.9	.702
		Age	53.1	19.3	.838	74.2	26.8	.738
		Net increase (V)	21.5	30.3	.434	14.9	60.9	.201
		Composition:						
		Pine	4.4	2.8	.486	4.0	3.6	.388
		Spruce	4.0	2.5	.674	4.5	3.3	.523
		B.L	1.6	1.7	.340	1.5	2.0	.206

Table 4.18(b). Means, root mean square errors and correlations by using different transformations.

Band combination	Number of P.C or C.V	variable	Compartments Mean	Compartments RMSE	Compartments Correlation	Image points Mean	Image points RMSE	Image points Correlation
		Data = ID-84 plus ID-85 for occasion 1 (Case I12P1)						
		Principal component transformation (standardized)						
1,2,3,4,5,7	3	Volume	118.9	48.9	.868	175.8	91.1	.677
		Age	49.8	18.8	.828	70.2	28.0	.678
		Composition:						
		Pine	4.5	2.1	.762	4.3	3.8	.544
		Spruce	3.8	2.2	.738	4.5	3.7	.587
		B.L	1.7	1.7	.688	1.2	3.1	.413
		Principal component analysis (non-standardized)						
1,2,3,4,5,7	3	Volume	118.9	50.7	.855	175.8	90.7	.681
		Age	49.8	20.4	.786	70.2	28.5	.669
		Composition:						
		Pine	4.5	2.0	.815	4.3	3.8	.593
		Spruce	3.8	2.1	.838	4.5	3.8	.638
		B.L	1.7	1.4	.808	1.2	3.0	.462
		Canonical variable transformation (for the volume on occasion 1)						
1,2,3,4,5,7	1	Volume	118.9	45.7	.893	175.8	88.8	.696
		Age	49.8	18.5	.838	70.2	27.4	.695

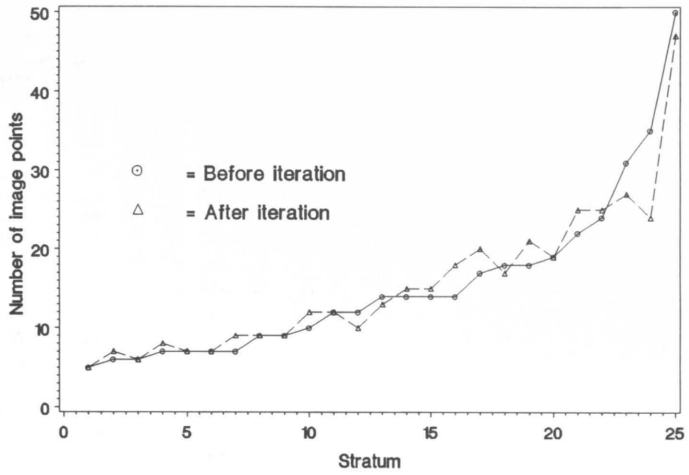

Figure 4.15. Changes of image points in strata before and after the ML iteration.

Table 4.19. Estimation accuracies of the qualitative variables by using different transformations.

Band combination	Number of stratifying factors	Compartments: Tax. class	Compartments: Site class	Compartments: Main species	Compartments: D.V class	Sample points: Tax. class	Sample points: Site class	Sample points: Main species	Sample points: D.V class
			Data = ID-84 plus ID-simul for occasion 2 (Case I12P12)						
			Principal component transformation (standardized)						
3,4,5,7	3	64	67	83	73	43	56	67	57
4,5,7	3	73	72	73	72	45	59	69	57
1,2,3,4,5,7	4	64	67	76	64	43	58	67	51
			Principal component transformation (non-standardized)						
1,2,3,4,5,7	3	64	66	76	73	45	58	69	51
3,4,5,7	3	63	69	78	67	45	59	67	49
			Canonical variable transformation (for main species)						
1,2,3,4,5,7	3	66	67	84	—	44	58	70	—
			Vegetation index						
1,2,3,4,5,7	2	64	64	73	67	44	55	67	57
			Data = ID-84 and ID-85 for occasion 1 (Case I12P1)						
			Principal component transformation (standardized)						
1,2,3,4,5,7	3	70	76	73	64	49	63	72	50
			Principal component transformation (non-standardized)						
1,2,3,4,5,7	3	70	76	76	50	50	61	74	46
			Canonical variable tranformation (for main species)						
2,3,4,5,7	3	—	—	78	—	—	—	73	—

Table 4.20. Means, root mean square errors and correlations by using different options in the stratification.

Sample phase	Transformation	Classifier	Variable	Compartments: Mean	Compartments: RMSE	Compartments: Correlation	Image points: Mean	Image points: RMSE	Image points: Correlation
				Data = ID-84 plus ID-simul for occasion 2 (Case I12P12)					
2	P.C	MD	Volume	145.6	49.4	.908	192.4	91.9	.687
			Age	54.2	20.9	.866	74.3	27.0	.726
			Net increase	20.8	36.2	.124	14.1	62.7	.163
			Composition:						
			Pine	4.6	3.2	.375	4.3	3.8	.327
			spruce	3.8	2.6	.635	4.5	3.3	.508
			B.L	1.6	2.2	−.061	1.2	2.2	.061
2	P.C	ML	Volume	145.6	50.4	.904	192.4	92.0	.686
			Age	54.2	19.9	.864	74.3	27.6	.722
			Net increase	20.8	35.5	.198	14.1	62.6	.166
			Composition:						
			Pine	4.6	3.1	.403	4.3	3.8	.311
			spruce	3.8	2.5	.704	4.5	3.3	.508
			B.L	1.6	2.1	.166	1.2	2.1	.126
				Data = ID-84 for occasion 1 (Case I1P1)					
2	P.C	MD	Volume	124.8	59.5	.818	178.3	93.7	.632
			Age	50.9	21.7	.775	70.5	29.3	.646
			Composition:						
			Pine	4.5	2.9	.481	4.2	3.6	.399
			spruce	3.8	2.5	.667	4.5	3.3	.510
			B.L	1.7	2.3	.176	1.3	2.1	.140
2	P.C	ML	Volume	124.8	59.3	.820	178.3	94.4	.640
			Age	50.9	21.7	.780	70.5	28.8	.646
			Composition:						
			Pine	4.5	3.0	.464	4.2	3.5	.442
			spruce	3.8	2.6	.623	4.5	3.3	.525
			B.L	1.7	2.2	.436	1.3	2.0	.227
2	C.V for growing stock	MD	Volume	124.8	58.3	.829	178.3	95.5	.635
			Age	50.9	20.3	.808	70.5	28.1	.660
2	C.V for growing stock	Equal interval	Volume	124.8	57.6	.835	178.3	93.7	.671
			Age	50.9	20.3	.805	70.5	28.1	.649
1	P.C	ML	Volume	124.8	61.9	.796	178.3	97.6	.609
			Age	50.9	22.1	.756	70.5	29.4	.632
			Composition:						
			Pine	4.5	2.9	.486	4.2	3.7	.367
			spruce	3.8	2.5	.681	4.5	3.3	.490
			B.L	1.7	2.3	.256	1.3	2.1	.162

Table 4.21. Estimation accuracies of the qualitative variables by uing different options for the stratification.

Sample phase	Transformation	Classifier	Compartments Tax. class	Site class	Main species	Dev. class	Image points Tax. class	Site class	Main species	Dev. class
			Data = ID-84 plus ID-simu1 for occasion 2 (Case I12P12)							
2	P.C	MD	56	60	72	63	42	56	66	46
2	P.C	ML	52	64	69	66	42	57	64	48
			Data = IDD84 for occasion 1 (Case I1P1)							
2	P.C	MD	58	63	67	50	42	54	68	43
2	P.C	ML	55	61	69	55	44	57	68	49
1	P.C	ML	58	63	72	52	41	54	69	41

should be emphasized that the lower limit of the image points in a stratum for each classifier is different, i.e. 2 for the MD and 5 for the ML. If the minimum limits of the numbers of sample plots in the strata were the same, the ML would give slightly better results than did MD.

The ML classifier can also be created from the large image sample, i.e. the image sample in the first phase. The advantage by using the image sample in the first phase is that the minimum number of image points in a stratum can be relatively large in comparison with the use of the permanent plot sample. However, the results obtained by using the ML classifier created from the large image sample has not given satisfactory results (see Table 4.20). This failure may be attributed to the fact that both the image and field variables are more strongly correlated with each other in the second phase sample than that in the large sample. In addition, the large sample can not be used for the partition into cut and non-cut subareas. The calculation is also time consuming. For instance, the ML classifier on the basis of the first phase sample in Table 4.20 was obtained after 36 iterations.

As a whole, the difference between these stratification options is not significant.

443. Supervised stratification

The training area of the supervised method in the two phase sampling is just the ground sample of the second phase and not the usual subjectively selected forest area.

For the variable of volume, each sample plot is classified into volume classes with an interval of 20 m^3/ha except for the first class (less than 10 m^3 /ha) and the last class (greater than 410 m^3 /ha). Other quantitative variables such as height, D.B.H, basal area, age and net increase were simultaneously classified as the volume classification was progressing.

Three models: ML-PTM-ML, ML-ML and ML were used in the supervised method. The ML-PTM-ML model was used for volume classes, main species and development classes based on the bitemporal image data: ID-84 plus ID-simu1 and measurements at two periods with a time interval of 5 years. The probability transition matrix presented in section 22 was based on the permanent plot sample. Based on the same bitemporal image data, the ML-ML model was used for those qualitative variables which did not change over the five year period. Besides, the ML-ML model was also used for both the quantitative and the qualitative variables based on the bitemporal imageries (ID-84 plus ID-85) and unitemporal measurements in the first period (the interval of the two image data is only nine months). It implies there is no any movement between classes for these variables. The ML model was used for the stacked image data on two occasions as well as for the single image data.

A comparison between the supervised (using only a single ML) and unsupervised method for most qualitative variables was presented by Peng (1987).

The normal distribution is assumed as a prerequisite for the use of the ML classifier. In addition, the proportions of the sample plots in the strata were initially used as the a priori probabilities for the qualitative variables. Equal probabilities as the a priori probabilities are assumed for the quantitative variables. The test based on the three criteria indicates that under the case in which the a priori probability is unknown, treating the a priori probability in this way is better than others in the study area. The MD classifier as a contrast is used only for the image data from a single occasion.

Tables 4.22 and 4.23 present the results, in which the supervised method appeared slightly better than the unsupervised method (refer to Tables 4.22 and 4.20) for estimating volume. However, for estimating the qualitative variables they are quite similar. Compared with the results from the unitemporal image data using a single ML, the ML-PTM-ML and ML-ML models also give better results, except for some qualitative variables such as the site class and the taxation class based on ID-84 plus ID-simu1 using the ML-ML model. One of the advantages of using the supervised method is that it optimizes the use of the ground sample information, provided that prerequisites for the ML are satisfied. However, a problem also derives from the sample. If the sample is not large enough for a variety of forest types to be represented or the statistical assumption of the normal distribution does not hold for some variables, biased estimates are likely to arise.

Table 4.22. Means, root mean square errors and correlations by using different updating techniques (supervised method).

Updating technique	Estimates	Compartments Mean	RMSE	Correlation	Image points Mean	RMSE	Correlation
		Data = ID-84 plus ID-simu1 for occasion 2 (Case I12P12)					
ML (stacked image data)	Volume	145.6	48.0	.906	192.4	90.2	.700
	Age	54.2	21.2	.817	74.3	26.6	.747
	Net increase	20.8	34.2	.342	14.1	64.2	.016
ML-PTL-ML	Volume	145.6	45.6	.915	192.4	92.4	.691
	Age	54.2	19.8	.847	74.3	26.3	.753
	Net increase	20.8	34.4	.318	14.1	64.2	.025
		Data = ID-84 PLUS ID-85 for occasion 1 (Case I12P1)					
ML (stacked image data)	Volume	124.8	55.2	.833	178.3	89.5	.697
	Age	50.9	20.1	.801	70.5	26.9	.712
ML-ML	Volume	124.8	55.8	.818	178.3	90.7	.704
	Age	50.9	20.0	.791	70.5	26.6	.716
		Data = ID-84 for occasion 1 (Case I1P1)					
ML	Volume	124.8	58.8	.810	178.3	95.3	.640
	Age	50.9	21.9	.760	70.5	28.8	.657
MD	Volume	124.8	64.4	.795	178.3	116.3	.618
	Age	50.9	24.5	.713	70.5	32.3	.619
		Data = ID-simu1 for occasion 2 (Case I2P2)					
ML	Volume	124.8	55.1	.904	178.3	96.3	.645
	Age	50.9	22.3	.821	70.5	29.3	.673

Table 4.23. Estimation accuracies of the qualitative variables by using different updating techniques (supervised method).

Updating technique	Compartments				Image points			
	Tax. class	Site class	Main species	Dev. class	Tax. class	Site class	Main species	Dev. class
	Data = ID-84 plus ID-simu1 for occasion 2 (Case I12P12)							
ML (stacked image data)	42	66	66	68	44	58	62	54
ML-PTM-ML	—	—	75	65	—	—	69	56
ML-ML	51	66	—	—	49	59	—	—
	Data = ID-84 plus ID-85 for occasion 1 (Case I12P1)							
ML (stacked image data)	60	74	66	55	48	61	65	51
ML-ML	65	78	69	55	49	63	71	50
	Data = ID-84 for occasion 1 (Case I1P1)							
ML	52	66	66	51	44	59	65	49
MD	14	25	42	40	09	20	37	34
	Data = ID-simu1 for occasion 2 (Case I2P2)							
ML	48	66	69	55	42	59	61	49

The MD classifier for the supervised method is not as good as the ML classifier, especially for the qualitative variables.

To estimate the net increase of volume, two alternatives can be selected for the supervised method. According to the test, the stratification based on merely the net increase only using the supervised method did not give the satisfactory results because of the weak correlation. The results listed in Table 4.23 come from the second method which simply follows the stratification by volume. The accuracy of the method is a little lower than that obtained by the unsupervised method. The estimate of the net increase of volume, following the volume stratification, could be expected to be better When the area is partitioned into cut and non-cut areas.

444. Regression estimation

The comparison between the stratification method and the regression methods shown in section 24, have been presented in a previous paper by Peng (1987). Both two methods gave similar results.

The important thing in using the regression estimation method, is the selection of the appropriate regression model. Since the responses of image data to forest differ in various parts of the distribution of stand characteristics, the segmented model should, perhaps, be applied in the manner of the model developed by Tomppo (1987). Also, in order to maintain the compatibility among field variables, the simultaneous equation model may need to be considered. Since the regression model is effective in many cases, the method remains promising. Of course, finding a good regression model requires much elaborate work.

45. Effects of updating methods

Two updating methods to handle the multitemporal image data have been discussed already. The first one is stacking multitemporal image data which was used for the unsupervised and supervised stratifications in sections 43 and 44. Another one is a recursive method including the ML-PTM-ML and ML-ML models. It was utilized in the supervised method in section 443. In reality, both updating methods can be used in either the supervised or the unsupervised manner to handle the multitemporal image data.

As described above, the stacked image data can be readily used for simultaneously estimating both the present state and changes in the forest, while the recursive method is mostly directed to the present state of the forest resources.

In Tables 4.24 and 4.25 the results of four methods concerning updating data are based on the real data: data ID-84 and ID-85. These methods are combined with the unsupervised method and used for estimating the current states of the compartment characteristics. It should be emphasized that the ML-PTM-ML and the ML-ML models used in the unsupervised stratification differ from the supervised one in the stratification factors as described in section 24. In the unsupervised method, the transition of the stratum is accomplished through a change of the spectral values of the image points, while for the supervised method, it is accomplished on the basis of the change of the stand characteristics of the sample plots. Although both transitions contain sampling errors, the former include an extra random error: the error of the change of spectral values of an image point over time.

In the event, the transition error of the unsupervised method may be larger than that of the supervised method. However, considering the statistical assumption of the normal distribution when using the ML classifier, the unsupervised method is, perhaps, easier to apply. Final results indicate that the accuracy of using the ML recursion models for the two methods are analogous.

The results of Tables 4.24 and 4.25 were obtained on the basis of the use of the two filters, one for volume and the other for tree species composition as discussed in section 413. The results are similar to those obtained using the stacked image data.

Time filtering can be also used for estimating the net increase. At the moment, the signs of the filter weights for the two imageries are opposite. However, merely a single difference filter would not produce an effective estimate for the net increase, because the net increase is also related to the current state of a field variable. For estimating the net increase, therefore, two kinds of filters are required at the same time: one for the current state and another for the net increase. In such a case, the stacked image data might meet the requirement since after principal component transformation of the stacked image data, the first two principal components often result in two types of eigenvectors which are similar to a summation filter and a difference filter respectively.

As in canonical variable transformations, the problem of time filtering based on correlations is whether the weights calculated from the sample are approximate to those calculted from the population. Naturally, if the sample is sufficiently large, it should be so.

Table 4.24 demonstrates that beyond the technique of using the stacked image data and the time filter, the estimate-modifying approach is also efficient. The method is straightforward but needs much computer time.

The presented results have been obtained without spatial filtering because the gains in the correlation for some important stand characteristics were rather weak.

The results in Tables 4.24 and 4.25 confirmed the inference. The accuracy of using spatial filtering is quite close to that without spactial filtering (see the technique "only using ID-85" in Tables 24 and 25) except the tree species composition (pine and spruce) which achieves more gains in the correlation by means of spatial filtering. It implies that spatial filtering may help in the estimation of those variables which are not very sensitive to the position of the image points, or less correlated with image data, such as species composition and most of the qualitative variables.

The test of updating data for sample case I1P12 is not in the present study since the basic method is the same as when using single image data for the stratification. The difference is only that the image data is old while the measurements are new. The partition of the cut area is necessary for this updating.

The key point of updating data in sample case I12P1 is how to normalize the two imageries to the same level. An attempt to normalizing ID-84 and ID-85 by using the multispectral ratio and vegetation indices failed in this study. In this case, the standardized principal component was chosen for the nor-

Table 4.24. Means, root mean square errors and correlations by using different updating techniques (Unsupervised method).

Updating technique	Variable	Compartments Mean	Compartments RMSE	Compartments Correlation	Image points Mean	Image points RMSE	Image points Correlation
		Data = ID-84 plus ID-85 for occasion 1 (Case I12P1)					
Stacked image data	Volume	124.8	56.3	.834	178.3	91.3	.672
	Age	50.9	20.3	.800	70.5	27.6	.685
	Composition:						
	Pine	4.5	2.5	.664	4.2	3.3	.527
	spruce	3.8	2.3	.690	4.5	3.1	.577
	B.L	1.7	2.0	.535	1.3	1.9	.387
ML-PTL-ML	Volume	124.8	57.9	.822	178.3	90.3	.678
	Age	50.9	20.3	.796	70.5	28.1	.670
	Composition:						
	Pine	4.5	2.5	.669	4.2	3.2	.554
	spruce	3.8	2.0	.821	4.5	3.0	.616
	B.L	1.7	1.9	.600	1.3	1.9	.425
ML-ML	Volume	124.8	57.2	.829	178.3	90.0	.681
	Age	50.9	19.9	.811	70.5	27.8	.680
	Composition:						
	Pine	4.5	2.5	.665	4.2	3.2	.555
	spruce	3.8	1.9	.832	4.5	3.0	.628
	B.L	1.7	1.8	.656	1.3	1.9	.454
Estimate-modifying	Volume	124.8	54.4	.853	178.3	—	—
	Age	50.9	20.0	.807	70.5	—	—
	Composition:						
	Pine	4.5	2.6	.650	4.2	—	—
	spruce	3.8	2.1	.777	4.5	—	—
	B.L	1.7	2.6	.430	1.3	—	—
Time filtering	Volume	124.8	56.2	.831	178.3	90.0	.684
	Age	50.9	19.8	.811	70.5	27.2	.700
	Composition:						
	Pine	4.5	2.8	.555	4.2	3.4	.500
	spruce	3.8	2.2	.753	4.5	3.0	.631
	B.L	1.7	2.1	.479	1.3	2.0	.252
		Data = ID-85 for occasion 1 (Case I1P1)					
Only using ID-85	Volume	124.8	59.6	.810	178.3	91.5	.669
	Age	50.9	21.3	.784	70.5	28.5	.658
	Composition:						
	Pine	4.5	2.5	.675	4.2	3.2	.558
	spruce	3.8	2.2	.721	4.5	3.1	.583
	B.L	1.7	1.8	.730	1.3	1.8	.484
Spatial filtering	Volume	124.8	58.7	.814	178.3	91.9	.662
based on ID-85	Age	50.9	22.3	.743	70.5	28.4	.660
	Composition:						
	Pine	4.5	2.4	.707	4.2	3.1	.591
	spruce	3.8	2.3	.710	4.5	3.1	.608
	B.L	1.7	1.9	.612	1.3	1.8	.470

Table 4.24 cont.

Updating technique	Variable	Compartments Mean	Compartments RMSE	Compartments Correlation	Image points Mean	Image points RMSE	Image points Correlation
Updating data based on	Volume	124.8	59.1	.812	178.3	92.3	.655
the old model	Age	50.9	22.1	.753	70.5	30.4	.600
	Composition:						
	Pine	4.5	2.7	.636	4.2	3.4	.476
	spruce	3.8	2.2	.776	4.5	3.0	.604
	B.L	1.7	2.4	.050	1.3	2.3	−.041

malization. The old image data and the measurements were used in clustering, building the MD classifier and for calculating the estimates of the stand characteristics in the strata. The new image data was used for determining the stratum code for the image points in the compartments based on the old MD classifier. The effect shown in Tables 4.24 and 4.25 are close to those obtained from sample case I1P1 (using image data ID-85).

Although the standardized principal transformation used in the study succeeded in normalizing the two imageries, there is still a problem of lacking the fresh ground observations. With a long inventory interval, the old ground observations may not cover all the combinations of the present forest. Further, the normalizing of image data may also remove the image changes generated from the forest growth. The technique of normalizing the image data and maintaining the effect of the forest growth requires further developement.

Table 4.25. Estimation accuracies of the qualitative variables by using different updating techniques (unsupervised method).

Updating technique	Compartments Tax. class	Compartments Site class	Compartments Main species	Compartments D.V class	Image points Tax. class	Image points Site class	Image points Main species	Image points D.V class
	Data = ID-84 and ID-85 for occasion 1 (Case I12P1)							
Stacked image data	63	69	75	49	48	64	72	47
ML-PTM-ML	63	67	73	53	47	61	73	47
ML-ML	63	66	75	55	47	61	73	46
Time filtering	61	69	73	50	46	61	74	46
Estimate-modifying	63	70	73	47	—	—	—	—
	Data = ID-85 for occasion 1 (Case I1P1)							
only using ID-85	63	70	73	44	48	64	72	48
Spatial filtering	63	73	72	53	48	63	74	46
Updating data based on the old model	53	52	73	46	43	53	72	43

5. EFFICIENCY ANALYSIS

51. Precision analysis

511. Estimation of the population parameters using the the multitemporal image and field data

The multiple correlation coefficient of the spectral bands with a field variable is equivalent to that of a canonical variable of these spectral bands with the field variable. In this connection, the following analysis is based on two canonical variables which are transformed with respect to a certain field variable on two occasions respectively.

In practice, the sample variances and the correlation coefficients will be used in the expressions below instead those for the population.

Let c_1 = canonical variable on occasion 1
c_2 = canonical variable on occasion 2
$\bar{c}_{1p}$ = mean value of the canonical variable of the permanent plot sample on occasion 1, i.e. $\sum_{i=1}^{np} c_{1,i} / n_p$
$\bar{c}_{1I}$ = mean value of the canonical variable of the image sub-sample on occasion 1, i.e. $\sum_{i=1}^{ni} c_{1,i} / n_I'$
c_{2p} = mean value of the canonical variable of the permanent plot sample on occasion 2
$\bar{c}_{2I}$ = mean value of the canonical variable of the image sample on occasion 2
x_1 = field variable on occasion 1
x_2 = field variable on occasion 2
$\bar{x}_{1p}$ = mean value of the field variable on occasion 1
$\bar{x}_{2p}$ = mean value of the field variable on occasion 2

Then, a minimum variance linear estimate $\hat{\bar{x}}_2$ of μ_2 (population mean of x_2) in Ware and Cunia's way (1962) can be rewritten as follows:

$$\hat{\bar{x}}_2 = \bar{x}_{2p} + A(\bar{c}_{1p} - \bar{c}_{1I}) + B(\bar{c}_{2p} - \bar{c}_{2I}) \quad (5.1)$$

where A and B are unknown coefficients to be estimated. Noting that pairs $\bar{x}_{2p}$ and $\bar{c}_{2p}$, $\bar{x}_{1p}$ and $\bar{c}_{1p}$, $\bar{c}_{2p}$, $\bar{c}_{1I}$ and $\bar{c}_{2I}$ are related to each other, we can express the variance of $\hat{\bar{x}}_2$ as follows

$$s^2_{\hat{\bar{x}}_2} = s^2_{x_2}/n_p + A^2 s^2_{c_1}(1/n_p + 1/n_I') + B^2 s^2_{c_2}(1/n_p + 1/n_I') + 2As_{x_2} s_{c_1} r_{x_2,c_1}/n_p + 2Bs_{x_2} s_{c_2} r_{x_2,c_2}/n_p + 2ABs_{c_1} s_{c_2} r_{c_1,c_2}/n_I' \quad (5.2)$$

where all the sample variances and correlation coefficients are calculated from the permanent plot sample.

Minimizing $s^2_{\hat{\bar{x}}_2}$ with respect of A, B, we have the following results:

$$A = f'(s_{x_2}/s_{c_2})(r_{x_2,c_1} r_{c_1,c_2} - r_{x_2,c_2})/(1 - r^2_{c_1,c_2})$$

$$B = f'(s_{x_2}/s_{c_1})(r_{x_2,c_2} r_{c_1,c_2} - r_{x_2,c_1})/(1 - r^2_{c_1,c_2})$$

and

$$s^2_{\hat{\bar{x}}_2} = s^2_{x_2}(1 - f' r^2_{x_2,c})/n_p \quad (5.3)$$

where $f' = n'/n_I'$ and $n' = n_p + n_I'$

$$r^2_{x_2,c} = (r^2_{x_2,c_1} + r^2_{x_2,c_2} - 2r_{x_2,c_1} r_{x_2,c_2} r_{c_1,c_2})/(1 - r^2_{c_1,c_2}) \quad (5.4)$$

It can be seen that $r_{x_2,c}$ is exactly the same as equation (23.7). It implies that the GLS coincides with time filtering which maximizes the correlation between the bitemporal image data and the field variable. It also means that the GLS does not only minimize the variance of the estimate of the mean of a field variable, but also results in a single image variable which has the highest correlation with the variable.

Formula (5.4) can be rewritten as the following expression:

$$|r_{x_2,c}| = |r_{x_2,c_2}| G_{x_2} \quad (5.5)$$

where G_{x_2} is the gain in the correlation

$$G_{x_2} = [1 + (q_{r_x} - r_{c_1,c_2})^2/(1 - r^2_{c_1,c_2})] \quad (5.6)$$

and

$$q_{r_x} = r_{x_2,c_1}/r_{x_2,c_2} \text{ (suppose } |r_{x_2,c_2}| > |r_{x_2,c_1}|)$$

From (5.5) and (5.6), it could be concluded that

(1) $|r_{x_2,c}| \geq |r_{x_2,c_2}|$ i.e. $G_{x_2} \geq 1$ holds in any cases.

If $r_{x_2,c_1} = r_{x_2,c_2} r_{c_1,c_2}$, i.e. $q_{r_x} = r_{c_1,c_2}$, then $r_{x_2,c} = r_{x_2,c_2}$ This is the case that the new image data does not contain any new information concerning the correlation between the image data and the field variable. In this case, the bitemporal image cannot improve the precision in estimating the current state of the field variable and it acts as a unitemporal image data. Beyond this exception, the bitemporal image data alway is more effective than the unitemporal image data.

(2) If $r_{c_1,c_2} > 0$ and $q_{r_x} > r_{c_1,c_2}$, $|r_{x_2,c}|$ will decrease with increase of r_{c_1,c_2}. Then the case with unmatched image data in the image subsample is more effective than the case with the matched image data in order to estimate the current state of the field variable. This is why case I1I2P12 in Table 4.12 is better than case I12P12 in estimating the current state. In many cases $q_{r_x} > r_{c_1,c_2}$. Therefore, the matched case is not best suited for estimating the current state of the field variable.

(3) If $r_{c_1,c_2} > 0$ and $q_{r_x} < r_{c_1,c_2}$, $|r_{x_2,c}|$ will increase with r_{c_1,c_2}. The case is opposite to the previous one but probably rarely occurs, unless very big change would appear in the forest. Based on the equations listed above, it is apparent that the correlation coefficient provides direct information on the precision of the estimation on the current state of the field variable (see (5.3)). To estimate the current state of the field variable, the correlation of the unitemporal image data with the field variable is still most important. The gain in the correlation by using the bitemporal image data depends upon how much new information is carried by the new image.

For estimating the change of the field variable during an interval, the estimate $\hat{D}$ and its variance $s^2_{\hat{D}}$ can be derived in the same way:

$$\hat{D} = \bar{x}_{2p} - \bar{x}_{1p} + A_D(\bar{c}_{1p} - \bar{c}_{1I}) + B_D(\bar{c}_{2p} - \bar{c}_{2I}) \quad (5.7)$$

where A_D and B_D are the parameters to be estimated, and after minimizing the variance of $\hat{D}$, we have

$$s^2_{\hat{D}} = s^2_D(1 - f' r^2_{D,c})/n_p \quad (5.8)$$

where

$$s^2_D = s^2_{x_1} + s^2_{x_2} - 2s_{x_1} s_{x_2} r_{x_1,x_2} \quad (5.9)$$

$$r^2_{D,c} = (r^2_{D,c_1} + r^2_{D,c_2} - 2r_{D,c_1} r_{D,c_2} r_{c_1,c_2})/(1 - r^2_{c_1,c_2}) \quad (5.10)$$

$$r_{D,c_1} = (s_{x_2} r_{x_2,c_1} - s_{x_1} r_{x_1,c_1})/s_D \quad (5.11)$$

$$r_{D,c_2} = (s_{x_2} r_{x_2,c_2} - s_{x_1} r_{x_1,c_2})/s_D \quad (5.12)$$

$$A = f'(s_D/s_{c_2})(r_{D,c_1} r_{c_1,c_2} - r_{D,c_2})/(1 - r_{c_1,c_2})$$

$$B = f'(s_D/s_{c_1})(r_{D,c_2} r_{c_1,c_2} - r_{D,c_1})/(1 - r^2_{c_1,c_2})$$

(5.10) can be also rewritten in the manner of expression (5.4)

$$|r_{D,c}| = |r_{D,c_2}| G_D \quad (5.13)$$

where

$$G_D = [1 + (q_{r_D} - r_{c_1,c_2})^2/(1 - r^2_{c_1,c_2})] \quad (5.14)$$

$q_{r_D} = r_{D,c_1}/r_{D,c_2}$ and assume $|q_{r_D}| \leq 1$.

Although (5.13) and (5.5) are identical in form, $|r_{D,c}|$ in (5.13) is often much lower than $|r_{x_2,c}|$ in (5.5) because $|r_{D,c_2}|$ in (5.12) is much lower than $|r_{x_2,c_2}|$ in (5.5). On the other hand, q_{r_D} is more commonly negative, and r_{c_1,c_2} is mostly positive. Then G_D will increase with r_{c_1,c_2}. It implies that the matched case is, more often, better than the unmatched case for estimating changes in the forest. In addition, the gain G_D is often greater than the gain G_{x_2} simply because, in comparison with the unitemporal image data, the bitemporal image data offers more information concerning the forest change.

If the change intensity is large as in the case of clear cutting, the increase in $|r_{D,c}|$ arises mainly due to the increase in $|r_{D,c_2}|$ rather than that in G_D. On the other hand, if the quality of the image data were to be improved, the major increase in $|r_{D,c}|$ might be due to the increase in G_D. In the case of Landsat TM, the increase in $|r_{D,c}|$ mostly relies on the r_{D,c_1} rather than G_D. In other words, the detection of forest change depends more on the nature of forest change than on the image data.

Table 5.1 presents the correlations between x_2 (and D) and the canonical variables for spectral bands, and the corresponding gains for different images and occasions.

In Table 5.1 the gain in the correlation concerned with the net increase of volume is

Table 5.1. Correlations of x_2 and D with the canonical variables and the associated gains.

For volume on the present occasion					For net increase of volume between two occasions			
$r_{1,2}$	r_{c_1,c_1}	r_{x_2,c_2}	$r_{x_2,c}$	G_{x_2}	r_{D,c_1}	r_{D,c_2}	$r_{D,c}$	G_D
Data = bitemporal image data (ID-84 plus ID-simu1)								
From occasion 1 to occasion 2:								
.502	−.592	−.643	−.715	1.11	.096	−.051	.150	1.56
From occasion 2 to occasion 3:								
.438	−.520	−.679	−.723	1.06	.141	−.507	−.649	1.28
Data = bitemporal image data: ID-84 plus ID-85								
Occasion 1:								
.785	−.637	−.636	−.675	1.06	–	–	–	–

greater than the gain in the correlation with the current state of volume, although the correlation for the net increase of volume is lower than that for the current state of volume.

In addition, the high correlation between the image variable and the net increase from occasion 2 to occasion 3 is primarily due to high r_{D,c_2} and not to gain G_D. The reason why r_{D,c_2} from occasion 2 to occasion 3 is so high is that the spectral values of the cut area are located at the end of the radiation distribution. In this case even the unitemporal image data can be used for effectively estimating the net increase.

In spite of the difficulty of detecting a small change with the aid of TM image data, the reduced correlation between measurements on two occaions could be partly offset by using the bitemporal image data. This is because the large change can be effectively separated out.

512. Effective ranges of the filter weights

The analysis made above is also applicable for the time filtering or spatial filtering based on maximizing the correlation between the image and field variables. However, the determination of the weights of the filters is a key step when filtering in a forest inventory. Although the optimum weights can be calculated theoretically, in practice the weights are estimated on the basis of the sample. It follows that the estimated weights might not be optimal. The applicability of the filters can be questioned if the weights are not optimal. In this section, we discuss the question of the effective weight ranges for the filter.

The effective weight range here means that the weight within the range will produce a weighted image variable which is more strongly correlated to the field variable than the original image variable.

The following expression is derived from (23.2)

$$r_{x,c} = (w_1 s_{c_1} r_{x,c_1} + w_0 s_{c_2} r_{x,c_2})/$$

$$(w_1^2 s_{c_1}^2 + w_0^2 s_{c_2}^2 + 2w_1 w_0 s_{c_1} s_{c_2} r_{c_1,c_2})^{1/2} \qquad (5.15)$$

where x denotes the field variable like x_2 or D.

Equation (5.15) can be rearranged as follows:

$$r_{x,c} = r_{x,c_2} (q_s q_w q_r + 1)/$$

$$(q_s^2 q_w^2 + 1 + 2q_s q_w r_{c_1,c_2})^{1/2}$$

where $q_s = s_{c_1} / s_{c_2}$

$q_w = w_1 / w_0$

$q_r = r_{x,c_1} / r_{x,c_2}$

Let $|r_{x,c_2}| \geq |r_{x,c_1}|$, then $|q_r| \leq 1$.

In order to enable $|r_{x,c}| > |r_{x,c_2}|$, we have

Table 5. 2. The optimum weights and the effective weight ranges for time filters.

For the current state of volume		For the net increase of volume between two occasions	
Optimum weight	Effective weight range	Optimum weight	Effective weight range
Data = bitemporal image data (ID=84 plus ID-simu1)			
From occasion 1 to occasion 2:			
$w_1 = .44$	$0 < w_1 < .84$	$w_1 = 5.43$	$w_1>1$ or $w_1<-.53$
$w_0 = .56$	$.26 < w_0 < 1.0$	$w_0=-4.43$	$w_0<0$ or $w_0>1.53$
From occasion 2 to occasion 3:			
$w_1 = .33$	$0 < w_1 < .85$	$w_1=-1.77$	$w_1<0$ or $w_1> 2.82$
$w_0 = .67$	$.15 < w < 1.0$	$w_0 = 2.77$	$w_0>1$ or $w_0<-1.82$
Data = bitemporal image data (ID-84 plus ID-85)			
Occasion 1:			
$w_1 = .50$	$.01< w_1 < 1.0$	—	—
$w_0 = .50$	$0 < w_0 < .99$	—	—

$$q_w > 2 (r_{c_1,c_2} - q_r)/[q_s (q_r^2 - 1)] \text{ if } q_w < 0 \qquad (5.16)$$

$$q_w < 2(r_{c_1,c_2} - q_r) / [q_s (q_r^2 - 1)] \text{ if } q_w > 0 \qquad (5.17)$$

When $s_{c_1} = s_{c_2}$, (5.16) and (5.17) can be simplified as follows:

$$q_w > 2(r_{c_1,c_2} - q_r) / (q_r^2 - 1) \text{ if } q_w < 0 \qquad (5.18)$$

$$q_w < 2(r_{c_1,c_2} - q_r) / (q_r^2 - 1) \text{ if } q_w > 0 \qquad (5.19)$$

Then the effective weight ranges of w_0 and w_1 can be obtained in accordance with $w_0 + w_1 = 1$ and q_w.

Table 5.2 is based on equations (5.5), (5.15), (5.18) and (5.19). From Table 5.2 it can be seen that the effective weight range is rather wide if the variances and correlations of the two original image variables (or the weights) for two occasions are close to each other. This is especially so if they are almost equal (see the results of the bitemporal image data ID-84 plus ID-85 in Tables 5.1 and 5.2). In this case, the effective weights cover almost the whole range from 0 to 1.The effective weight ranges for the time difference filters are larger than those for the time summation filters. A spectial feature of weights of the difference filter is that they are situated outside range 0−1. It seems that for time filtering the weights of filters may not be the optimal, though in many cases some gain in the correlation still can be obtained to varying degrees.

The weights of the spatial filter differ from the time filter in that it gives more weights to the central image pixel or the first nearest pixel for most spectral bands. In other words, the weight of the central pixel or the first nearest pixel is closed to 1. Consequently, the effective weight range for these filters becomes narrow. Accordingly, there is a danger that the weights from the sample may be located outside the effective range. In this case the correlation becomes weaker after filtering. On the other hand, if the weight of the central pixel approaches 1, the gain in the correlation is so small that it can almost be ignored. Under the circustance, spatial filtering for these bands is not essential.

513. Estimation of a compartment characteristic

Let x_c be a random variable in a compartment, then x_c can be expressed as follows:

$$x_c = \mu_c + (x_c - \mu_c) = \mu_c + \varepsilon \qquad (5.20)$$

where μ_c = mean value of x_c in the compartment

$\varepsilon = x_c - \mu_c$ = random error with 0 mean value and the variance of x_c in the compartment

In stratified sampling, with a random distribution of the sample plots, a certain characteristic of an arbitrary image point in the compartment, can be similarly estimated from

$$\hat{x}_{c,i} = \bar{x}_j + \varepsilon_j \qquad (5.21)$$

where $\hat{x}_{c,i}$ = estimate of the characteristic of interest at image point i in the compartment

$\bar{x}_j$ = sample mean value of the characteristic in stratum j to which the image point belongs

ε_j = random error with 0 mean value and the variance of the characteristic in stratum j

Note that both $\bar{x}_j$ and ε_j in (5.21) are random variables at the moment. Suppose that $\bar{x}_j$ and ε_j are independent of each other, then the variance of $\hat{x}_{c,i}$ within a stratum can be approximately denoted by the following expression:

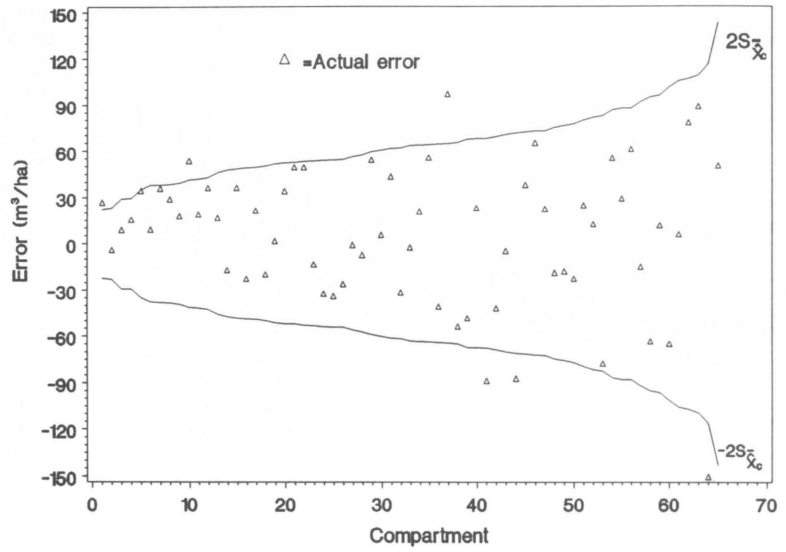

Figure 5.1. Standard errors and actual errors of estimates of volume in the compartments (which are arranged in a ascending order by positive standard errors of volume).

$$s^2_{\bar{x}_{c,j}} = s^2_{\bar{x}_j} + s^2_{x_j} \qquad (5.22)$$

where $s^2_{\bar{x}_j}$ = sample variance of $\bar{x}_j$

$s^2_{x_j}$ = variance estimate of ε_j

It is apparent that for the case of n'_{c_j} image points drawn from stratum j and when $\bar{x}_j$ is still used as the estimate of the mean of these image points, equation (5.22) will become

$$s^2_{\bar{x}_{c,j}} = s^2_{\bar{x}_j} + s^2_{x_j} / n'_{c_j} \qquad (5.23)$$

Equation (5.23) implies that the first part in the right hand side, i.e. the variance of the stratum mean value, does not change with an increase in the number of image points as long as the mean value is used as the estimate of these image points.

If there are n'_c image points are systematically or randomly allocated in a compartment, the variance of the average value of estimate $\hat{x}_j$ over these image points can be approximately expressed as follows:

$$s^2_{\hat{\bar{x}}_c} = \sum_j w_j s^2_{\bar{x}_j} + \sum_j w_j s^2_{x_j} / n'_c \quad j = 1, 2, \ldots, L_c \qquad (5.24)$$

where $w_j = n'_{c_j} / n'_c$

L_c = number of strata in the compartment

In practice, the plots within a stratum may not be distributed according to the statistical assumptions, especially in a large forest area. Then equation (5.24) may lead to bias.

Figure 5.1 illustrates the standard errors $s_{\hat{\bar{x}}_c}$ calculated from (5.24), and the actual errors, which are the differences between the estimates and measurements of volume for all 65 compartments. It can be seen that 90 % of the actual errors fall in the range of $\pm\, 2s_{\hat{\bar{x}}_c}$. As autocorrelation exists between the neighboring image points, the variances in (5.24) might be underestimated.

Assume that the first part in the right-hand of (5.24) could be replaced by s^2_x / n_p, where s^2_x is the sample (permanent plots) variance of the field variable, and $\Sigma\, w_j\, s^2_{x_j}$ could be approximately denoted by the residual mean square of a linear model formed by the image and field variables, then the following expression can be derived from (5.24)

$$n'_c / [n'_c / n_p / (1-r^2) + 1] = t^2\, c^2\, (1-r^2) / E^2 \qquad (5.25)$$

where t = t-statistic

c = coefficient of variation of the field variable, %

E = allowable error for the estimate in the compartment, %

r = correlation coefficient between the field and image variables

(5.25) can be used for investigating the effect of the correlation on the precision of the estimates in the compartments with different sizes. Of course, (5.25) is not adequate for every compartment, but it can help us to see the relationship between the correlation coefficient, the precision and the compartment size. The distributions and the variation of the compartments in (5.25) represent an average level in the investigated area.

Assume that an image point in a compartment represents a forest area of .09 hectares (30 m × 30 m). Under the condition of c = 70 % for the volume in the study area and different r-values, Table 5.3 shows the desired numbers of the image points in the assumed compartment for the given E based on equation (5.25).

According to (5.25), for an allowable error of 30 % the minimum number of image points in a compartment in the study is 12. In this case, 51 % of compartments can attain the given precision. Actually, about 60 % of compartments in the area reached this level (see Figure 4.14). When the correlation rises to .95, with an allowable error of 20 %, the minimum number of image points in a compartment is 2.2. about 82 % of the compartments should attain the given precision according to (5.25). Actually, about 90 % of compartments in the area reached this level based on data ID-simu2 in which volume is highly correlated to the image data.

In Table 5.3, we find that image data with a TM-like quality remains ineffective for a small compartment, e.g. 1 hectare. It can also be seen that the size of the compartment has an effect on the the estimate, though the relationship between E and n'_c weakens with the increase of n'_c, especially when n'_c is greater than n_p. Figure 5.2 demonstrates the relationship between the number of image points and E.

By using the supervised method, the variance of the estimates for each of image points

Table 5.3. Correlations, precisions and numbers of the image points in compartments.

	r = .7	r = .8	r = .9
E = 30 %:			
n'_c	12	8	5
Area (ha)	1.0	.7	.5
E = 20 %:			
n'_c	26	18	10
Area (ha)	2.3	1.6	.9
E = 10 %:			
n'_c	101	71	38
Area (ha)	9.1	6.4	3.4

in the compartment comes from two sources: one is the probabilities (proportions) of strata; another refers to the variances of the mean values of the variable in all the possible classes. Assume that the probability (proportion) and the mean value of the field variable in the class are independent of each other, then the final variance of the estimate of the variable at an image point can be derived according to the theory on the error propagation of two independent variables.

52. The number of permanent sample plots and image points

The number of sample plots for a variable can be derived from equation (5.3). Accordingly

$$n_p = t^2\, c^2\, (1 - f'\, r^2) / E^2 \qquad (5.26)$$

where c = coefficient of the variation of a field variable, %

E = allowable error, %

t = t-statistic

r = correlation coefficient between the image variable and the field variable

$f' = n'_i / n'$

When r, E and c are given, the question is how to decide f '.

The total cost of the two-phase sampling can be expressed as follows:

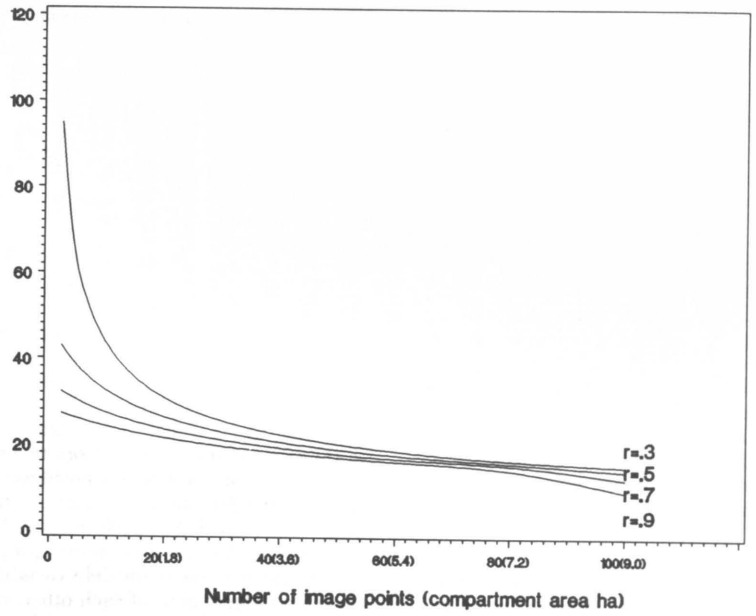

Figure 5.2. Precisions and numbers of image points for the compartment.

$$c_T = c_F + c_{TI} + c_{Tp} \quad (5.27)$$

where c_F = fixed cost
c_{TI} = total cost of the image points
c_{Tp} = total cost of the permanent sample plots

The total cost of the permanent sample plots can be estimated on the basis of the average cost of a permanent sample plot. The total cost of the image points may not be so estimated. The average cost of an image point depends on how the points are selected and charged.

If the image material used in the forest inventory could be picked and charged by the small image windows which are around the image points or the sample plots, the number of the permanent sample plots and the image points can be calculated by (5.26) and by the following expression (Cochran 1977, p. 341)

$$n_p/n' = [c_I (1-r^2)/r^2 c_p]^{1/2} \quad (5.28)$$

where c_I = cost of the unit image point
c_p = cost of the unit permanent sample plot

Suppose that the window size of the image point is 7 × 7 pixels (210 × 210 m), the cost of a single image point in Finland is shown as follows:

Number of image points	Cost of the unit image point
1 000	2.6 FM
5 000	.9 FM
10 000	.7 FM
> 20 000	.6 FM

In order to evaluate the cost of a unit permanent sample plot, we have to confine the discussion to some given conditions.

On the basis of the national forest inventory in southern Finland during recent years,

(1) the sample plots are specified as i) a circular plot of .03 hectares and ii) a relascope plot with BAF 2;
(2) the number of the sample trees measured accurately for each sample plot is about two on average;
(3) the distance between sample plots is 400 m, i.e. in a large area the lay-out of the sample plots would be non-uniform or tractwise;
(4) the basic work in a sample plot includes determining the locations of the plot and trees, tree tally, measuring sample trees and stump survey;
(5) the working group in the field work consists of three persons using the car as the means of travel.

Table 5.4. The costs of the permanent sample plots.

Traveling distance (km/day)	Completed number of the sample plots per group in a working day		Cost of the unit sample plot (FM)	
	Circular plot	relascope plot	Circular plot	Relascope plot
20	4.6	6.2	343	258
50	4.3	5.8	386	295
80	4.0	5.4	437	338

Under the above assumptions, the main difference in the costs of the permanent sample plots in a large area compared with a small area is determined by the travelling time.

According to the results of the national forest inventory in Finland during 1984–1985, and following the assumptions specified above, the costs of the permanent sample plots with respect to distance are presented in Table 5.4.

Comparing the results listed in Table 5.4 with those concerning the cost of the unit image point listed above, the ratio c_I/c_p is placed within the range 1/100 to 1/700.

It should be noted that the ratio c_I/c_p obtained above is mostly for the net increase of volume. If the variables of interest are concerned with proportions such as land-use classes and main species, as could be expected, the ratio c_I/c_p would be much larger than that for the net increase of volume. Even for the volume, the ratio might be greater than 1/200 since an inventory for this purpose may only require temporary sample plots.

Table 5.5 presents the values of n_p/n' with regard to different r-values and the ratio c_p/c_I. The best n_P/n' is around 1/11 for r = .6 under c_I/c_p = 1/200.

When the allowable size of the image material which should be purchased is at least a quarter of the image scene other than the image window around the image point, the total cost of the image points largely depend on the investigated area rather than on the number of the image points. In this case, the prerequisite of using the image data profitably in the two-phase sampling is that

$$f' r^2 > c_{TI}/c_{TP} \quad (5.29)$$

Table 5.5. Ratio n_p/n' and $1\text{-}f'r^2$ as a function of r and c_p/c_I.

	c_p/c_I = 100		c_p/c_I = 200		c_p/c_I = 300		c_p/c_I = 600	
r	n_p/n'	$1\text{-}f'r^2$	n_p/n'	$1\text{-}f'r^2$	n_p/n'	$1\text{-}f'r^2$	n_p/n'	$1\text{-}f'r^2$
.2	.49	.980	.35	.974	.28	.971	.20	.968
.4	.23	.877	.16	.866	.13	.861	.09	.768
.6	.13	.687	.09	.672	.08	.669	.05	.658
.8	.08	.411	.05	.392	.04	.386	.03	.379
.9	.05	.230	.03	.218	.03	.214	.02	.206

Figure 5.3 illustrates the profitable region of using image data in the CFI in relation to c_I/c_p and $f'r^2$.

Since the price of the image data is rather low, in most cases the image data used in the forest inventory would be finacially acceptable.

53. The feasibility of using satellite imagery

In Table 5.5 $(1-f'r^2)$ indicates the reduction of the permanent sample plots by means of the two-phase sampling.

If the fixed cost is excluded , the cost ratio of the CFI with the image data to the CFI without the image data, for the same given precision, can be expressed as follows:

$$e_c = (1-f'r^2)[1 + (r^2 c_I/c_p)^{1/2}/(1-r^2)^{1/2}] \quad (5.30)$$

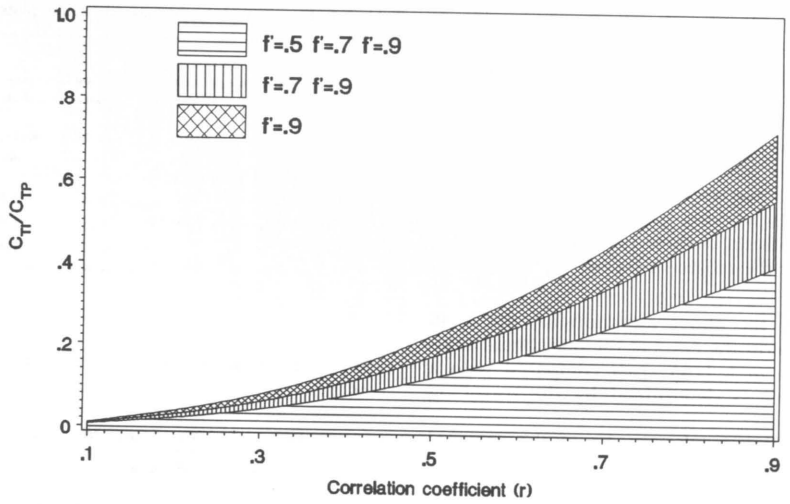

Figure 5.3. Rational areas of C_{TI}/C_{TP}.

The e_c with regard to the different f', c_I/c_p, and r are presented in Table 5.6. It is clear that under the assumption that the image data can be picked and charged in terms of the image windows around the image points, the use of the permanent sample plots with the image data is effective, especially for those variables which are highly correlated with the image variable.

The cost of a compartmentwise estimation using satellite imagery consists of two parts: one is the cost of the image material and the computer processing time used in the estimation of the compartments; the other is the shared unit area cost from the CFI in the whole area.

Since the cost of the first part of the compartmentwise estimation is rather low (less than 1 FM/ha), the main expenditure of the compartmentwise estimation arises from the second part which depends on the extent of the inventory population in the two-phase sampling.

Suppose the numbers of sample plots are 500, 1 000 and 2 000, and the associated forest inventory areas are 2 000, 100 000 and 500 000 hectares, then the costs (with circular plots and relascope plots in parentheses) are 9 (7) FM/ha,4 (3) FM/ha and 2 (1) FM/ha respectively under the assumptions given in section 5.2.

Table 5.6. Cost ratio of an inventory with image data to an inventory without image data.

	f' = .8			f'=.9		
	c_I/c_p			c_I/c_p		
r	1/100	1/300	1/600	1/100	1/300	1/600
.2	.988	.979	.976	.984	.975	.972
.4	.910	.894	.888	.893	.878	.871
.6	.765	.743	.734	.727	.705	.697
.8	.553	.526	.515	.481	.457	.447
.9	.425	.394	.382	.327	.303	.294

In comparison with the cost of the traditional compartmentwise survey (i.e. total cost is around 45 FM/ha, with field work is around 20–30 FM in recent years) the cost of the comparmentwise estimation when using satellite imagery listed in the previous paragraph remains rather small, especially if the sampling population is large. An important prerequisite for this comparison is that the estimation must be reliable.

For operative forest planning which requires rather precise estimates for every comparment, the comparment-oriented estimation using image data could not offer satisfactory estimates for the small compartments. This problem can be partly solved with the help of the supplementary information such as old inventory results or map material. Extra field work, however, is inevitable in operative forest planning. How much extra field work should be added depends on the accuracies of the estimates to which the estimation aspires and the given precision requirement.

In a continuous forest inventory of a large area, the comparment-oriented estimation is an extra benefit. With its low cost, the estimation might reduce the cost of the operative forest planning.

6. DISCUSSION AND CONCLUSIONS

The study has focused on how to combine multitemporal image and field data in both continuous forest inventories and compartmentwise estimations.

The integration of the image data with permanent sample plots is a natural extention of the traditional SPR. With its minimum variance, the GLS method has been shown to be an effective way of handling a variety of cases.

For estimating the current state of a field variable which has a fairly high correlation with the image data, the combination of image data and sample plots is demonstrating quite effective. Perhaps the unitemporal image data is enough for the estimation. The gains in the correlation when using Landsat TM bitemporal image data are around 5–10 % in the study area.

For estimating change in the forest, the role of multitemporal imageries in a continuous forest inventory is that of a "classifier" which classifies a large change into smaller changes. As a result, the effect of the correlation reduction on estimaing forest change will be alleviated by multitemporal image data. Bitemporal image data can effectively detect large changes such as clear cutting. The advantage of partitioning the large change becomes evident in this case. To determine a small change, such as thinning, the TM image data proved to be ineffective in the study area. The estimation precision in this case depended mostly on permanent sample plots.

Availability of cheap image data compared with laborious compartmentwise surveying, as well as the presence of permanent sample plots over a large area further encourages the compartment-oriented estimation.

The application of the multitemporal image data to the compartmentwise estimation can be accomplished using a space-time model (see Bennett 1979) as follows:

$$Y_t = SU_t \qquad (6.1)$$

where Y_t : output
U_t : input
S : transfer function

In (6.1) the image data, with its spatial and temporal distribution, can be viewed as the input and the estimates of the target variables would be the output.

In reality, it seems that the input and output in (6.1) should be exchanged, i.e. the image data should be the output and vice versa. For the purpose of the present application, (6.1) can be thought of as the inverse transformation of the real model. The transfer function is the key part of the model. Indeed, most parts of this investigation deal with the transfer function, which includes: the spatial filter, time filter, transformation, discriminant function, estimation models for compartments, etc.

The filtering for both spatial and time series can be used for maximizing the correlation of the filtered image variable with the target variable. The gain in the correlation can be estimated through the sample.

Where the imagery is well registered, any gain in the correlation by using the filtering of spatial series for most quantitative variables is likely to be low. The filtering may help to improve the correlation for only those variables which are less correlated with the image variables or which change over space smoothly. Spatial filtering is therefore suitable for special applications, e.g. the classification of the site class.

The filtering of time series for multitemporal imageries with a short interval is more effective than spatial filtering. It is convenient to handle multitemporal image data for estimating the current state of a field variable. For estimating both the current state and change of a field variable simultaneously, a transformation such as P.C or C.V is convenient.

The advantage of time filtering is that it can maintain the respective feature for every spectral band after filtering so that the filtered material can be used in other applications.

In a multiparameter inventory, the principal component transformation, especially the standardized one, corresponds well to the unsupervised method. When multitemporal image data are available, the selection of only the important bands for the transformations should perhaps be considered.

The canonical variable transformation can be specialized for a certain target variable (especially in the case of quantitative variables). It might be used to enhance the estimation effect of a variable peculiarly. Both the P.C and C.V transformations can complement each other.

The problem with the vegetaion index transformation is how to determine the effective transformation coefficients. The vegetation index transformation employed in this investigation were effective in the estimation, but it did not succeed in normalizing the image data for the biomass.

Pre-stratification is necessary. In particular, the area should be divided into cut and non-cut subareas when estimating forest changes.

Clustering can result in clusters which are, to a large extent, a response to the actual distribution of the objectives. It may also produce the over-large clusters. The ML iteration may be helpful for adjusting the strata. Equal interval classifying may be more effective for a homogeneous forest area. Both MD (minimum distance) and ML (maximum likelihood) classifiers are recommended for the unsupervised method because the difference between them is small. Of the two, the MD is less limited. The ML classifier is limited by the minimum number of the sample plots in a stratum. However, where the conditions for the ML classifier are met, it is likely to be better than the alternative.

With respect to the supervised method, the ML classifier has also to be considered in many cases, especially for the qualitative variables.

On the whole, the unsupervised method is fairly adaptable and able to make all the field variables compatible with each other. The estimation accuracies of the major stand characteristics when using the method are almost the same as those achieved when using methods, as demonstrated in this study. These properties are particularly suitable for a multiparameter forest inventory. However, the method may not be the best for all the variables of interest. The shortcomings could be compensated by means of transformations or other pertinent methods.

Stacking the multitemporal image data is a straightforward updating method. It enables the estimation of both the current state and the change of a field variable to be carried out simultaneously.

Without fresh field measurements, the updating of data using only new image data and old models remains problematic. The main difficulty is the normalization of the multitemporal image data.

The precision analysis indicated that for estimating the current state of a field variable, the unitemporal image data perhaps is sufficient. The gain in the correlation for the current state when using bitemporal image data varies from 5 % to 10 % in this study. Image data such as Landsat TM can effectively reveal only large changes. Its efficiency to detect small changes remains poor, although the gain in the correlation when using bitemporal image data for estimating forest change is higher than that in estimates of the current state.

With a short interval and normalized image data, equal weights for a time filter can achieve almost the maximum gain in the correlation for some quantitative variables. At least the effective range of the weights of the time filter are rather large.

Contrary to time filters, the effective range of the weights of a spatial filter may be rather narrow. The precisions of estimates of compartment characteristics depend to a great extent on the correlations, the variation of the characteristics in the area and the compartment size.

For image data such as Landsat TM, the precisions of most compartment characteristics in small compartments of the size less than 1–2 hectares in Finland remain low.

Operative forest planning probably requires extra field work beyond the compartment-oriented estimation when using image data. Although the inventory results obtained with the aid of image data could satisfy the demands of strategic forest planning, some estimates of the stand characteristics which are almost uncorrelated with the image data, such as stoniness, still require checking with the help of ancilliary information, e.g. old forest inventory results and map material.

As long as the image points in the first phase can be selected in terms of image points and associated image windows, the use of

image data is effecient for most field variables in a large forest inventory.

It should be pointed out that the present investigation has spent a great deal of time on the simulation of the multitemporal data by means of trial and error in order to obtain realistic image material. Although the statistical nature of the simulated material was close to realistic, there may be differences between them. Nevertheless, the emphasis of the study has been on the methodological issuses in using multitemporal data rather than real figures. Furthermore, the real data were used to verify the results obtained from the simulated data in many cases. The discussion and conclusions above, are also based on this verification.

7. SUMMARY

Purposes of the study

The study is concerned with the methodology and efficiency of integrating multitemporal image data with permanent sample plots in a continuous forest inventory and compartmentwise estimation.

Material

The study area (192.8 hectares) is located in Hyytiälä, Finland. 1472 relascope sample plots were measured in the field, of which 387 sample plots were used as the permanent sample plots. Two Landsat-5 TM imageries with an interval of nine months were available for the study.

The remeasurements of the sample plots and the associated multitemporal image data for the coming occasions were simulated using the MELA programme and regression models. The correlations between the image data and the important quantitative and qualitative variables were tested with respect to the spectral bands.

Estimation methods

Two estimation methods were used for the population: the generalized least squares (GLS) and two-phase sampling for stratification (TPS). The main method is the GLS estimation. It can cope with a variety of sample cases with minimum variance. The GLS used in the study is designed for estimating the current state and change, as well as the class area transition of field variables based on multitemporal image and field data.

There are also two estimation methods which were applied to the compartmentwise estimation in the study: TPS and regression estimation.

TPS includes two sub-methods, i.e. the supervised and unsupervised methods. The unsupervised method is the main method for the compartmentwise estimation.

A number of statistical techniques or options for the data preprocessing and the stratification are presented and compared. The data preprocessing includes the compartment delineation, image registration, filtering and transformation.

Filtering for both the time and spatial series aimed at maximizing the correlation between the image and the field variable. The optimum weights of a filter and the gain in the correlation can be estimated from the sample.

Two types of spatial filters were assumed. One is the filtering window of size 3 × 3 pixels. The other one is the filter which covers the nearest two or three pixels to an arbitrary image point. The time filtering dealt with only two time points.

Three transformation options were tested. They are the principal component tranformation, the canonical variable tranformation and the vegetation index transformation. In the principal component transformtion, both the standardized and non-standardized methods were examined.

The canonical transformation was computed on the basis of the image and field sample. It was used for maximizing the correlation between the transformed image variable and a special field variable in the study.

The vegetation index transformation was originally developed for extracting the image component concerned with the biomass. Only the first two components, i.e. brightness and greenness were extracted using an othogonal transformation in the study.

In the stratification step, some basic classification options were presented. These options were K-means clustering or equal interval classifying, and the MD (minimum distance) classifier or ML (maximum likelihood) classifier. In addition, the R-square value which here is a ratio of the variances between strata to the total variance, was used for determining the number of strata.

To test the regression estimation, exponential regression models were developed for estimating volume and net increase. Log-linear and logistic regression models were intro-

duced for the qualitative models.

Updating methods concerned with handling multitemporal image and field data through the estimation methods were also presented. Stacking all the available data and making a recursion for the estimates from one occasion to another were two basic ways used in handling the multitemporal data.

Stacking multitemporal data can be used for estimating the current state and change of a certain field variable simultaneously. It is the main updating method via the unsupervised method.

The ML cascade and estimate-modifier are the two recursive updating methods. The ML cascade was initially designed for the supervised method, it can be also used for the unsupervised method.

Results

The study area was delineated into 68 compartments. The image data was registered by shifting the image position and checking the correlations.

By using multitemporal image data, the estimations of the GLS and TPS for the population were conducted for two periods with different cuttings. The results for five sample cases were given for a comparison. For estimating the current states of field variables, the method appeared quite effective. For estimating forest change, the improvement held only for large changes such as clear cutting. The probability transition matrices for the main species and development classes, using GLS, were listed.

A spatial filtering window with 3x3 pixels and a filter composed of the two nearest pixels were tested. The result indicated that the gain in the correlation for volume is low. Higher gains were obtained for the tree species composition.

Two real image data were used for testing the time filtering. The gain in the correlation was higher than that obtained from spatial filtering.

The transformations made on the basis of stacked bitemporal image data indicated that the first principal component or canonical variable was noticably correlated with the current states and the second principal component or canonical variable with forest changes.

The effects of using a part of the bands of multitemporal image data for the transformation appeared to be the same as or even better than when using all the spectral bands with respect to the first three transformed variables for stratification.

For the real data, the canonical transformation gave better estimates than did the principal component transformation.

The results in terms of working steps, using the unsupervised method for the compartmentwise estimation (P.C transformation, K-mean clustering and MD classifier), were illustrated by tables and figures. The number of strata was 34.

The root mean square error and the correlation between the estimates and measurements, as well as the estimation accuracy for the qualitative variables, were used as the criteria for checking the effects of the compartmentwise estimations.

The comparisons were made for the different estimation methods and statistical options in accordance with the three criteria.

According to the test, the effect of using equal interval classifying is almost the same as that of using clustering for some important variables. The experiment also showed that clustering may produce over-large strata if the investigated area is homogeneous.

The difference between the MD and ML classifiers were small when using the unsupervised method. For the supervised method, however, the ML classifier was better than the MD, especially for the qualitative variables.

By using the ML classifier, the estimation effect when using the supervised method was similar to effects when using the unsupervised method together with the regression estimation.

Pre-stratification proved to be necessary. In particular, the whole area should be partitioned into cut and non-cut sub-areas in order to estimate the net increase. Without this partition, the net increase in the cut compartments were overestimated.

All the updating methods used in the study resulted in similar effects. For estimating the net increase, the "stacking" method appeared more convenient and better than the others. In the absence of new measurements, the key point of updating based on only the fresh image data and old models is the image normalization.

Efficiency analysis

The formulas derived for the efficiency analysis were based on the Ware and Cunia's way.

The precision analysis was conducted for estimates in both the population and compartments. It was demonstrated that the GLS and time filtering resulted in consistent effects. The gain in the correlation when using the bitemporal image is dependent on the relevant correlations. Since the sensitivity of the image data to the change of middle aged and mature forest are very weak, detecting thinning remains difficult.

The precision of estimates in the compartments can also be estimated. According to the analysis, a high precision is not attained when using the TM image data for the small compartments.

The effective range of the weights of the filters can be estimated by the given formulas. The range of the filters concerning the time series is quite wide, but the range might be narrower for the spatial filter.

Based on experimental data recently obtained from the national forest inventory together with some necessary assumptions, the cost of the permanent sample plots and image points were calculated. Efficiency analysis indicated that if the image data can be selected and purchased in terms of image points and surrounding areas, the integration of the permanent plots and multitemporal image data can be beneficial for most variables.

The compartmentwise estimation is not expensive, but the precision, especially for small compartments, might be low. The application of the method to operative management planning is more difficult and was not studied here.

Conclusions

As a traditional estimation method for sampling with the partial replacement, the generalized least squares estimation used for both the quantitative and qualitative variables works well in the case of the permanent sample plots and multitemporal image data.

The image data is effective for estimating the current state of the field variables and detecting large change in them. For detecting small changes, the TM image data seems unsatisfactory. The partitions of a cut area in the compartmentwise estimation is, therefore, necessary.

If the image data are well registered, the gain in the correlation when using spatial filtering is likely to be low for some important variables.

With the unsupervised method, the use of stacked multitemporal data for the multiparameter inventory appears adaptable and compatible. It is therefore recommended. The method can be further enhanced by selecting different statistical transformation and classification techniques.

REFERENCES

Andson T. W. 1984. An introduction to multivariate statistical analysis. Second edition. John Wiley & Sons. New York.

Badwar G. D., Carnes J. G., & Austin W. W. 1982. Use of Landsat-derived temporal profiles for corn-soybean feature extraction and classification. Remote Sensing of Environment. Vol. 12(1):57–59.

Bennett B. J. 1979. Spatial time series. Pion Limited. London.

Cochran W.G. 1977. Sampling techniques. Third edition. John Wiley & Sons. New York.

Cox D. R. 1972. The analysis of binary data. Methuen & Co Ltd. London.

Cruse T., Hägglund B., Jonasson H., Ranneby B., & Swärd J. 1985. Designing a new national forest survey for Sweden. Swedish University of Agricultural Sciences, Faculty of Forestry.

Cunia T. 1965. Continuous forest inventory with partial replacement of samples and multiple regression. For. Sci. 11:480–502.

— & Chevrou R. B. 1969. Sampling with partial replacement on three or more occasions. For. Sci. 15(2):204–224.

Curran P. J. 1985. Principles of remote sensing. Longman. London.

Dixon B. L. & Howitt R. E. 1979. Continuous forest inventory using a linear filter. For. Sci. 25(4):675–689.

Everitt B. S. 1979. Unresolved problems in cluster analysis. Biometrics 35:169–181.

Everitt B. S. 1980. Cluster analysis. Heineman Educational Books Ltd. London.

Frayer W. E. & Furnival G. M. 1967. Area change estimate from sampling with partial replacement. For. Sci. 13:72–77.

Freiberger W. F. (ed.). 1960. The International Dictionary of Applied Mathematics. Van Nostrand. Princeton, N.J.

Goetz A.F.H., Billingsley F. C., Gillespie A. R., Abrams M. J., Squires R. L., Shoemaker E. M., Luchitta I. & Elston D. P. 1975. Application of ERTS images and image processing to regional geologic problems and geologic mapping in Northern Arizona. Jet Propulsion Laboratory Technical Report 32–1597 prepared for NASA contract 7–100. California Inst. of Technology.

Goldberg M., Schlaps D., Alvo M., & Karam G. 1982 Monitoring and change detection with Landsat imagery. Proc. of the 6th International Conference on Pattern Recognition. Munich. Vol. 1. Computer Society Press. pp. 523–526.

Hand D. J. 1981. Discrimination and classification. John Wiley & Sons. New York.

Hansen M. H., Hurwitz W. N. & Madow W. G. 1953. Sample survey methods and theory. John Wiley & Sons.

Harvey A. C. 1981. Time series models. Philip Allan. Deddington.

Hartigen J. A. 1975. Clustering Algorithms. John Wiley & Sons. New York.

Hazard J. W. 1977. Estimating Area in sampling forest populations on two successive occasions. For. Sci. 253–267.

— & Promnitz L. C. 1974. Design of successive forest inventories: optimization by convex mathematical programing. For. Sci., 20: 117–127.

Häme T. 1987. Satellite image-aided change detection. University of Helsinki, Department of Forest Mensuration and Management. Research notes 19: 47–59.

Jaakkola S. 1986. Use of the LANDSAT MSS for forest inventory and regional management: the European experience. Remote sensing:reviews. 2: 165–213.

— & Saukkola P. 1979. Timber volume estimation and cutting opportunity mapping using multispectral remote sensing techniques. Photogrammetric Journal of Finland 8 (1).

Jackson R. D. 1983. Spectral indices in N-space. Remote sensing of environment 13:409–421.

Jessen R.J. 1942. Statistical investigation of a sample survey for obtaining farm facts. Iowa Agr. Exp. Sta. Res. Bull. 304.

Kauth R. J. & Thomas G. S. 1976. The tasselled cap – a graphic description of the spectral- temporal development of agricultural crops as seen by Landsat. Proc. Symposium on machine processing of remotely sensed data. IEEE 76CH 1103-1MPRSD. pp. 41–51.

Kilkki P. 1985. Timber management planning. University of Joensuu, Faculty of Forestry, Silva Carelica 5. 160 pp.

— & Päivinen R. 1987. Reference sample plots to combine field measurements and satellite data in forest inventory. University of Helsinki, Department of Forest Mensuration and Management, Reseach Notes 19: 209–215.

Kuusela K. & Salminen S. 1969. The 5th National Forest Inventory in Finland. Communicationes Instituti Forestalis Fenniae 69(4).

Loetsch F. & Haller K. E. 1973. Forest Inventory. Second edition. BLV Verlagsgesellschaft. München.

Malila W. A. 1980. Change vector analysis: An approach for detecting forest changes with Landsat. Proc. of the Machine Processing of Remotely Sensed Data Symposium. pp. 326–335.

MacQueen J. B. 1967. Some methods for classification and analysis of multivariate observations. Proceedings of the Fifth Berkeley Symposium on Mathematical Statistics and Probability, 1, 281–297.

McCullagh P. & J. A. Nelder F.R.S. 1983. Generalized linear models. Chapman and Hall. London.

Newton C. M., T. Cunia and Bickford C. A. 1974. Multivariate estimators for sampling with partial replacement on two occasions. For. Sci. 20(2):106–116.

Niblack W. 1985 An introduction to digital image processing. Strandberg.

Nyyssönen A. 1967. Remeasured sample plots in forest inventory. Norwegian Forest Research Institute, Vollebekk, Norway.

— , Kilkki P. & Mikkola E. 1967. On the precision of some methods of forest inventory. Acta Forestalia Fennica 81. 60 pp.

Peng Shikui. 1982. A study of continuous forest inventory on more than two occasions (in Chinese, abstract in English). Journal of Nanjing Technological College of Forest Products. No. 1.

— 1986. A comparison of replacement strategies in continuous forest inventory. Silva Fennica 20(3):245–250.

— 1987. An alternative way of integrating multitemporal image data with permanent plots for the continuous forest inventory and the compartmentwise survey. University of Helsinki, Department of Forest Mensuration and Management, Research Notes 19:159–174.

— & Zhu Mingde. 1985. Kalman's linear filtering and its application to the estimation of forest resource dynamics (in Chinese, Abstract in English). Sivae Sinicae 21(2).

Poso S. & Kujala M. 1971. Ryhmitetty ilmakuva- ja maasto-otanta Inarin, Utsjoen ja Enontekiön metsien inventoinnissa. Summary: Groupwise sampling based on photo and field plots in forest inventoryof Inari, Utsjoki and Enontekiö. Folia Forestalia 132.

— & Kujala M. 1978. A method for National Forest Inventory in northern Finland. Communicationes Instituti Forestalis Fenniae 93(1).

— , Häme T. &Paananen R. 1984. A method of estimating the stand characteristics of a forest compartment using satellite imagery. Silva Fennica 18(3):261–292.

— , Paananen R. & Similä M. 1987. Forest inventory by compartments using satellite imagery. Silva Fennica 21(1):69–74.

Press R. J. & Wilson S. 1978. Choosing between logistic regression and discriminant analysis. Journal of the American Statistical Association 73: 699–705.

Richardson, A. J. & Wiegand C. L. 1977. Distinguishing vegetation from soil background information. Photogrammetric engineering and remote sensing 43(12): 1541–1552.

Rouse J. W. Jr., Hass R. H., Schell J. A., & Deering D. W. 1973. Monitoring vegetation systems in the Great Plains with ERTS. Proc. Third ERTS Symposium, NASA SP-351, Vol. I: 309–317.

Rubinstein R. Y. 1981. Simulation and the Monte Carlo Method. John Wiley & Sons. New York.

SAS institute Inc. 1982. SAS user's guide: statistics. 1982 edition. SAS institute Inc. Cary, NC, USA.

— 1985. SAS user's guide: statistics. Version 5 edition. SAS institute Inc. Cary, NC, USA.

Saukkola P. 1982. Clear-cut monitoring with satellite imagery (in Finnish, abstract in English). Technical Research Center of Finland, Research Reports 89.

— & Jaakkola S. 1983. Numerical image interpretation in forest inventory and mensuration (in Finnish, abstract in English). Technical Research center of Finland, Research reports 151.

Scott C.T. 1984. A new look at sampling with partial replacement. For. Sci. 30:157–166.

Showengerdt R. A. 1983. Techniques for Image Processing and Classification in Remote Sensing. Academic Press. New York.

Siitonen M. 1983. A long term forestry planning system based on data from the Finnish national forest inventory. University of Helsinki, Department of Forest Mensuration and Management, Research notes 17.

Singh A. & Harrison A. 1985 Standardized principal components. Int. J. Remote sensing 6(6):883–896.

Spurr S. H. 1952. Forest Inventory. The Ronald Press Company. New York. 476 pp.

Stott C. B. & Semmens G. 1962. Our changing inventory methods and the C.F.I. in North America. Proc. 5th World For. Congr., Seattle, 1:451–454.

Swain P. H. 1978. Bayesian classification in a time-varying environment. LARS technical report 030178. Purdue University, laboratory for applications of remote sensing.

Swain P. H. & Davis S. M. (eds.). 1978. Remote Sensing: the Quantitative Approach. New York. McGraw-Hill.

Theil H. 1971. Principles of Econometrics. John Wiley and Sons. New York.

Thompson D. R. & Wehmanen O. A. 1979. Using Landsat digital data to detect moisture stress. Photogrammetric Eng. and remote sensing 45(2):201–207.

Tomppo E. 1987. Stand delineation and estimation of stand variates by means of satellite images. University of Helsinki, Department of Forest Mensuration and Management, Research notes 19: 60–76.

Tou, J.T. & Gonzalez R. C. 1975. Pattern Recognition Principles. Second edition. Reading, Mass. Addison-Wesley.

Ware K. D. & Cunia T. 1962. Continuous forest inventory with partial replacement of samples. For. Sci. Monog.

Wiegand C. L. & Richardson A. J. 1982. Comparisons among a new soil index and other two- and four dimensional vegetation indices. Proceedings of the 48th Annual meeting, Amer. Soc. Photogramm. pp. 211–227.

Total of 69 references

Appendix 1. Parameters and statistics of the simulation models

Model 1 (sub-model 1)

	Class score					Regression
	1	2	3	4	5	coefficient
Band 1						
Solution:						
Constant = 49.4117						
Site class		0	−0.023	0.433	0.669	
Tax. class	0	0.550	0.449	0.290	.247	
G						−0.0313
ln (D + 3)						−0.8671
Residual mean squares: 2.1555						
R-square : .271						
Band 2						
Solution:						
Constant = 19.7967						
Site class		0	−0.262	0.101	0.046	
Tax. class	0	0.094	0.060	0.105	0.137	
G						−0.0229
ln (D + 3)						−0.8039
Residual mean squares: 0.9811						
R-square: 0.378						
Band 3						
Solution:						
Constant = 18.0817						
Site class		0	−0.170	0.438	0.498	
Tax. class	0	0.399	0.253	0.174	0.098	
G						−0.0287
ln (D + 3)						−1.3387
Residual mean squares: 1.8284						
R-square: 0.432						
Band 4						
Solution:						
Contant = 44.1484						
Site class		0	−0.497	−0.530	−1.282	
Tax. class	0	1.380	−0.149	−0.370	−0.927	
G						−0.1431
ln (D + 3)						−4.0957
Residual mean squares: 18.2175						
R-square = 0.442						
Band 5						
Solution:						
Constant = 38.9749						
Site class		0	0.351	2.534	2.529	

Appendix 1 cont.

	Class score					Regression
	1	2	3	4	5	coefficient
Tax. class	0	1.746	0.555	0.418	.0001	
G						−0.133
ln (D + 3)						−6.0833
Residual mean squares: 29.9558						
R-square: 0.481						
Band 6						
Solution:						
Constant = 102.3486						
Site class		0	0.192	1.066	1.721	
Tax. class	0	0.230	0.164	0.213	0.574	
G						−0.0089
ln (D + 3)						−0.5165
Residual mean squares: 1.8590						
R-square: 0.272						
Band 7						
Solution:						
Constant = 12.8333						
Site class		0	1.063	1.872	1.995	
Tax. class	0	0.455	0.178	0.084	0.052	
G						−0.0405
ln (D +3)						−2.0717
Residual mean squares: 4.1439						
R-square: 0.433						

Appendix 1 cont.

Model 1 (sub-model 2)

	Class score									Regression
	0	1	2	3	4	5	6	7	8	coefficient
Band 1										
Solution:										
Constant = 49.3878										
Stoniness		0	−0.235	−0.657	−0.310	−0.425	−0.379	−0.168	−0.259	
Main species	0	−0.920	−1.123	−0.899	−1.321		−1.375			
H										−0.0653
D										0.0206
A										−0.7693
ln (G + 3)										0.00001
P										0.1494
S										0.1101
B										0.1792
Residual mean squares: 2.0698										
R-square : 0.302										
Band 2										
Solution:										
Constant = 18.6990										
Stoniness		0	−0.044	−0.910	0.031	−0.069	−0.039	−0.127	−0.075	
Main species	0	−0.095	−0.240	0.092	−0.072		−1.171			
H										−0.0688
D										0.0151
A										−0.3274
ln (G + 3)										−0.0025
P										0.0548
S										0.0003
B										0.0797
Residual mean squares: 0.8773										
R-square : 0.4458										
Band 3										
Solution:										
Constant = 16.9193										
Stoniness		0	−0.115	−0.976	−0.176	−0.647	−0.873	−0.162	−0.109	
Main species	0	−0.440	−0.676	−0.060	−0.490		−1.932			
H										−0.0615
D										0.0081
A										−0.9364
ln (G + 3)										−0.0010
P										0.1410
S										0.0634
B										0.1794
Residual mean squares: 1.6576										
R-square : 0.487										

Appendix 1 cont.

	Class score									Regression
	0	1	2	3	4	5	6	7	8	coefficient
Band 4										
Solution:										
Constant = 36.0648										
Stoniness		0	−0.190	−2.949	−0.374	−0.118	−1.646	−0.080	−0.041	
Main species	0	−0.858	−2.048	−1.075	−2.286		6.397			
H										0.3485
D										0.1019
A										−1.2682
ln (G + 3)										−0.0362
P										0.2856
S										0.3809
B										0.8504
Residual mean squares: 15.6388										
R-square : 0.522										
Band 5										
Solution:										
Constant = 37.4390										
Stoniness		0	−0.546	−3.925	−0.075	−3.902	−2.657	−0.143	−0.1565	
Main species	0	−3.459	−4.662	−2.662	−4.953		−7.0721			
H										−0.3848
D										0.1342
A										−4.0907
ln (G + 3)										−0.0053
P										0.3465
S										0.0308
B										0.7721
Residual mean squares: 25.6425										
R-square: 0.557										
Band 6										
Solution:										
Constant = 103.4016										
Stoniness		0	−0.215	−1.182	−0.178	−0.622	0.067	0.391	0.273	
Main species	0	−0.808	−0.957	−0.082	−0.526		−1.072			
H										−0.0234
D										−0.0239
A										−0.4329
ln (G + 3)										0.0084
P										0.0956
S										−0.0194
B										−0.0092
Residual mean squares: 1.8545										
R-square : 0.275										

Appendix 1 cont.

Model 2

	Regression coefficient					
	Constant	H	ln (H+3)	V	ln (V+10)	$[\ln(V+10)]^2$
Band 1						
Solution:	52.7813	−0.0051	−0.4199	−0.0016	−1.7031	0.1523
Residual mean squares: 2.1436						
R-square : 0.275						
Band 2						
Solution:	21.6680	−0.0502	−0.3984	−0.0052	−1.5547	0.2275
Residual mean squares: 0.9622						
R-square : 0.391						
Band 3						
Solution:	23.8477	−0.0253	−0.8623	−0.0075	−3.4922	0.4478
Residual mean squares: 1.8144						
R-square : 0.437						
Band 4						
Solution:	39.7227	−0.3994	0.8770	−0.0026	−2.0586	0.1309
Residual mean squares: 17.6198						
R-square : 0.460						
Band 5						
Solution:	67.7148	0.0731	−7.7715	−0.0421	−14.5898	2.0737
Residual mean squares: 28.8866						
R-square: 0.500						
Band 6						
Solution:	106.9531	−0.0771	0.6406	−0.0068	−3.0625	0.4023
Residual mean squares: 2.1834						
R-square : .143						
Band 7						
Solution:	27.0273	0.0591	−2.8457	−0.0176	−6.7275	0.9392
Residual mean squares: 3.9635						
R-square : 0.458						

Appendix 2. Inventory results of one compartment based on the image stratification (An example)

Compartment no. = 0	image points = 24 Mean	S.D.	area = 66966 M^2 C.V (%)
Age (year)	89.93	27.89	31.01
Height (m)	20.32	3.90	19.22
D.B.H (cm)	25.62	6.24	24.37
Basal area (m^2)	22.81	8.64	37.87
Volume (m^3)	231.48	102.05	44.08
Composition (10 %):			
Pine	3.74	3.37	90.06
Spruce	5.43	3.29	60.66
Broad leaved spesies	0.83	1.41	170.07
Net increase (m^3/ha)	10.50	76.04	723.97
Total growth (m^3/ha)	32.05	12.59	39.30
Total drain (m^3/ha)	21.54	71.81	333.31
Including:			
Cutting (m^3/ha)	20.73	71.81	346.48
Mortality (m^3/ha)	0.82	1.52	186.34

	Class code										
	0	1	2	3	4	5	6	7	8	9	Total
Site class	0.00	24.00	0.00	0.00	0.00	0.00	0.00	0.00	0.00	0.00	24.00
Soil class	0.00	19.59	1.88	2.53	0.00	0.00	0.00	0.00	0.00	0.00	24.00
Site class	0.00	0.00	4.94	14.11	2.99	1.96	0.00	0.00	0.00	0.00	24.00
Stoniness	0.00	13.99	3.47	0.36	1.76	0.51	0.03	1.86	2.02	0.00	24.00
Taxation class	0.00	3.07	11.27	5.70	3.38	0.57	0.00	0.00	0.00	0.00	24.00
Forest class	0.00	22.05	1.06	0.89	0.00	0.00	0.00	0.00	0.00	0.00	24.00
Main species	0.00	9.53	14.01	0.03	0.35	0.00	0.00	0.08	0.00	0.00	24.00
Dev. class	0.00	0.84	2.64	4.22	14.45	1.84	0.00	0.00	0.00	0.00	24.00

ACTA FORESTALIA FENNICA

180 Simula, M. 1983. Productivity differentials in the Finnish forest industry. Seloste: Tuottavuuden vaihtelu Suomen metsäteollisuudessa.
181 Pohtila, E. & Pohjola, T. 1983. Lehvästöruiskutuksen ajoitus kasvukauden aikana. Summary: The timing of foliage spraying during the growing season.
182 Kilkki, P. 1983. Sample trees in timber volume estimation. Seloste: Koepuut puuston tilavuuden estimoinnissa.
183 Mikkonen, E. 1983. Eräiden matemaattisen ohjelmoinnin menetelmien käyttö puunkorjuun ja kuljetuksen sekä tehdaskäsittelyn menetelmävalinnan apuvälineenä. Abstract: The usefulness of some techniques of the mathematical programming as a tool for the choice of timber harvesting system.
184 Westman, C. J. 1983. Taimitarhamaiden fysikaalisia ja kemiallisia ominaisuuksia sekä niiden suhde orgaanisen aineen määrään. Summary: Physical and physico-chemical properties of forest tree nursery soils and their relation to the amount of organic matter.
185 Kauppi, P. 1984. Stress, strain, and injury: Scots pine transplants from lifting to acclimation on the planting site. Tiivistelmä: Metsänviljelytaimien vaurioituminen noston ja istutuksen välillä.
186 Henttonen, H. 1984. The dependence of annual ring indices on some climatic factors. Seloste: Vuosilustoindeksien riippuvuus ilmastotekijöistä.
187 Smolander, H. 1984. Measurement of fluctuating irradiance in field studies of photosynthesis. Seloste: Säteilyn vaihtelun mittaaminen fotosynteesin maastotutkimuksissa.
188 Pulkki, R. 1984. A spatial database – heuristic programming system for aiding decisionmaking in long-distance transport of wood. Seloste: Sijaintitietokanta – heuristinen ohjelmointijärjestelmä puutavaran kaukokuljetuksen päätöksenteossa.
189 Heliövaara, K. & Väisänen, R. 1984. Effects of modern forestry on northwestern European forest invertebrates: a synthesis. Seloste: Nykyaikaisen metsänkäsittelyn vaikutukset luoteiseurooppalaisen metsän selkärangattomiin: synteesi.
190 Suomen Metsätieteellinen Seura 75 vuotta. The Society of Forestry in Finland – 75 years. 1984.
191 Silvola, J., Välijoki, J. & Aaltonen, H. 1985. Effect of draining and fertilization on soil respiration at three ameliorated peatland sites. Seloste: Ojituksen ja lannoituksen vaikutus maahengitykseen kolmella suomuuttumalla.
192 Kuusipalo, J. 1985. An ecological study of upland forest site classification in southern Finland. Seloste: Ekologinen tutkimus Etelä-Suomen kangasmetsien kasvupaikkaluokituksesta.
193 Keltikangas, M., Laine, J., Puttonen, P. & Seppälä, K. 1986. Vuosina 1930–1978 metsäojitetut suot: Ojitusalueiden inventoinnin tuloksia. Summary: Peatlands drained for forestry in 1930–1978: Results from field surveys of drained areas.
194 Vehkamäki, S. 1986. The economic basis of forest policy. A study on the goals and means of forest policy. Seloste: Metsäpolitiikan taloudelliset perusteet. Tutkimus metsäpolitiikan tavoitteista ja keinoista.
195 Huhta, V., Hyvönen R., Koskenniemi A., Vilkamaa P., Kaasalainen P. & Sulander M. 1986. Response of soil fauna to fertilization and manipulation of pH in coniferous forests. Seloste: Lannoituksen ja pH-muutoksen vaikutus kangasmetsän maaperäeläimistöön.
196 Luomajoki, A. 1986. Timing of microsporogenesis in trees with reference to climatic adaptation. A review. Seloste: Mikrosporogeneesin ajoitus ja puulajien ilmastollinen sopeutuminen.
197 Oker-Blom, P. 1986. Photosynthetic radiation regime and canopy structure in modeled forest stands. Tiivistelmä: Metsikön valoilmasto ja latvuston rakenne.
198 Westman, C. J. 1987. Site classification in estimation of fertilization effects on drained mires. Seloste: Kasvupaikkojen luokitus lannoitusvaikutuksen arvioinnissa ojitetuilla rämeillä.
199 Leikola, M. 1987. Suomalaiset metsätieteelliset väitöskirjat ja niiden laatijat. Summary: Academic dissertations and doctors in forestry sciences in Finland.
200 Peng Shikui. 1987. On the combination of multitemporal satellite and field data for forest inventories. Tiivistelmä: Moniaikaisen satelliitti- ja maastoaineiston yhteiskäyttö metsien inventoinnissa.
201 Nygren, M. 1987. Germination characteristics of autumn collected Pinus sylvestris seeds. Seloste: Männyn siementen itämistunnukset syyskeräyksissä.

Kannattajajäsenet – Supporting members

CENTRALSKOGSNÄMNDEN SKOGSKULTUR
SUOMEN METSÄTEOLLISUUDEN KESKUSLIITTO
OSUUSKUNTA METSÄLIITTO
KESKUSOSUUSLIIKE HANKKIJA
OY WILH. SCHAUMAN AB
KEMIRA OY
METSÄ-SERLA OY
KYMMENE OY
KESKUSMETSÄLAUTAKUNTA TAPIO
KOIVUKESKUS
A. AHLSTRÖM OSAKEYHTIÖ
TEOLLISUUDEN PUUYHDISTYS
OY TAMPELLA AB
KAJAANI OY
KEMI OY
MAATALOUSTUOTTAJAIN KESKUSLIITTO
VAKUUTUSOSAKEYHTIÖ POHJOLA
VEITSILUOTO OSAKEYHTIÖ
OSUUSPANKKIEN KESKUSPANKKI OY
SUOMEN SAHANOMISTAJAYHDISTYS
OY HACKMAN AB
YHTYNEET PAPERITEHTAAT OSAKEYHTIÖ
RAUMA REPOLA OY
JAAKKO PÖYRY OY
KANSALLIS-OSAKE-PANKKI
SOTKA OY
THOMESTO OY
SAASTAMOINEN OY
OY KESKUSLABORATORIO
METSÄNJALOSTUSSÄÄTIÖ
SUOMEN METSÄNHOITAJALIITTO
SUOMEN 4H-LIITTO
SUOMEN PUULEVYTEOLLISUUSLIITTO R.Y.
OY W. ROSENLEW AB
METSÄMIESTEN SÄÄTIÖ
SÄÄSTÖPANKKIEN KESKUS-OSAKE-PANKKI
ENSO-GUTZEIT OY

ISBN 951-651-0787-7

Karisto Oy:n kirjapaino
Hämeenlinna 1987